

ICE JAM FLOODING ON THE LOUP RIVER STUDY REPORT

LOUP RIVER HYDROELECTRIC PROJECT

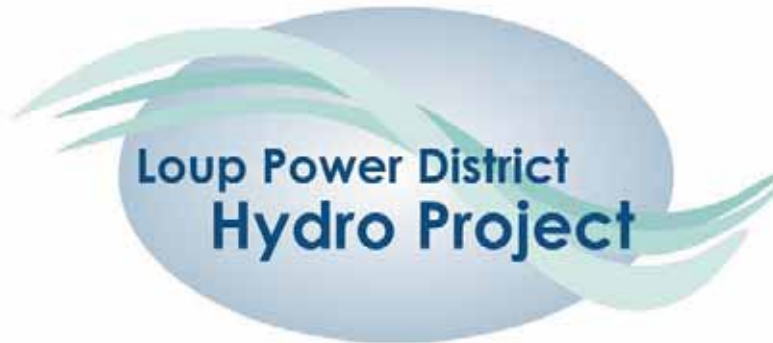
FERC PROJECT No. 1256

ICE JAM FLOODING ON THE LOUP RIVER



FEBRUARY 11, 2011

STUDY 12.0 - ICE JAM FLOODING ON THE LOUP RIVER



**Loup River Hydroelectric Project
FERC Project No. 1256**

Study 12.0 Ice Jam Flooding on the Loup River

February 11, 2011

© 2011 Loup River Public Power District

Prepared for:

Loup Power District
2404 15th Street
Columbus, NE 68602

Prepared by:



**US Army Corps
of Engineers**

1616 Capitol Avenue, Suite 9000
Omaha, NE 68102

Roger L. Kay, P.E., Jesse M. Brown, Alex J. Flanigan, Laurel J. Hamilton, and Neil W. Vohl, P.E.

STUDY 12.0 ICE JAM FLOODING ON THE LOUP RIVER..... 1

1. INTRODUCTION 1

2. GOALS AND OBJECTIVES OF STUDY 2

3. STUDY AREA 2

4. METHODOLOGY 3

 4.1 History of Flooding 3

 4.2 Compilation of Meteorologic Data 11

 4.3 HEC-RAS Modeling 16

 4.4 DynaRICE Modeling 18

5. RESULTS AND DISCUSSION 18

 5.1 History of Flooding 18

 5.2 Analysis of Meteorologic Data 20

 5.3 HEC-RAS Modeling Results 29

 5.4 DynaRICE Modeling Results 34

 5.5 Summary and Conclusions 34

6. STUDY VARIANCE 34

7. REFERENCES 34

List of Tables

Table 4-1. Backwater Affected Stages - Loup River at Columbus 7

Table 4-2. Peak Backwater Affected Stages - Loup River at Genoa 9

Table 4-3. Notable Nebraska Ice Jam Flooding 11

Table 4-4. Typical C Values for modified Stefan Equation 15

Table 5-1. Documented Significant Ice Jam Floods Before and After 1937 19

Table 5-2. Peak AFDD 30-Year Average 24

Table 5-3. Trends in AFDD_{max} and Julian Date by Decade 26

Table 5-4. Computed Range of Ice Thickness in Ice Jam Years 27

List of Attachments

- Attachment A Statistical Analysis of AFDD
- Attachment B Trend Analysis
- Attachment C Ice Thickness
- Attachment D Relationship Between Snow Cover and/or Rain and Ice Jams
- Attachment E DynaRICE Modeling of Ice Transport on the Loup River

STUDY 12.0 ICE JAM FLOODING ON THE LOUP RIVER

1. INTRODUCTION

The Project is located in Nance and Platte counties, where water is diverted from the Loup River and routed through the 35-mile-long Loup Power Canal, which empties into the Platte River near Columbus. The Project includes various hydraulic structures, two powerhouses, and two regulating reservoirs. The portion of the Loup River from the Diversion Weir to the confluence with the Platte River is called the Loup River bypass reach.

At the point of diversion, a low weir across the Loup River creates sufficient head to divert a variable portion of river flow (not to exceed 3,500 cfs) through an Intake Gate Structure. The diverted water is then routed through the Loup Power Canal, which empties into the Platte River just downstream of the Loup River confluence at Columbus. The portion of Loup River flow that is not diverted into the Loup Power Canal passes over the Diversion Weir or through the adjacent Sluice Gate Structure and continues downstream. According to long-term gage records, approximately 69 percent of the total Loup River flow is diverted into the Loup Power Canal for Project purposes on an annual basis.

Project operations in winter include special procedures to deal with cold temperatures and ice conditions. Frazil ice, also known as slush ice because of its appearance, is formed only in turbulent supercooled water. According to the U.S. Army Corps of Engineers (USACE), frazil ice is most often seen in early to mid-winter and can accumulate to form an ice cover or an ice jam (USACE, July 1994). When frazil ice is observed in the river at the Diversion Weir, District operating procedures require gate operators to close the intake gates and cease admitting water to the canal. When conditions change and frazil ice is no longer observed near the Diversion Weir, the operators open the intake gates and resume diversion of water into the canal.

Historical records show that severe ice jams have occurred in the lower Loup River and the lower Platte River with some regularity since long before District hydroelectric operations began in the late 1930s. In March 1993, a combination of ice jams and rapid snowmelt resulted in severe flooding in the lower Platte River basin. The two areas most impacted were the south side of the Loup River in Columbus and the area immediately downstream of the Elkhorn River and Platte River confluence near Ashland, Nebraska. Over 74,000 acres were flooded, and damages exceeded \$25 million (USACE, January 1996). This wide-spread and devastating event prompted two related studies by USACE on ice jam formation and resultant flooding in the lower Platte River basin. The two USACE reports are titled “Lower Platte River Ice Jam Flooding” (July 1994) and “Ice Jam Flooding and Mitigation: Lower Platte River Basin, Nebraska” (January 1996).

The USACE reports do not identify any responsible parties, structures, or events related to the ice jam formation or resultant flooding. The USACE reports do mention that some local citizens expressed the opinion that water level fluctuations caused by Project operations may exacerbate ice jam formation and flood impacts in the Loup River bypass reach. The reports explain that there was insufficient information available at the time to perform a quantitative analysis on the potential impacts of Project operations on ice jam formation. It was recommended that an ice reporting program be initiated under the Nebraska Natural Resources Commission, now the Nebraska Department of Natural Resources (NDNR). Both reports concluded with a statement that “A recommended future study would be to evaluate the effect, if any, that Project operations have on ice conditions downstream” (USACE, July 1994 and January 1996). Subsequently, NDNR initiated the Nebraska Ice Reporting program and has gathered ice data at various stations from 1994 to the present.

2. GOALS AND OBJECTIVES OF STUDY

The goal of the study of ice jam flooding on the Loup River is to evaluate the impact of Project operations on ice jam flooding on the Loup and Platte rivers between Fullerton, Nebraska, and North Bend, Nebraska. The study will also develop an ice jam and/or breakup predictive model (limited to examination of Project effects), as well as identify operational or structural measures to mitigate or minimize Project effects on ice jam formation and subsequent flooding, if it is demonstrated that operation of the Project materially impacts ice jam formation on the Loup and Platte rivers.

The objectives of the study of ice jam flooding on the Loup River are as follows:

1. To evaluate the effect of Project operations on hydrology, sediment transport, and channel hydraulics on ice processes in the Loup and lower Platte rivers
2. To develop an ice jam and/or breakup predictive model to evaluate Project effects
3. To identify structural and nonstructural methods for the prevention and mitigation of ice jams, should it be demonstrated that operation of the Project materially impacts ice jam formation on the Loup and Platte Rivers.

3. STUDY AREA

The study area includes the Loup River from Fullerton (approximately 7 miles upstream of the Loup Power Canal Headworks) to the confluence with the Platte River (the Loup River bypass reach), the Platte River from just upstream of the confluence of the Loup and Platte rivers to North Bend, and the Loup Power Canal from the Headworks to the Tailrace Canal confluence with the Platte River below the Loup-Platte confluence.

4. METHODOLOGY

Several methods were employed to determine if the operation of the Loup Power Canal contributes materially to the formation of ice jams along the study reach. These methods included a review of flood history, a statistical overview of meteorologic data, and hydraulic modeling of the study area.

4.1 History of Flooding

A review of all available records was conducted to determine when significant flood events occurred along the study reach. The flood history was heavily influenced by Nance County Journal articles. These accounts are some of the only records of floods before the 1930's. Following are brief descriptions of some of the most notable floods along the study reach.

4.1.1 Significant Floods in Lower Loup Basin

Flood of 1848 or 1849

Ice jam flooding occurred in either early March 1848 or March 1849. According to pioneer accounts, the Platte and Loup valleys flooded from bluff to bluff. The flood inundated nearly all present day Columbus. An entire tribe of Pawnee Indians supposedly perished in the flood between present day Fullerton and Spaulding. Floodwaters killed many wild animals that were swept downstream into the Missouri River (*Nance County Journal*, 1923).

Flood March 1881

Multiple deaths caused by ice jam flooding occurred on March 19th. Many rural residents escaped floodwaters by spending days stuck in tall trees. Railroad tracks suffered heavy damages. Flood damages in Columbus reached 11th St. Multiple homes in Columbus were destroyed. 80% of the Loup River Bridge was destroyed. Large herds of livestock were lost in the floodwaters (Andreas, 1882; *Nance County Journal*, 1923).

Flood May 1904

Spaulding, NE, along the Cedar River, received 7" of rain. Cedar Rapids rainfall exceeded 4". Many tributary bridges were destroyed. The Cedar River inundated much of Fullerton, NE. Fullerton's stockyards and grain elevator were flooded. Railroad tracks were washed out near Fullerton (*Nance County Journal*, 1904). Newspaper articles made no mention of flooding on the Loup River.

Flood of February 1905

Picture shows the destruction of the Loup River Bridge, which was destroyed during an ice jam flood. The photo shows the water has receded, but large ice pads over 20" thick are scattered around the remains of the bridge.

Flood of February 1907

Stages rose more than 5 feet per hour as a result of ice jam flooding on February 13th. Four Columbus locals drowned trying to escape the floodwaters. Most of southern Columbus was underwater, including the stockyards and railroad. Areas along Shell Creek and the Platte River were also flooded (USACE, 2010).

Flood of March 1910

An ice jam formed upstream of the Union Pacific Railroad bridge, damaging both Union Pacific and Burlington lines. Many Columbus streets were buried in a foot of mud. The Platte River Wagon Bridge was swept away by ice flows, according to photos.

Flood of March 1912

On March 29th, collapse of bridge due to ice flow causes flooding along Loup River. A Railroad Bridge was swept away. Some Columbus streets were covered in a foot of mud. Pawnee Park was also flooded (*Nance County Journal*, 1923).

Flood June 1923

Heavy rainfall caused severe flooding in most of the Loup River Basin. Extensive agricultural damage sustained on Loup River and Cedar River, Beaver Creek, Looking Glass Creek and Lost Creek. Columbus was flooded to 6th Street. Railroad tracks between Genoa and Fullerton were severely damaged including some bridges. This flood was supposedly the worst flood ever seen, to that point in time. The Loup Basin experienced 1 million dollars in flood damages, according to a local newspaper (*Nance County Journal*, 1923).

Flood of April 26, 1935

A 7” rain fell near Columbus causing extensive flooding. 18” of floodwater stood in the southwest section of Columbus. US Highway 30-81 was inundated along with Pawnee Park. Stream flows peaked at 41,500 cfs and stages crested at 9.5 ft. No damage estimates are available (USACE, 1967).

Flood of March 1936

Ice jam flooding on the Cedar River washed out the east-west road near the Union Pacific depot in Fullerton, NE. The flood created a 450 feet wide by 20 feet deep gully through the east west road. Many families were forced to evacuate as homes along the Loup River and Cedar River were flooded. The Fullerton golf course and numerous farmland acres were inundated (*Nance County Journal*, 1936). No other documentation of Loup River flooding.

Flood of February 1941

One inch of rain over the Cedar River Basin compounded ice jam flooding along the Loup and Cedar Rivers. The ice jam was approximately $\frac{3}{4}$ miles long. Many roads were closed and the KND Highway was washed out. A sink hole at the Fullerton Stock Yards swallowed a rail car as it grew to cover over $\frac{1}{2}$ acre. The Union Pacific depot at Belgrade was also flooded (*Nance County Journal*, 1941).

Flood of June 23, 1947

Large portions of the Loup Basin received 6” of rain on June 21st and 22nd. Localized areas accumulated over 8”. Flooding peaked in Columbus on June 23rd. 112 city blocks comprised of 500 residences were inundated. Commercial businesses, the railroad switchyard, Pawnee Park, Wagner Lake and the golf course were also flooded. Evacuations of over 900 families were made. Stream flows peaked at 85,000 cfs and stages crested at 12.0 ft. Damages were estimated at \$388,000 (USACE, 1967).

Floods of February 1948

Ice jams on the Loup River caused two separate floods in Columbus. The first ice jam formed downstream of U.S. Highway 30-81 bridge between February 14th – 21st. No damages were estimated. Another ice jam formed at the same location on February 28th. The southwest section of Columbus was inundated. Damages were estimated as \$72,000 (USACE, 1967). It is unknown if the first jam remained in place or not, which would have contributed to the second period of flooding.

Flood of March 1960

Snowmelt runoff caused flooding from the Loup confluence to Columbus from March 22nd-26th. The flood was responsible for one death in Columbus. The peak discharge was 52,000 cfs and stages crested at 10.5 ft. Damages were estimated as \$236,000 (USACE, 1967).

Flood of August 1966

A large storm system produced over six inches of rainfall in much of the Loup River Basin. Sixteen inches of rain fell at the storm’s center near Walbach, NE. Flooding occurred throughout the Loup River Basin from Aug 12th – 14th. The southwest portion of Columbus experienced severe flooding. 634 houses and 24 businesses were inundated. The Union Pacific Railroad tracks, Pawnee Park, the golf course and Wagner Lake were also flooded. 1,000 Columbus families were evacuated. Damages were estimated at \$1,435,000 (USACE, 1967). The Loup River at Columbus estimated peak discharge was 119,000 cfs, but this flow is suspect, since the Platte River at North Bend downstream peaked at only 72,500 cfs on the same day (USACE, 1994).

Flood of March 1969

An ice jam formed ½ mile downstream of Highway 30-81 Bridge at Columbus in the evening of March 17th. At its largest, the jam extended ½ mile east and west of the Highway 30-81 Bridge. The jam was successfully blasted out on March 21st. Damages included some commercial businesses flooded and road washouts. Multiple rural homes were also flooded. Before 1993, the March 1969 flood was the highest recorded ice affected stage at Columbus (USACE, 1994).

Flood of February 1971

A 3-5 mile long ice jam formed at Genoa as a result of ice break up and a storm event, according to the Nebraska Civil Defense. The jam was in place from February 20th through 24th, or longer. Little flood information is known about this event. Areas southeast of Columbus were inundated (USACE, 1994).

Flood of March 7, 1993

The ice jam formed on March 7th, upstream of the Highway 30-81 Bridge at Columbus. Highway 30-81 was closed as both approaches to the bridge were inundated. Flood issues extended into Nance County affecting Fullerton, NE. The ice jam produced a stage at Columbus that was equivalent to an open water flow of 200,000 cfs. High water mark surveys showed stages reach elevation 1449.31 ft- msl (nearly 9 feet above flood stage). Some residents claimed the floodwaters were 4-5 feet higher than the levels of the Flood of August 1966, the highest open-water stage recorded. Many residents consider the Ice Jam of 1993 the worst flood of his or her lifetime (USACE, 1994).

4.1.2 Other Ice Related Floods

The documented events listed below are other ice related incidences. The information in this section was found in CRREL's ice jam database (USACE, 2010).

The table below shows the backwater affected stages due to ice on the Loup River at Columbus. For comparison, flood stage at Columbus is 11 feet. Available information about an event is also documented in this section; any event without further information is described as backwater from ice.

Table 4-1. Backwater Affected Stages - Loup River at Columbus

Date	Stage, ft	Date	Stage, ft
24 Dec 2007	N/A	11 Jan 1975	7.46
6 Dec 2006	N/A	10 Jan 1974	6.7
14 Dec 2003	N/A	20 Jan 1973	7.4
5 Mar 2003	N/A	3 Jan 1970	8.0
29 Nov 1993	N/A	15 Feb 1966	N/A
14 Mar 1979	N/A	16 Feb 1963	6.04
15 Mar 1978	8.87	17 Feb 1961	6.38
24 Feb 1977	6.36	5 Mar 1959	6.18
3 Jan 1976	8.58	26 Feb 1958	7.53

December 2007

Minor ice jam overflows were reported on the Loup River near Columbus NE, by the National Weather Service, Omaha/Valley NE, in a Hydrologic Statement released 518pm CST, Mon 24 Dec 2007. The jam stretched from its confluence with the Platte River to near the highway 81 bridge.

December 2006

At 435PM CST on Wednesday, December 6, 2006, the National Weather Service issued a flood advisory for the Loup River near Columbus. Platte County Emergency Management reported an ice jam on the Loup River from about 2 miles east of Columbus to about 2 miles west of the city. The upstream end of the jam was about 1 mile west of the Highway 81/30 bridge near the Black Bridge (railroad bridge). The jam had caused water levels to rise about 2 feet that afternoon. On Thursday, December 7, at 402 AM there was no report of any change in the situation. Flooding was taking place in low-lying areas. It was thought that additional releases of water into the river might help clear up the jam. Platte County Emergency Management observed ice levels rising near the railroad bridge at 1111 AM CST. At 949 PM, the NWS reported that water levels were increasing due to water NOT being diverted into the Loup River Power Canal (upstream from the jam), thus increasing flows and potentially melting the ice. Temperatures were expected to rise into the 50's on Saturday but stay in the 20's overnight. At 1147 PM Friday evening, the ice was reported to have backed up to a point about 4 miles upstream from Black Bridge. Platte County Emergency Management officials reported that water levels had risen significantly and water was flowing under the jam with an open channel near the wastewater treatment plant. The gage upstream at Genoa was steady and Loup Power was to continue allowing flow to remain in the Loup River, hopefully to assist with

meltout as temperatures were going to rise. At 1159 AM Saturday 9 December 2006, the NWS reported that Platte County Emergency Management officials found conditions unchanged, with a large amount of ice in the channel; however, water was flowing beneath the jam to open water on the Platte River. No flooding was occurring at that time.

December 2003

The NWS reported on 14 December 2003 that an ice jam on the Loup River near Columbus, NE continued to cause lowland flooding between the Loup and Platte rivers. Ditches were reported to be water filled near the intersection of highways 30 and 81 just south of Columbus. On 18 Dec the NWS reported that the jam continued past the railroad bridge and had seen some breakup action at the tail race. Ice chunk movement was noted on the Platte.

March 2003

The NWS reported at 635 PM that an ice jam was reported early Wednesday evening on the Loup River southeast of Columbus near the area where the Loup merges with the Platte River. This ice jam was causing some minor lowland flooding. Some cabins in the area may have been affected. At 805 PM the NWS reported that the ice jam on the Loup River appeared to be growing in size. The jam extended from near 13th Avenue downstream to the mouth of the Loup. The NWS reported on March 6 that the ice jam on the Loup River was still in place but did not appear to be solid. There were some areas of open water. Ice in the river extended from about ½-mile east of the inlet of the Loup Power Canal upstream to about 1 mile west of the Highway 81 Bridge southwest of Columbus. No flooding was occurring at 4 PM Thursday but some very minor overflows near the inlets to some small creeks.

November 1993

The jam lasted from 11/29/93 to 12/05/93. The toe of the jam was near the old Burlington Northern Railroad Bridge on the Platte River, with the length of jam more than 4 miles expanding up the Loup River. Damages were minimal - water was observed flowing through the golf course and pasture land.

March 1979

On March 14, 1979, an ice jam formed upstream from the Union Pacific Railroad bridge. This jam extended about one-half mile above the bridge and caused lowland flooding. The jam eventually failed and moved downstream, rejamming downstream from the Highway 81 Bridge. Backwater from the jam reached bank level at the bridge before the jam failed on March 15, 1979.

February 1966

An additional ice jam was reported in Nebraska Civil Defense records on February 15, 1966 (memorandum of aerial reconnaissance, William J. Clark, February 16, 1966). This ice jam, located in the Wagner Lake-Sand Pit area west of Columbus (upstream from the gage), caused overbank flooding. No other more specific information regarding jam formation or extent was given.

The following table shows the backwater affected stages due to ice on the Loup River at Genoa. Available information about an event is also documented in this section.

Table 4-2. Peak Backwater Affected Stages - Loup River at Genoa

Date	Stage, ft	Date	Stage, ft
9 March 2010	13.82	15 March 1979	10.87
10 February 2009	9.5	18 March 1978	12.12
23 Jan 2005	8.15	23 February 1977	10.2
28 February 2004	9.49	9 February 1976	8.79
12 March 2001	9.7	3 March 1975	8.36
17 Jan 1997	9.7	15 February 1974	9.12
26 February 1996	11.7	21 Jan 1973	8.36
10 March 1993	9.4	28 February 1972	9.21
10 March 1989	9.4	19 February 1971	10.37
24 February 1988	8.99	23 February 1970	8.59
27 Jan 1986	10.14	19 March 1969	10.80
27 February 1985	9.43	1 Apr 1965	10.33
17 February 1983	9.35	18 Dec 1963	7.83
21 February 1982	12.35	16 February 1962	10.00
30 Dec 1981	11.83	16 March 1948	7.61
18 Jan 1980	10.79	12 March 1929	7.31

Less is known about Genoa peak stages and their temporal relationship to ice jams before 1962. But of the 22 years of record between 1929 and 1962, 10 of the 22 peak stages were affected by backwater in some way; it is likely that these are also ice-affected, but it is not documented as such. It is also possible that additional years had peak stages affected by backwater, but were not annotated as such.

March 2010

Flooding was caused by river ice breakup. Temperatures increased in early March and were accompanied by rain and snowmelt runoff. The Loup River at Genoa gage recorded a stage of 13.82 ft. The record stage is 13.93 ft. Water was seen flowing over Highway 39 south of Genoa as result of the ice jam.

February 2009

An ice jam formed, causing minor flooding 3-4 miles upstream of the Highway 39 Bridge near Genoa.

February 2007

There was widespread flooding on the Loup River and neighboring tributaries. Ice problems were mentioned but no direct mention of an ice jam. A family living within 1/8 mile of Loup River was forced to evacuate as water encroached their backyard.

March 2004

The yearly maximum stage and discharge was caused by ice-affected backwater. A discharge of 9,000 cfs on March 1st and a stage of 9.49 ft on February 28th at the Genoa gage were recorded.

March 2001

Stages reached 9.7 ft at the Genoa gage and 11-12 ft near the Highway 39 bridge as a result of ice movement. Moderate flooding reported.

February 1997

An ice bridge formed between the Loup Power Canal Headworks and Highway 39 Bridge in mid-January. The bridge then froze in place. Stages reached 9.7 ft at Genoa. Up to 5,000 cfs were diverted through the Loup Power Canal Headworks during the peak.

February 1996

An ice jam formed downstream of the Highway 39 bridge. The jam was four miles long.

February 1995

An ice jam caused lowland flooding near the Highway 39 Bridge near Genoa.

Jan 1994

An ice jam produced minor Loup River flooding downstream of Genoa.

February 1982

A one mile long ice jam formed, causing lowland flooding. Stages reached 12.35 ft at the Loup River at Genoa gage.

Other rivers in Nebraska are susceptible to ice jam flooding. The following table shows some major ice jam flooding on other Nebraska rivers. Please note this list contains only major events of the past 50 years.

Table 4-3. Notable Nebraska Ice Jam Flooding

Date	City, River
3/2010	West Point, Elkhorn
3/2009	North Bend, Platte
2/2007	West Point/Waterloo, Elkhorn
3/2001	Ashland, Platte
3/1994	West Point, Elkhorn
3/1993	Ashland, Platte
2/1982	Norfolk, Elkhorn
2/1982	North Bend/Louisville, Platte
3/1978	West Point, Elkhorn
3/1978	North Bend, Platte
3/1978	Fremont/Valley, Platte
3/1971	Ashland, Platte
3/1960	West Point, Elkhorn
3/1960	Grand Island, Platte

4.2 Compilation of Meteorologic Data

Applicable meteorological information near the study area was used. Meteorological data was collected from NOAA’s National Climactic Data Center. Data from the following sites was included:

- Columbus 3NE, NE (POR 1894-2010)
- Genoa 2W, NE (POR 1893-2010)
- St. Paul 4N, NE (POR 1900-2009)
- Madison, NE (POR 1895-1994)
- David City, NE (POR 1897-2010)

Columbus and Genoa were used as primary stations because they are within the study area. Both weather stations are at similar latitude, providing valid data comparison. Columbus and Genoa also have the same number of complete water year observations. St. Paul is a secondary station for this study; St. Paul is south of Genoa and Columbus and St. Paul's period of record extends back only to Water Year 1900. The other two stations were primarily used to extend the other stations' record of missing values.

Temperature, snowfall, snow depth and precipitation were collected for each station. Temperature data provided daily maximum and minimum, although a fair number of data were missing at each station. In order to have a complete period of record with no missing temperature data, multiple regression equations were developed relating each stations high and low temperatures with all possible combinations of the other 4 stations to synthesize missing records in the data, depending on how many stations had a valid temperature measurement on the same date.

One measure of a winter's severity can be computed via accumulated freezing degree days (AFDD). Freezing degree days are calculated using the following equation:

$$FDD = (32 - T_{ave})$$

where: FDD = Freezing Degree Day

T_{ave} = Average Daily Air Temperature, °F

An average daily temperature below freezing produces a positive FDD value, while an average daily temperature above freezing produces a negative FDD value. FDD are cumulatively summed throughout the winter, providing accumulated freezing degree days (AFDD). AFDD has a lower limit of zero. AFDD accumulates with freezing temperatures through the winter once daily average air temperatures consistently stay below freezing. AFDD decreases as warmer temperatures arrive, and eventually reach zero in the spring.

4.2.1 Ice Thickness Computations

Ice thickness measurements, with corresponding AFDD, can be used in the modified Stefan equation (see Section 4.2.4) to estimate historical ice thickness. Ice thickness measurements are intermittently collected by the USGS. The USGS provided ice thickness measurements taken during the last 60 years at the following sites:

- North Loup River at St. Paul, NE
- Middle Loup River at St. Paul, NE
- Loup River at Genoa, NE
- Loup River at Columbus, NE

Thirty ice measurements from these four sites were used in the analysis. Most measurements were taken at Columbus or Genoa. Most measurements were taken during years with high peak AFDD.

4.2.2 Statistical Analysis of AFDD

Statistical analyses were performed on the AFDD data from Genoa, Columbus and St. Paul. The probabilities of reaching different AFDD values were found. The following analyses were performed:

- AFDD Required to Initially Impact Power Canal operations
- AFDD Required to Form Intact Ice Cover in Bypass Reach
- Peak AFDD Histogram
- Peak AFDD Frequency Analysis
- Monthly Change in AFDD Frequency Analysis
 - Processed the change in AFDD during January, February and from February 28/29 to that year's peak AFDD (in years when AFDD peaks March 1 or later)
- AFDD₋₂₁ Frequency Analysis
 - Examined the change in AFDD during the 21 days leading up to peak AFDD (hereafter referred to as AFDD₋₂₁)
- AFDD₊₇ Frequency Analysis
 - Studied the change in AFDD during the 7 days following peak AFDD (hereafter referred to as AFDD₊₇)
- Relationship between peak AFDD and Loup River discharge increases

All statistical analyses are available in Attachment A. Documented ice jams in 1881 and 1848/1849 could not be included in statistical analyses due to a lack of meteorological information.

4.2.3 Temporal Trends in AFDD

AFDD trend analyses were performed to see if AFDD data has changed over time. The following AFDD trend analyses were completed for Genoa, Columbus and St. Paul:

- Peak AFDD Trend Analysis
- Monthly Change in AFDD Trend Analysis
 - Processed monthly AFDD change in January, February and from February 28/29 to that year's peak AFDD over time

- Peak AFDD Averages over Time
 - Analyzed the changes in average during each of the following durations
 - 30 year average
 - 10 year average
 - 5 year average
- AFDD₋₂₁ Trend Analysis
 - Examined the change in AFDD during 21 days leading up to peak AFDD over time
- AFDD₊₇ Trend Analysis
 - Studied the change in AFDD during the 7 days after peak AFDD over time
- Julian Date of AFDD_{max}
 - Studied the change and variability in date of AFDD_{max} over time

Thirty year peak AFDD averages were analyzed for each site. Columbus and Genoa have three completed thirty year periods and the majority of the fourth. For consistency, St. Paul data was analyzed from over the same thirty year periods used for Columbus and Genoa. This ignored years 1900-1923 of the St. Paul record.

All trend analyses are available in Attachment B. Documented ice jams in 1881 and 1848/1849 could not be included in analyses due to a lack of meteorological information.

4.2.4 Estimate Ice Thickness for Historic Ice Jams

Ice growth is inversely proportional to temperature. Ice continues to grow as the atmosphere removes energy from the ice. Ice growth, or ice thickness, can be difficult to predict due to conditions like snow cover, tree and bank shelter and wind pitch. The modified Stefan equation estimates ice thickness with only two easily accessible variables. According to “Engineering and Design: Ice Engineering Manual 1110-2-1612”, the modified Stefan equation makes the following assumptions:

- Ice is a homogeneous, horizon layer
- The ice is growing only at its horizontal interface with the water
- The thermal conditions in the ice are quasi-steady
- The heat flux from the water is negligible
- The heat fluxes are in the vertical direction only

- The heat loss rate from the ice surface to the atmosphere is a linear function of the temperature difference between the ice surface and the air

$$t = C \times \sqrt{AFDD}$$

where: t = ice thickness, in

AFDD = Accumulated Freezing Degree Days, °F

C = Empirical Coefficient

C can be calculated with the modified Stefan equation using measured ice thicknesses and corresponding AFDD. Generalized C values are shown in the table below.

Table 4-4. Typical C Values for modified Stefan Equation

Ice cover condition	C
Windy lake w/o snow	0.8
Average lake w/ snow	0.5-0.7
Average river w/ snow	0.4-0.5
Sheltered small river	0.2-0.4

The modified Stefan equation was then used to calculate ice thicknesses using peak AFDD data. This method gives little weight to snow cover, wind effects and other ice thickness factors. While the modified Stefan equation can provide accurate ice thickness estimates under ideal conditions, other conditions can cause the ice thickness estimates to deviate from the true value.

Ice thickness was measured sporadically by the USGS from 1948-2010. Thirty measurements were used from this time period. Ice thickness computations are shown in Attachment C.

4.2.5 Relationship Between Snow Cover and/or Rain and Ice Jams

Snow depth and snow accumulation data from Columbus and Genoa was analyzed. Snow accumulation refers to the yearly total snow accumulated. Snow depth refers to the measured depth of snow at any time during the year. A frequency analysis of yearly snow accumulation was performed. During snow depth analysis, Genoa data was used when Columbus data was not reported and vice versa. Snow depth measurements were consistently recorded from the 1970 to present. Earlier years have sporadic snow depth measurements that are not useful in snow depth analysis.

To analyze the temporal relationship of snow cover and temperatures, daily mean temperatures were plotted with snow depths. This plot shows cold periods and corresponding snow depths during those periods. If the ice has a deep snow cover

through the coldest parts of winter, the ice will not likely be as thick and strong as the ice cover from a cold, snowless winter.

Snow accumulations during AFDD₋₂₁ and AFDD₊₇ periods were studied, searching for a relationship between snow accumulation near the peak AFDD. Only years with documented ice jams were analyzed.

Documented flood years will be evaluated to see if any rainstorms were present near breakup and if those storms affected ice jamming.

4.3 HEC-RAS Modeling

An HEC-RAS model was constructed to model flow conditions on the Loup River under ice-affected conditions utilizing surveyed cross-sections, an existing hydraulic model and a digital elevation model (DEM) representing ground elevations outside the main channel. 110 georeferenced cross-sections were surveyed between bank lines from just downstream of the Loup Power Canal Headworks to just upstream of the Union Pacific Railroad Bridge west of Columbus. These surveyed cross-sections were combined with an existing hydraulic model extending from approximately one mile downstream of the Platte-Loup confluence to upstream of the Union Pacific Railroad Bridge west of Columbus. These georeferenced cross-sections were overlain on a DEM and extended in ArcGIS to include potential overbank flow areas. HEC-GeoRAS was used to cut new cross-sections based on these extended cross-sections, and then the previous hydraulic model cross-sections were merged with the newly cut cross-sections to create a new geometry.

The model geometry was then calibrated to match the latest rating curve at the Genoa gage with flows up to 3,000 cfs, in order to obtain an “n” value for the channel. Higher flows were then used to calibrate the overbank “n” values to the Genoa gage rating curve. The calibrated model was then used to verify hydraulic parameters from the Sediment Transport study for open water conditions under the assumption of both Effective and Dominant Discharge for the current operating plan and assuming no flow diversion took place.

4.3.1 Ice Formation and Freezeup Jam Formation

A new geometry was created for each flow condition and ice information, listed below, was entered in each HEC-RAS cross section using the ice cover table feature. Ice was incorporated into the channels and not the overbanks. Flows modeled included the 10-, 25-, 50-, 75-, and 90% by duration flows for the months of November, December, and January (typical months for ice cover to form).

- Open water velocity < 1 ft/s; ice n = 0.008; ice thickness = 0.333 ft
- Open water velocity 1 - 2.25 ft/s; ice n = 0.01; ice thickness = 0.333 ft
- Open water velocity 2.25 – 5 ft/s; ice n = 0.015; ice thickness = 0.5ft (50% increase)

- Open water velocity > 5 ft/s; ice not included

The geometry was rerun with ice. Velocities were again evaluated at each cross section. At cross sections where velocities were >5 ft/s, ice was removed. Where velocities were <5 ft/s, ice was added. The geometries were rerun again and velocities were evaluated.

For a few cross sections, velocity results would jump above and below the 5 ft/s mark depending on the addition/removal of ice. These cross sections were assigned no ice cover with the assumption that ice may form but cause an increase in velocity. This increase will dissipate any accumulated ice.

Once the ice characteristics were determined, the resulting ice thickness, roughness and cumulative volume were noted for each cross section. This process was repeated for an ice thickness increased by 50%.

Ice jam locations were identified using the ice jam feature in RAS. The ice cover geometry was adjusted to allow jamming at all cross sections and was run with the 10% December flow. Ice thicknesses generated at each jam were noted and ice roughness values were determined for frazil freeze up jams. The ice jam thicknesses were made permanent (jam thicknesses were not recalculated) and the new frazil ice roughness was copied into the ice cover table and was made fixed values. The model was rerun.

The ice jam and ice cover plans were compared and locations of the largest and most likely jams were identified based on available channel flow area, ice thickness, profile increase, change in channel geometry and constrictions and bends in the river.

4.3.2 Ice Breakup and Breakup Jam Formation

In order to compute ice breakup jam accurately, the volume of ice available for a jam must be known. In order to estimate the volume of ice available, the HEC-RAS model was used to compute the volume of ice at a range of flows typical of the pre-breakup period (10-, 25-, 50-, 75-, and 90% flows by duration for February, since most jams occur in either February or early March). A new geometry was created for each February flow condition, and ice information was entered in each RAS cross section using the ice cover table feature. A floating ice cover of 13-inches and 19.5-inches was modeled for each of the February flow durations. These ice thicknesses were chosen based on average AFDD and 1-standard deviation above average AFDD coupled with average “C” coefficient from the modified Stefan equation. Ice was incorporated into the channels, and not the overbanks, for each cross section. Default ice table values were used, and RAS calculated the ice roughness values. Ice volumes for the model reach were compared for each flow. Since the volumes did not differ significantly, only the 50% flow ice volumes were used for computation of the breakup ice jam.

New geometries were created to model the break up jams for each of the two ice cover thicknesses and for the flood frequency events, tabulated as follows:

<u>Event</u>	<u>Current Operations</u>	<u>No Flow Diversion</u>
50-Year	41,700 cfs	42,400 cfs
20-Year	28,500 cfs	30,700 cfs
10-Year	20,800 cfs	23,600 cfs
5-Year	14,600 cfs	17,600 cfs
2-Year	8,000 cfs	10,700 cfs

An initial ice thickness was entered in the ice cover table at cross sections where jams are likely to form and sustain, as identified in previous modeling of ice jams from freeze-in ice. At four identified locations, ice jams did not properly form. The jam locations of concern were shifted upstream or downstream by one cross section which yielded a better fitting jam shape and size. These newly identified cross sections were used as the starting location of the jam. The extent of the jam to the upstream cross section was determined based on available ice from the analysis above; the volume was reduced by half to account for broken ice pieces that are pushed and lost onto the overbanks and for ice that melts during transport.

4.4 DynaRICE Modeling

The transport of ice floes is beyond the capability of a one-dimensional model such as HEC-RAS. However, the two-dimensional DynaRICE ice-hydraulic numerical model has been successfully used to simulate ice transport through various channels and hydraulic structures as well as ice jam initiation. The main objective of the dynamic ice modeling is to detect differences in ice formation and ice jamming processes with and without diversions into the power canal owing to significant geometry changes due to differences in sediment transport processes, should they exist. Details of the DynaRICE modeling methodology are presented in Attachment E.

5. RESULTS AND DISCUSSION

Results of the analysis presented in the previous section are described below.

5.1 History of Flooding

The following table shows the number of documented significant floods during the period of record. The period from 1848-1893 does not have the necessary meteorological information for statistical analysis. The statistical analyses used the period of 1893-1936 as the period of record before the beginning of District operations.

Table 5-1. Documented Significant Ice Jam Floods Before and After 1937

	Documented Ice Jam Floods	Documented Runoff Floods
1848-1936 (88 years) ¹	7	3
1893-1936 (43 years) ²	5	3
1937-2010 (73 years)	5	3

Notes:

- ¹ Inconsistent record before late 1800’s. More undocumented events may have occurred between 1848 and late 1800’s.
- ² 1893-1936 was used as period of record before construction of Canal.

Both periods had years with high peak AFDD and other factors contributing to ice jams. But since the beginning of the District’s operations, the probability of a significant ice jam appears to have remained the same or even decreased. This decreased probability of ice jams cannot be credited to the District’s operations, but it does discount the idea the District’s operations have increased the frequency of documented ice jam floods.

It is notable that in every year that a significant ice jam has occurred on the Loup River since the commencement of District operations, that significant ice jams have occurred on other Nebraska Rivers of similar characteristics, such as the Platte and/or Elkhorn River. This tends to support the occurrence of ice jams as a natural process that occurs fairly predictably, given the right set of ice and meteorologic conditions preceding the ice event, irrespective of District operations.

This review of flood history and frequency of occurrence does not conclusively prove, or disprove, a connection between District operations and ice jam occurrence or severity. It is possible that the perception level of locals has changed over time; that is to say, an ice jam flood occurrence may not be considered notable by locals until the flooding reaches a certain threshold, and that threshold may differ among individuals and by location and may vary over time. The perception level also tends to increase following a significant flood event, and tends to increase with increased awareness of a problem.

Floodplain development may contribute to the severity of an individual ice jam flood; for instance, the 1993 flood event at Columbus may have been significantly higher due to the placement of the Whitetail residential development on the right overbank of the Loup as well as an increased height in the Highway 81 roadway perpendicular to flow on the right overbank. However, it is sometimes easy to overlook local floodplain development, over which a local community may be able to exert some influence, and seek to place blame on other factors, which may be beyond the local community’s influence. It is also possible that the construction of local flood

protection measures may protect communities and/or individuals from flooding that may have been considered significant previously, but is no longer considered significant due to the flood protection measures now in place. Other information, such as USGS gage records, do not predate District operations, so it is very difficult to assess if District operations contribute to increasing (or decreasing) the severity of a particular jam.

5.2 Analysis of Meteorologic Data

5.2.1 Ice Thickness Computations

Ice thickness calculations using the modified Stefan equation are based on an empirical coefficient, C , and the AFDD. C is found using previous ice measurements in the modified Stefan's equation and back-calculating to find a C value. This study used available ice thickness and AFDD data to back-calculate C . Most calculated C values ranged from 0.4-0.7, with an average of 0.56. The calculated C values were reasonable when compared to standard values and known values for similar rivers in the region.

5.2.2 Statistical Analysis of AFDD

Analysis of the USGS stream gage stations for the Loup Power Canal and at Genoa gages were correlated with the onset of FDD and evaluated to determine the average AFDD upon which Canal operations had to be adjusted, allowing significantly more water to flow through the bypass reach. On average, an AFDD value of 11 was reached before significant flows were bypassed (i.e. flows into the Canal were typically less than a few hundred cfs for a day or more). This does not take into account short periods when flows may be bypassed for a few hours during a cold night prior to AFDD accumulating, but these short duration events have very little impact on the total volume of water passed into the bypass reach on a daily basis, and the volume of ice associated with such bypass flows is rather small compared to the ice production potential of the entire bypass reach. It is likely that, prior to significant flow diversion through the bypass reach, that some shore ice starts to form in various reaches of the bypass reach; as the flows in the bypass reach increase, this shore ice is lifted and broken from shore, contributing a greater volume of ice in the bypass reach than would be expected if there had been a steady flow of water through the bypass reach. However, this volume of shore ice is a rather small component of the total ice volume and should not contribute materially to increased stages or freezeup jams in the reach. The annual AFDD required before Canal operations are altered to allow significant flow in the bypass channel are presented in Attachment A.

Likewise, the flow records at the Loup Power Canal and at Genoa gages were examined to determine when Canal operations allowed a significant increase in flow back into the Canal, indicating a stable ice cover had formed in the bypass reach (or most of it) and especially upstream of the Canal, and these dates were correlated to

AFDD. On average, the AFDD required to produce a stable ice cover in which frazil ice was no longer present at the Headworks was 108. This is a typical value for many streams at which to form a stable ice cover, with little or no further frazil ice production. It was noted in a number of years that weather conditions were such that the initial ice cover apparently either partially broke up or substantially melted, causing a new round of flows passing down the bypass reach, indicating further ice movement from upstream. However, in such cases, only the initial freezeup of the river was considered, since movement of the ice upstream of the Headworks could in no way be attributed to the operation of the Canal. The AFDD required for Canal operations to resume normal, or at least winter, operations are presented in Attachment A.

Statistical analysis of the peak AFDD was compared to the documented history of Loup River ice jam floods. Most ice jam flooding occurs when AFDD exceed 1,000. 1,000 AFDD has a 20% chance of exceedance in any year. 70% of the documented **significant** ice jam floods **since 1905** corresponded to above 1,000 AFDD at Genoa; however, ice jams have also occurred in years with average AFDD. The Flood of 1907 inundated much of southern Columbus and caused four fatalities. This devastating ice jam formed after a winter with near average AFDD. Similar trends were seen at Columbus and St. Paul. A table showing yearly peak AFDD for all three sites is in Attachment C. Statistical analysis of peak AFDD is available in Attachment A.

Revised 03/08/11

A limited correlation can be drawn between ice jam flooding and high AFDD. Years with high AFDD totals have an increased chance, but not certainty, of ice jam flooding. Ice jams normally do not form with average to below average AFDD, but large floods have occurred in years with near average AFDD.

Since the District's operations began, no available data shows any relationship between ice jams forming with lower AFDD.

Statistical analysis of the AFDD_{.21} was compared to the documented history of the Loup River ice jam floods. **60%** of the documented **significant** floods **since 1905** had AFDD_{.21} above the 50% chance of exceedance in any year. At Genoa, there were **only two** occurrences, **1918 and 1893**, with high AFDD and above 50 % probability AFDD_{.21} where no flooding was documented. Similar results were seen at St. Paul and Columbus. While it appears larger AFDD_{.21} influence ice jam flooding, no direct correlation between ice jam flooding and AFDD_{.21} can be drawn. No data shows changes in flood frequency correlated to AFDD_{.21} since 1937. No trends between the District's operations and floods correlated to AFDD_{.21} can be made. Statistical analysis of AFDD_{.21} is shown in Attachment A.

Revised 03/08/11

Statistical analysis of the AFDD₊₇ post peak AFDD seven day change was compared to the documented history of the Loup River ice jam floods in the study area. 70% of the documented floods had an AFDD₊₇ above the 50% chance of exceedance in any

year. However, half the years with above 1000 peak AFDD and above average AFDD₊₇ experienced no flooding.

The AFDD₊₇ has some correlation to ice jam flooding, but a direct correlation between ice jam flooding and AFDD₊₇ cannot be made. No correlation between the effects of AFDD₊₇ and District operations can be made. Statistical analyses of the AFDD₊₇ are shown in Attachment A.

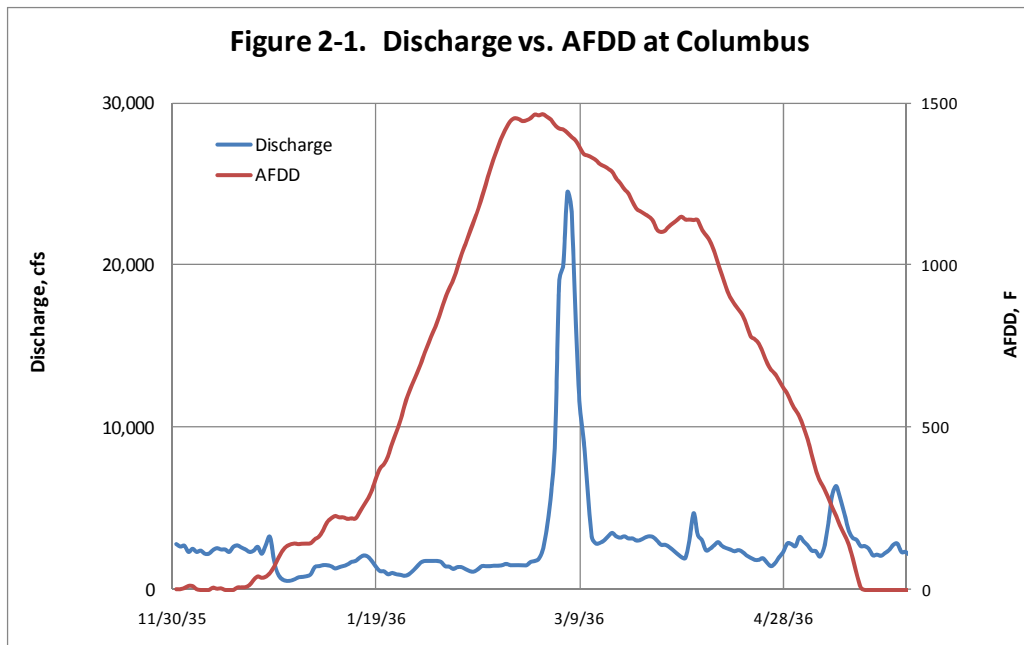
Years with high AFDD and above 50% probability AFDD₋₂₁ and AFDD₊₇ were also analyzed. Of the seven years where all three of the events occurred at Genoa, **significant** ice jams were documented in **1905, 1910, 1912, and 1936**. 1893, 1960 and 1965 exceeded all three criteria, but no ice jam flooding was documented. Similar results were seen at St. Paul and Columbus. This specific analysis included years with peak AFDD values above 1,000.

Revised 03/08/11

Statistical analysis of monthly change in AFDD was prepared for all three sites. All **significant ice jam** flood years showed above average accumulation of AFDD, **with one exception**. But no other trends were found between ice jam flooding and general monthly accumulation of AFDD. All statistical analyses are available in Attachment A.

Revised 03/08/11

There is a strong correlation between a peak in AFDD and Loup River discharge. Plotting discharges and AFDD at Genoa or Columbus shows increases in discharge as AFDD decline from a peak, which is to be expected. An example of this is shown in the figure below.



cover will often cause a large peak in discharge after AFDD peak, even though an ice jam may or may not occur.

Temperature, snow depth, snow accumulation and other data sets are available digitally in a .dss file format upon request.

5.2.3 Temporal Trends in AFDD

Trend analyses were performed on peak AFDD at all three sites, comparing all data sets to the period of record. AFDD in any year is random. A low AFDD year may be followed by a year with an exceptionally high AFDD. None of the data sets showed an obvious trend over time when taken in aggregate. Regression analysis showed a decrease in peak AFDD during the period of record, indicating a slight increase in overall temperatures. But the R^2 correlation coefficients associated with these trend lines were low, between 0.015-0.03. The current trend line may show decreasing peak AFDD, but the low R^2 values prove this trend is not a reliable indicator for future peak AFDD values. All trend analyses are found in Attachment B.

Thirty year peak AFDD averages were analyzed for each site. At each location, the thirty year average changed based on the meteorological cycles occurring during the thirty year period. All three sites had a period of high peak AFDD average followed by a period of lower peak AFDD average. The peak AFDD 30 year averages are shown in the table below. This trend of a moving average is likely to continue as meteorological cycles continue into the future. Based on past data and the length of our current cycle, these sites are likely approaching a period of higher peak AFDD within the next ten years. A plot of the 5, 10 and 30 year AFDD averages at Columbus is shown in the following figure:

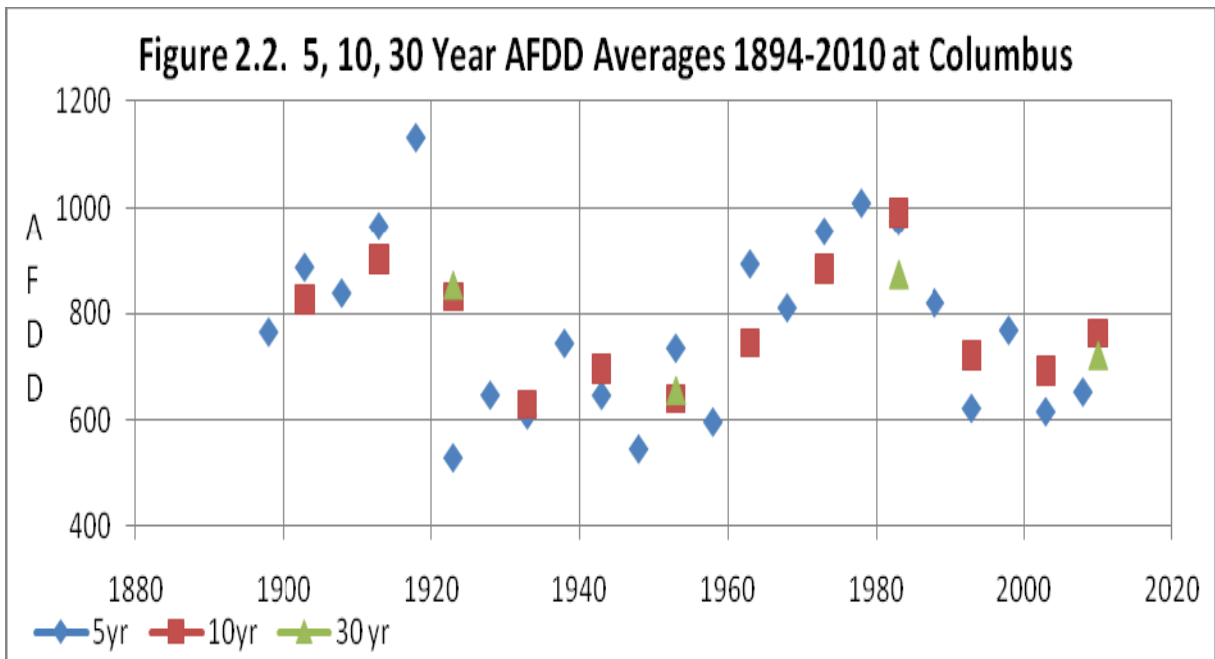


Table 5-2. Peak AFDD 30-Year Average

	Genoa	Columbus	St. Paul
1894 – 1923	822	853	-
1924 – 1953	656	<u>655</u>	614
1954 – 1983	831	872	809
1984 – 2010	<u>636</u>	721	<u>600</u>

Notes:

No St. Paul data available before 1900. Calculated 1st 30 yr. average beginning in 1924.

The 1984-2010 average does not contain a full 30 year record.

The highest peak AFDD 30 yr. average is bolded and the lowest peak AFDD 30 yr. average is underlined

The preceding table shows the thirty year AFDD average at each site. The analysis of five and ten year peak AFDD averages showed a trend of twenty-five to thirty-five year up and down cycles of AFDD. The ten and five year averages show more detail than the thirty year average, but the cyclical trend is the same for all three averages. This cyclic trend was especially visible in the Columbus and Genoa data sets. The St. Paul data set showed the cyclic trends, but not as visibly as the others. St. Paul is at lower latitude than Columbus and Genoa, which may explain St. Paul's slight variation from the cyclic trend. The five, ten and thirty year averages for all three sites are shown in Attachment B.

Of the ten documented significant ice jam floods in the study area, 4 ice jam floods occurred during the high AFDD cycle of the 1890's-1920's. These floods occurred before the construction of the Loup Power Canal. During the second high AFDD 30 cycle from the 1950's-1980's, 3 ice jam floods occurred. These floods occurred after the construction of the Loup Power Canal. Although changes have been made to the Loup River and its operations since 1937, the frequency of documented ice jam floods did not increase. It does appear, however, that the frequency of ice jam flooding may be influenced by cyclic changes in climate. Since these cyclic changes are multi-decadal and for the most part genteel, with episodic exceptions, there may be a perception that other factors (i.e. the Loup Power District Canal) are to blame for a particular ice jam.

Trend analyses were produced for AFDD monthly changes. These analyses did not confirm an obvious trend over time. Monthly change trend lines provided little evidence of any trends. A site may have one monthly change that shows a slight AFDD change increase, while another month for the same site may show a slight decrease. These correlation coefficient R^2 values do not support any trends. R^2 values for the monthly change analyses range from 0.03 to less than 0.001. The

unpredictability of AFDD monthly changes is evidence that no trends in AFDD monthly changes.

Another trend analyzed was the date of the maximum AFDD. Generally, the date of maximum AFDD is a good precursor to determining when the river ice will begin to breakup, although in some years, most noticeably 1993, the breakup occurs prior to the maximum AFDD being achieved. In order to compare the date, the Julian date (J.D.) of the water year (starting on October 1) of the maximum AFDD was computed for each year. A plot of the data shows a trend towards the AFDD maximum value being reached on an earlier date; however, the correlation coefficient R^2 values were very small, indicating no significant trend. When the AFDD_{max} and Julian Date values are averaged by decade, the trends in average AFDD and Julian Date of AFDD_{max} show the same general cyclical trends; however, the standard deviations of the values do not. The standard deviation of the AFDD_{max} does not deviate significantly with time, as should be expected, but the standard deviation of the Julian Date shows a pronounced increase during the 1990s and to a lesser extent during the 2000s, as shown in the following table. The cause of this pronounced variability in the Julian Date of AFDD_{max} is not readily apparent; however, it may indicate a more variable weather pattern with more sustained warming periods, generally occurring earlier, during the course of winter in the last twenty years. All trend analyses are shown in Attachment B.

Table 5-3. Trends in AFDD_{max} and Julian Date by Decade

Decade	Genoa				Columbus				St. Paul			
	Ave. J.D. of AFDD _{max}	St. Dev. of J.D. of AFDD _{max}	Ave. AFDD	St. Dev. of AFDD	Ave. J.D. of AFDD _{max}	St. Dev. of J.D. of AFDD _{max}	Ave. AFDD	St. Dev. of AFDD	Ave. J.D. of AFDD _{max}	St. Dev. of J.D. of AFDD _{max}	Ave. AFDD	St. Dev. of AFDD
1890s	164	14.3	929	268	161	13.2	842	365	n/a	n/a	n/a	n/a
1900s	146	11.9	793	308	146	11.7	841	336	146	11.9	634	284
1910s	157	14.3	875	389	158	11.5	987	412	157	14.3	803	331
1920s	138	16.8	624	229	141	15.7	647	237	136	24.1	649	264
1930s	144	16.6	668	436	143	16.0	641	418	138	21.6	626	393
1940s	163	12.2	643	267	153	19.7	648	251	157	17.1	573	264
1950s	151	18.0	682	250	147	17.1	662	248	141	21.0	671	252
1960s	153	14.6	816	279	154	13.8	863	266	154	14.5	824	273
1970s	147	14.9	967	398	147	14.1	1036	400	146	14.6	988	425
1980s	141	14.5	704	329	142	15.6	759	329	142	15.6	759	329
1990s	136	32.9	597	329	136	37.8	652	317	134	38.0	638	338
2000s	141	22.0	628	313	149	15.5	766	335	139	23.6	539	261

Trend analyses were performed for the AFDD₋₂₁ and the AFDD₊₇ day change. Conflicting trends occurred at the different sites. No obvious trends are visible. Trend lines showed a slight decrease in the AFDD₋₂₁ at all three locations, but the trend line's R² correlation coefficients were insignificant. This slight decrease may be tied to, or be indicative of, the increased variability in when the AFDD_{max} is occurring. However, it does not reinforce the presence of a trend. All trend analyses are shown in Attachment B. Temperature, snow depth, snow accumulation and other data sets are available digitally in a .dss file format upon request.

5.2.4 Estimation of Ice Thickness for Historic Ice Jams

Ice thickness calculations using the modified Stefan equation are based on an empirical coefficient, C, and the AFDD. C is found using previous ice measurements in Stefan's equation and back-calculating to find a C value. This study used available ice thickness and AFDD data to back-calculate C. Most calculated C values ranged from 0.4-0.7, with an average of 0.52. The calculated C values were reasonable when compared to standard values and known values for similar rivers in the region.

The possibility of unaccounted conditions affecting ice thickness estimates warranted the calculation of a range of thicknesses. Ice thicknesses were calculated using C values of 0.4 and 0.6. The estimated ice thicknesses for the documented ice jams are shown in the following table.

Table 5-4. Computed Range of Ice Thickness in Ice Jam Years

Documented Ice Jam Floods	Ice Thickness, inches (C = 0.4)	Ice Thickness, inches (C=0.6)
1905	14.5	21.6
1907	10.9	16.4
1910	13.7	20.5
1911	15.0	22.5
1936	15.6	23.4
1948	11.6	17.3
1960	13.6	20.4
1969	13.9	20.8
1971	11.6	17.4
1993	13.2	19.8 ¹

Note:

¹ Estimated ice thicknesses on 08 March 1993 were near 12", approximately 1 week after peak AFDD

Ice thickness is a factor in ice jam floods, but there are many instances where thick ice did not cause documented ice jam flooding. There have been twenty instances where +18” ice thicknesses were estimated, but no documented ice jam flooding occurred. No changes to ice thickness were estimated since the beginning of the District’s operations. Unfortunately, there are no ice thickness measurements prior to 1937, other than estimation from a photo of the 1905 ice jam. Without these pre-1937 thickness measurements, the District’s operations affects, if any, on Loup River ice thickness cannot be determined using these methods. Ice thickness estimates and measurements are both listed in Attachment C.

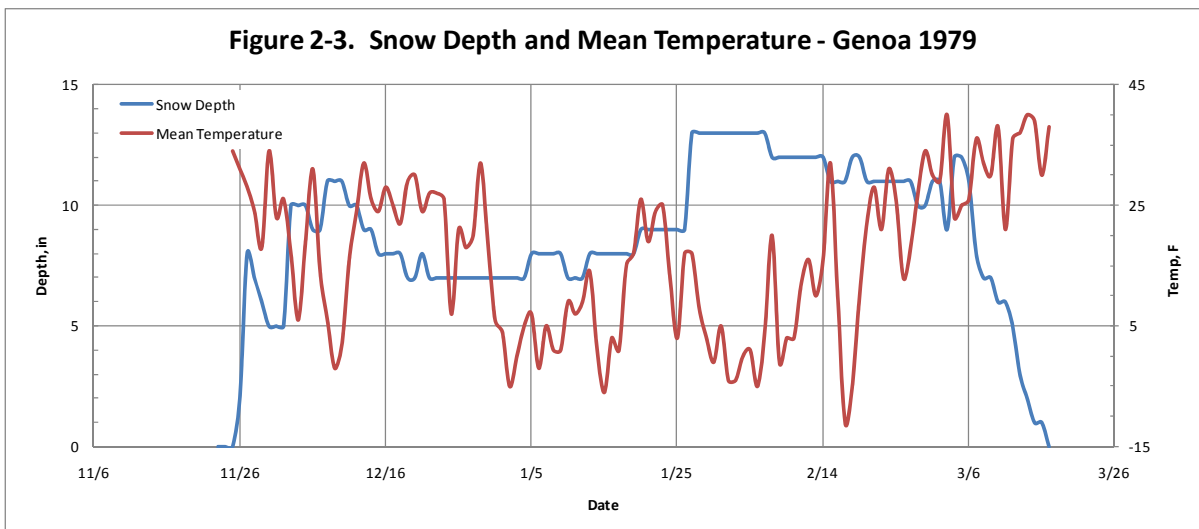
5.2.5 Relationship Between Snow Cover and/or Rain and Ice Jams

Ice jam flooding appears to occur on years with above 50% probability snow accumulations. Of the ten documented **significant** ice jam floods **since 1905**, eight occurred in years with above a 50% probability snow accumulation. Six of the ten documented ice jam floods occurred in years with above a 20% probability snow accumulation.

The plots of snow depth and mean temperatures provided a clear view of when cold weather occurred and if snow cover was present. Frigid temperatures can thicken and strengthen the ice, but if sufficient snow cover is present, even the coldest temperatures will only marginally affect the ice.

Examples of ice insulation are evident in 2010 and 1979. Both years had extremely cold temperatures through much of the winter. But a thick snow cover was present during the sub zero temperatures, and both years failed to produce extensive ice jam flooding in the study area. See below the plot of the 1979 snow depth and average daily temperature at Genoa.

Revised 03/08/11



A larger version of Figure 2-3 and a plot of the 2010 snow depth and mean temperature at Columbus are shown in Attachment D.

Examples correlating cold temperatures and no snow cover to ice jams were not found. Consistent snow depth data before the 1950's was not available; hence a similar analysis could not be performed for earlier ice jams.

Snow generally accumulates during the 21 day period prior to peak AFDD. 80% of **the** documented ice jams **since 1905** had snow accumulation during the 21 day period prior to peak AFDD. 50% of the documented ice jams saw accumulations above 4" of snow during the 21 day period prior to peak AFDD. Although snowfall during the 21 day period before peak AFDD may be a factor in ice jam flooding, this snowfall is not the major cause.

Revised 03/08/11

Rainfall was **noted** during only the 1941 and 1971 ice jam floods. According to accounts in the Nance County Journal, the 1941 ice jam flooding was intensified by a 1" rainfall runoff. Most of the damage from this ice jam was in Fullerton, NE, upstream of the study area. Over 1.5" of rain fell as an ice jam formed at Genoa. The ice jam grew to five miles long and caused flooding from at least February 24th through March 6th. With only two **noted** rainfall events affecting ice jam flooding, a clear relationship between ice jams and rainfall cannot be made. However, it is widely accepted that rainfall-runoff events occurring concurrently with river ice breakup leads to an increased risk of damaging ice jams forming.

Revised 03/08/11

Revised 03/08/11

5.3 HEC-RAS Modeling Results


5.3.1 Ice Production and Freezeup Jams

Nine jam locations within the reach were identified. Jams were allowed to form specifically at these locations. There were several potential locations for jams; however the available ice to form the jams was limited based on the ice thicknesses for the 4" floating ice cover plan. Therefore, jam proximity was considered when identifying locations. Once jam locations were selected, the size of the jam was adjusted so the jam's ice volume was between 100% and 125% of the available floating ice between jam locations as computed in the ice cover plan. If ice volume in a jam was >125%, thicknesses at the upstream end of the jam were manually reduced. The 9 jam locations are shown graphically in Figure 12-4. As expected, the no-diversion alternative produced higher stages due to the greater flow in the bypass reach. This does not mean that Canal operations reduce the risk of flooding, but it does not appear that Canal operations have the detrimental effect that some have postulated. Perhaps somewhat surprisingly, there was no difference between no-diversion and diversion flows in producing stretches of river where velocities are too great to sustain a stable ice cover (except via upstream progression of a downstream ice cover increasing dynamically from upstream ice transport). These areas are shown graphically in Figure 12-5. This indicates that regardless of Canal operation, there are certain reaches of river that can, in the right circumstances, produce significant volumes of frazil ice, which would materially impact the potential for ice jams to occur.

Figure 12-4. Ice Jam Locations Due to Frazil Ice



Legend

 Frazil Ice Jam Locations

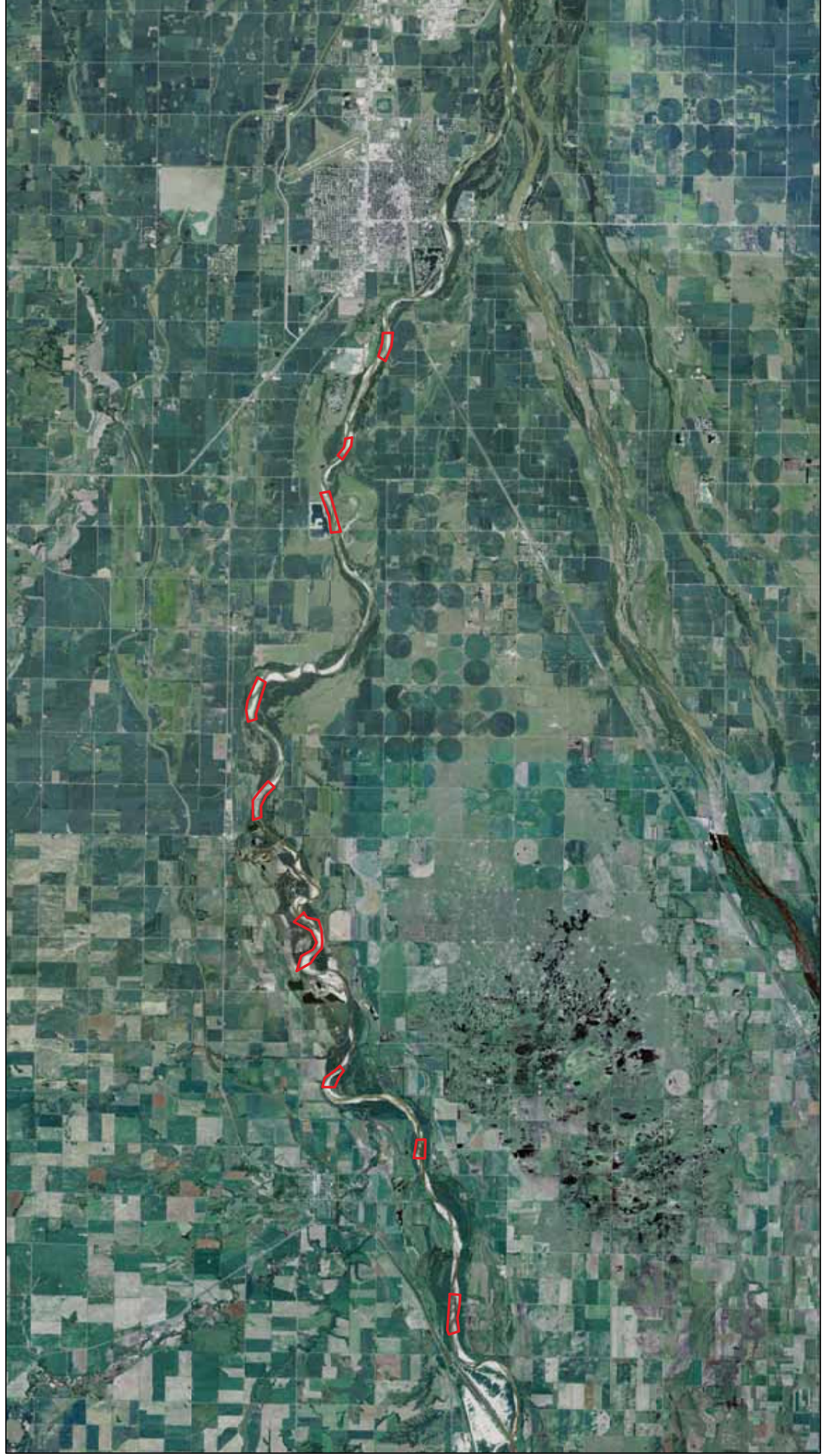
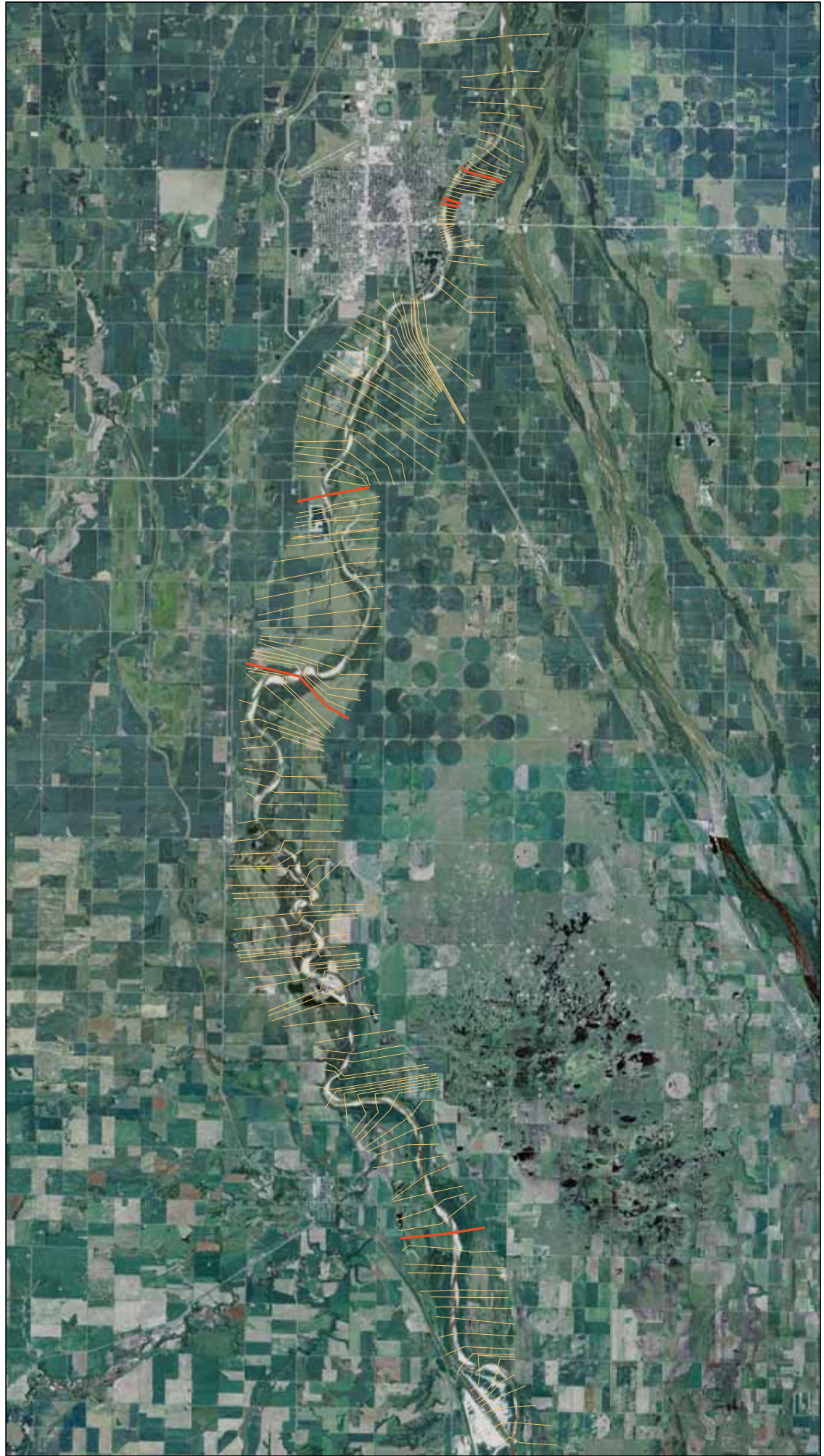


Figure 12-5. High Velocity Locations with Frazil Ice Cover



Legend

— High Velocity (>5 fps)



5.3.2 Ice Breakup and Breakup Jam Formation


RAS calculated the thickness of the jam and corresponding ice roughness value, and default ice values were used. The extent of each jam was adjusted until the approximate target volume of available ice was achieved. In general, ice jam volumes ranged from 40-60% of available ice, while the target volume was 50%. In those instances where the volume fell outside that range, a smaller jam was allowed to form and floating ice cover was used for upstream cross sections to achieve a volume within the target range. The eight likely breakup jam locations used in this analysis, with respect to the RAS model, are shown on Figure 12-6. As expected, the no-diversion alternative produces higher stages due to the greater flow and increased volume of ice in the bypass reach. It should be noted that the HEC-RAS model does not self-predict an ice jam downstream of the Highway 81 bridge **(without significant thickening of the downstream ice cover)**, as occurred in 1969 and 1993, although other ice jam locations in the HEC-RAS model seem to correlate with historical accounts of various ice jams. Rather, this location would have to be manually input to model an ice jam at this location. This location was modeled in previous reports (USACE, April 1996) with HEC-2 and ICETHK; however, the jam location was manually input in that report as well. Since this location has previously been modeled with the same geometry, it was not modeled for this report.

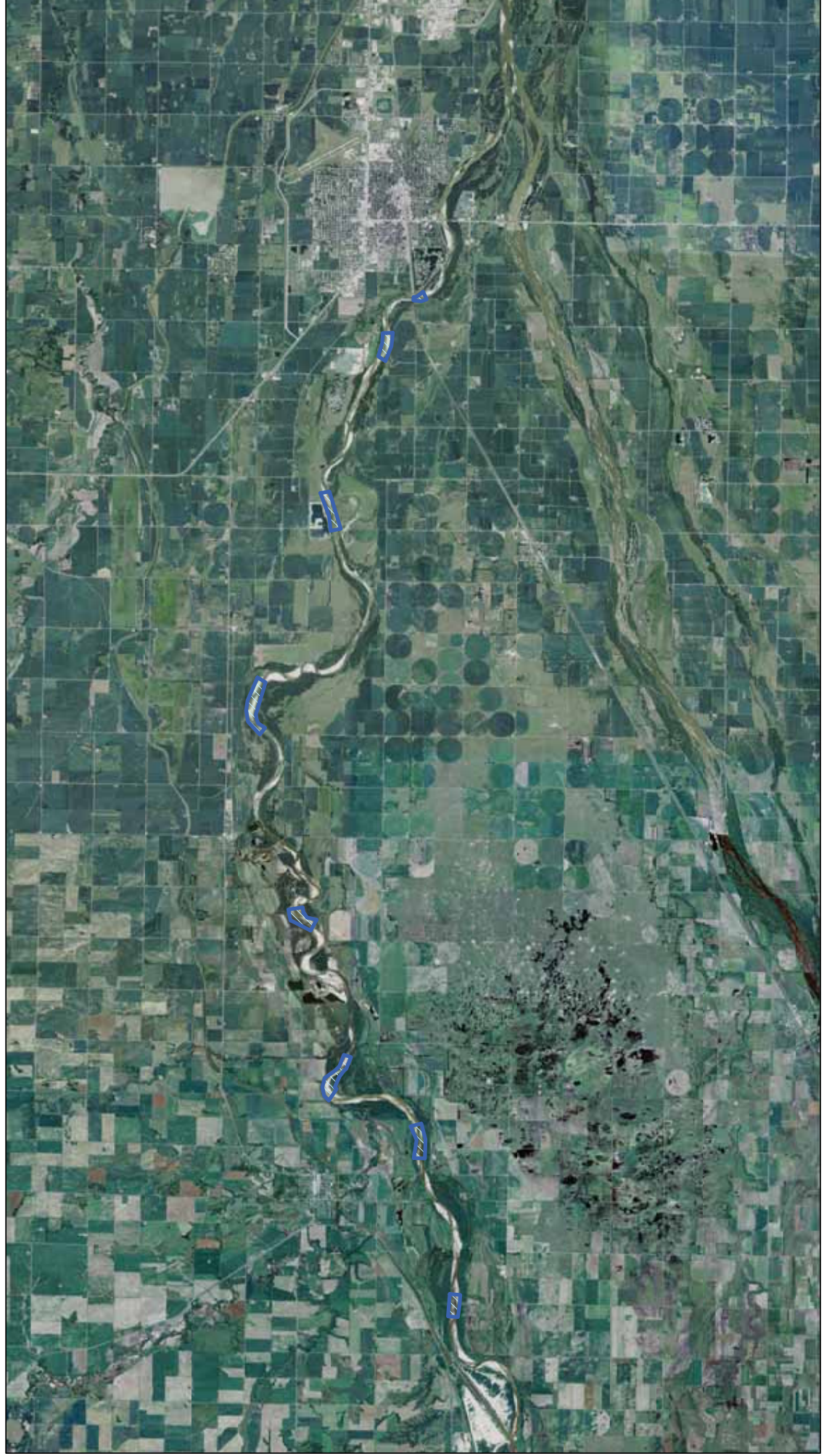
Revised 03/08/11

Figure 12-6. Ice Jam Locations Due to Break-up Ice



Legend

 Break-up Ice Jam Locations



5.4 DynaRICE Modeling Results

Results of the DynaRICE modeling efforts are presented in Attachment E.

5.5 Summary and Conclusions

A review of flood history shows that the occurrence of significant ice jam flooding has not increased since the Loup Power Canal commenced operations. A lack of historical data precludes a similar comparison of minor ice-affected flooding; however, a thorough review of climatological data and use of hydraulic models does not show a difference in the occurrence of minor ice-affected flooding due to operation of the Power Canal. Other factors, such as climatic variability and floodplain developments may lead to an increased flood risk during an ice jam; however, as these factors are often subtle over time, they may be overlooked as a cause of increased flood risk. It is the opinion of the authors that the Loup Power Canal has not significantly changed the ice regime of the Loup River between the Headworks and its confluence with the Platte, nor has it increased the risk of significant ice jam flooding.

6. STUDY VARIANCE

The Study Plan Determination specified that the DynaRICE modeling effort would only be required “in those locations where significant geometry changes due to differences in sediment transport can be demonstrated under the no diversion or alternative operating condition.” Owing to delays in obtaining various other study components and delays in obtaining cross-section data for the HEC-RAS model due to high water on the Loup River, it was decided to initiate the DynaRICE modeling effort prior to a determination of whether there were significant geometry changes due to differences in sediment transport. This was done to allow initial DynaRICE efforts to begin, so that if a difference in sediment transport were demonstrated, the DynaRICE modeling effort would not delay production of this report. Once it was conclusively determined that there were no significant geometry changes due to sediment transport, no further DynaRICE modeling was performed. However, the results of the study to-date are presented as Attachment E of this report.

7. REFERENCES

Andreas, A.T. (1882). “History of the State of Nebraska.” Chicago, Illinois: The Western Historical Company.

Nance County Journal, “On a rampage. the cedar river on a big high lonesome.” (1904, May 26).

Nance County Journal, “Five times has rivers flooded valleys.” (1923, June 21).

Nance County Journal, “Ice, rain cause cedar to flood; damage is done.” (1941, February 20)

- Nance County Journal*, “Roadbed washed by floodwaters.” (1936, March 12)
- NDNR. *Listing of Nebraska Ice Report Sites*. Retrieved on March 17, 2009.
<http://dnrdata.dnr.ne.gov/Icejam/listing.asp>.
- NDNR. February 9, 2009. Letter from Brian P. Dunnigan, Director, to Kimberly D. Bose, Secretary, Federal Energy Regulatory Commission, regarding a study request.
- NDNR. June 25, 2009. Letter from Jean E. Angell, Legal Counsel, NDNR, to Neal Suess, President/CEO, Loup Power District, regarding comments on the District’s Proposed Study Plan.
- USACE, 1967. *Detailed project report, Loup River at Columbus, Ne*. Omaha, NE: USACE, Omaha District.
- USACE, July 1994. “Lower Platte River Ice Jam Flooding.” U.S. Army Corps of Engineers, Omaha District.
- USACE, January 1996. “Ice Jam Flooding and Mitigation: Lower Platte River Basin, Nebraska, Special Report 96-1.” U.S. Army Corps of Engineers, Cold Regions Research and Engineering Laboratory, Hanover, NH.
- USACE, April 1996. “Lower Platte River and Tributaries, Nebraska.” U.S. Army Corps of Engineers, Omaha District.
- USACE, 2002. “EM 1110-2-1612 - Engineering and Design Ice Engineering.” U.S. Army Corps of Engineers, Washington, D.C.
- USACE, 2010. Cold Regions Research and Engineering Laboratory *Ice jam database* Hanover, NH: Retrieved from <https://rsgis.crrel.usace.army.mil/icejam/>

ATTACHMENT A

STATISTICAL ANALYSIS OF AFDD

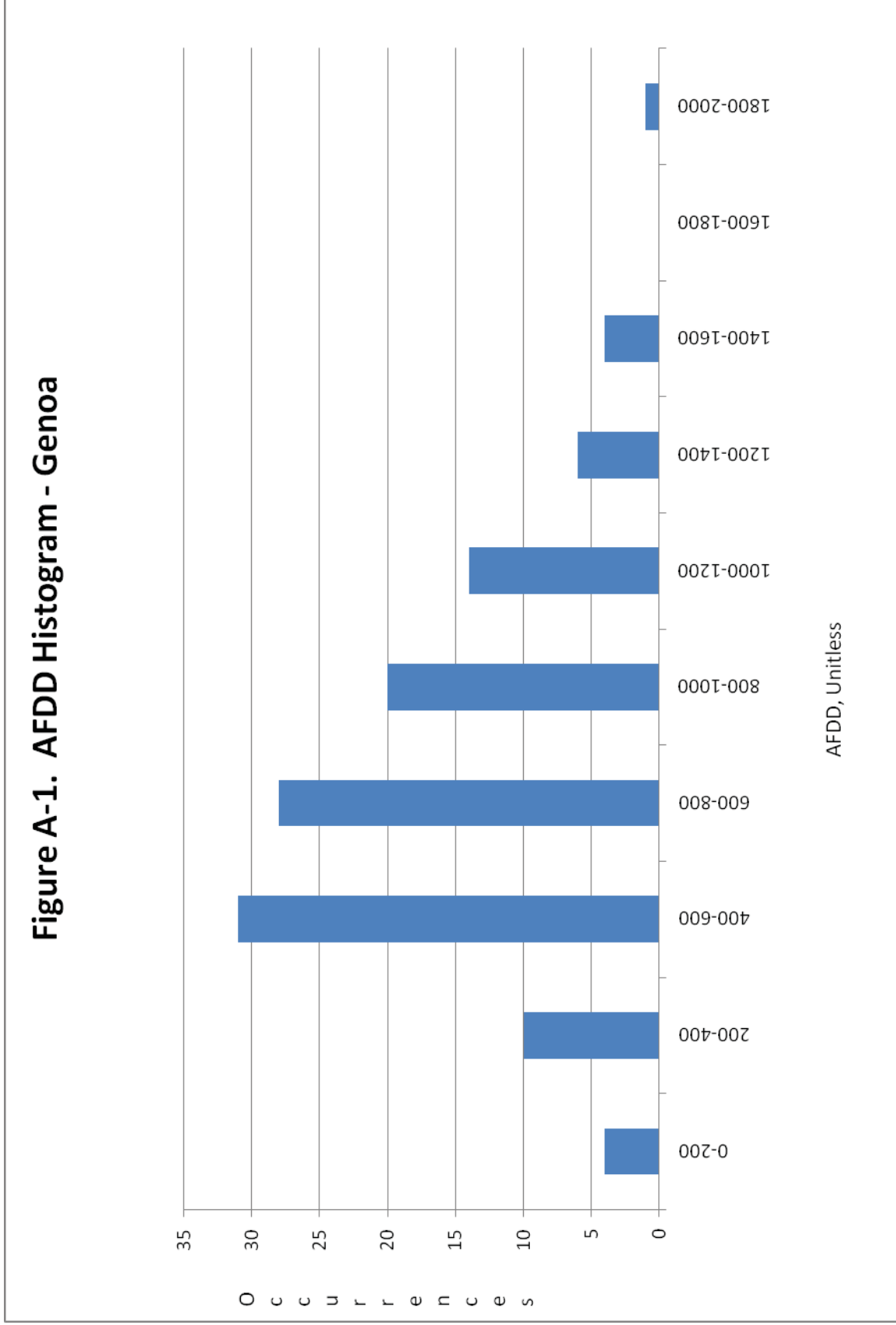
Table A-1. AFDD Required to Produce Significant Frazil Production and Alter Canal Operations to Significantly Increase Flows in Bypass Reach, by Water Year

Water Year	AFDD	Water Year	AFDD	Water Year	AFDD
1944	10	1967	19.5	1990	10.5
1945	8	1968	13.5	1991	5
1946	13.5	1969	16.5	1992	10.5
1947	16	1970	13.5	1993	7.5
1948	16.5	1971	15	1994	5
1949	10	1972	17	1995	13
1950	9.5	1973	19.5	1996	14
1951	16.5	1974	5.5	1997	18
1952	6.5	1975	5	1998	14.5
1953	9	1976	3.5	1999	22.5
1954	2	1977	26	2000	6
1955	5	1978	28	2001	1
1956	19.5	1979	15.5	2002	8
1957	15.5	1980	9	2003	6
1958	13.5	1981	2.5	2004	3.5
1959	20.5	1982	8	2005	6.5
1960	6	1983	6	2006	8
1961	5.5	1984	9.5	2007	9.5
1962	1.5	1985	17.5	2008	17.5
1963	9	1986	13.5		
1964	1	1987	16	Average	10.9
1965	8	1988	8.5	Median	9.5
1966	3.5	1989	5	St. Dev.	6.2

Table A-2. AFDD Required to Produce Stable Ice Cover, by Water Year

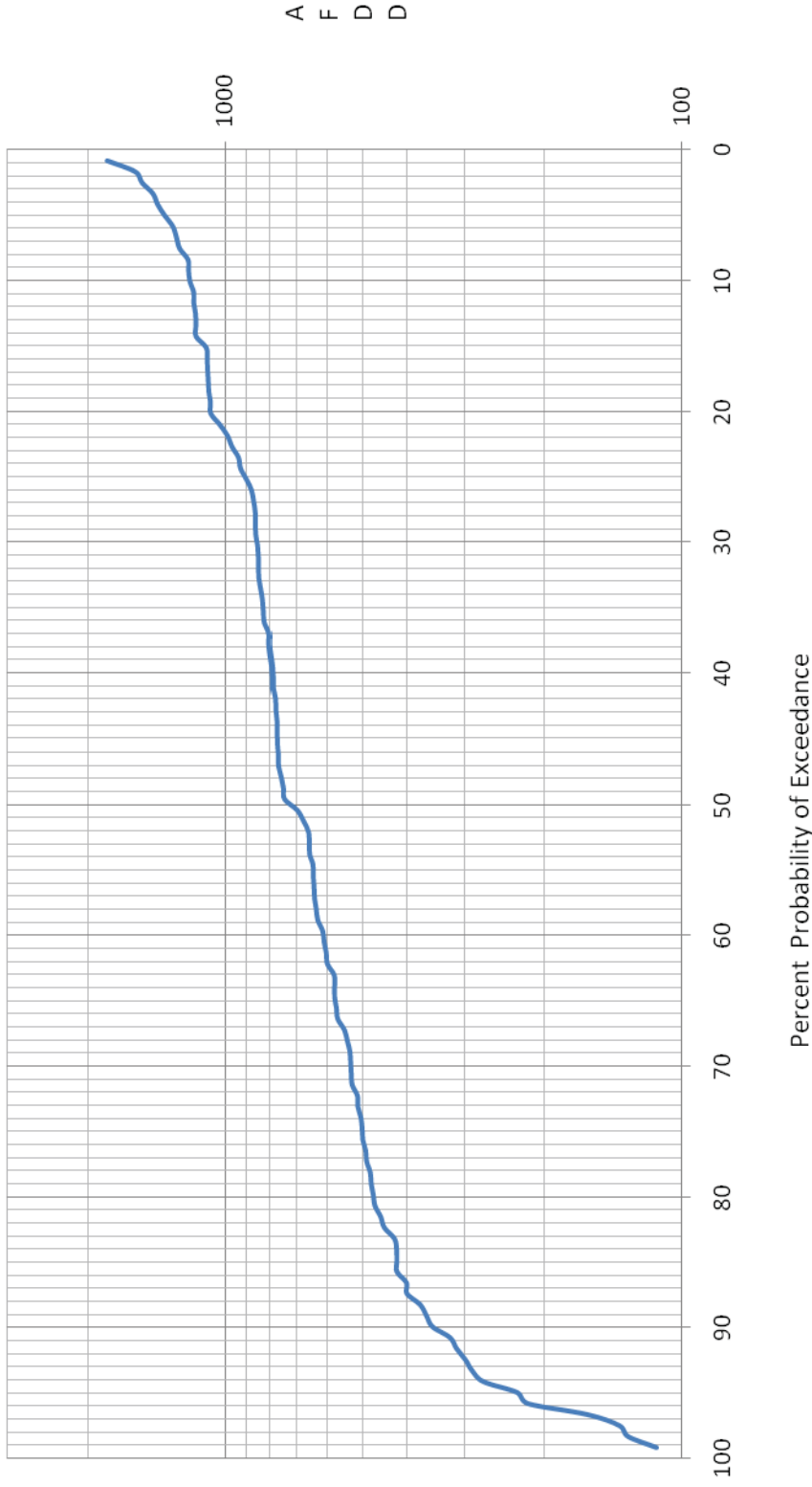
Water Year	AFDD	Water Year	AFDD	Water Year	AFDD
1944	60	1967	69.5	1990	225.5
1945	151.5	1968	144	1991	188.5
1946	42.5	1969	107.5	1992	57
1947	147	1970	51.5	1993	101
1948	65.5	1971	43	1994	112
1949	72.5	1972	90.5	1995	177
1950	119.5	1973	82	1996	109
1951	84.5	1974	119.5	1997	62.5
1952	88.5	1975	170.5	1998	152
1953	218.5	1976	183.5	1999	163
1954	99	1977	119	2000	75
1955	67	1978	64	2001	134.5
1956	70	1979	189.5	2002	158.5
1957	62.5	1980	150	2003	126
1958	122.5	1981	89.5	2004	67
1959	74	1982	100.5	2005	151.5
1960	124.5	1983	127	2006	51
1961	84.5	1984	134.5	2007	62
1962	67.5	1985	112.5	2008	58.5
1963	63	1986	311		
1964	47.5	1987	83	Average	107.7
1965	81.5	1988	100.5	Median	99.0
1966	64	1989	52	St. Dev.	51.9

Figure A-1. AFDD Histogram - Genoa



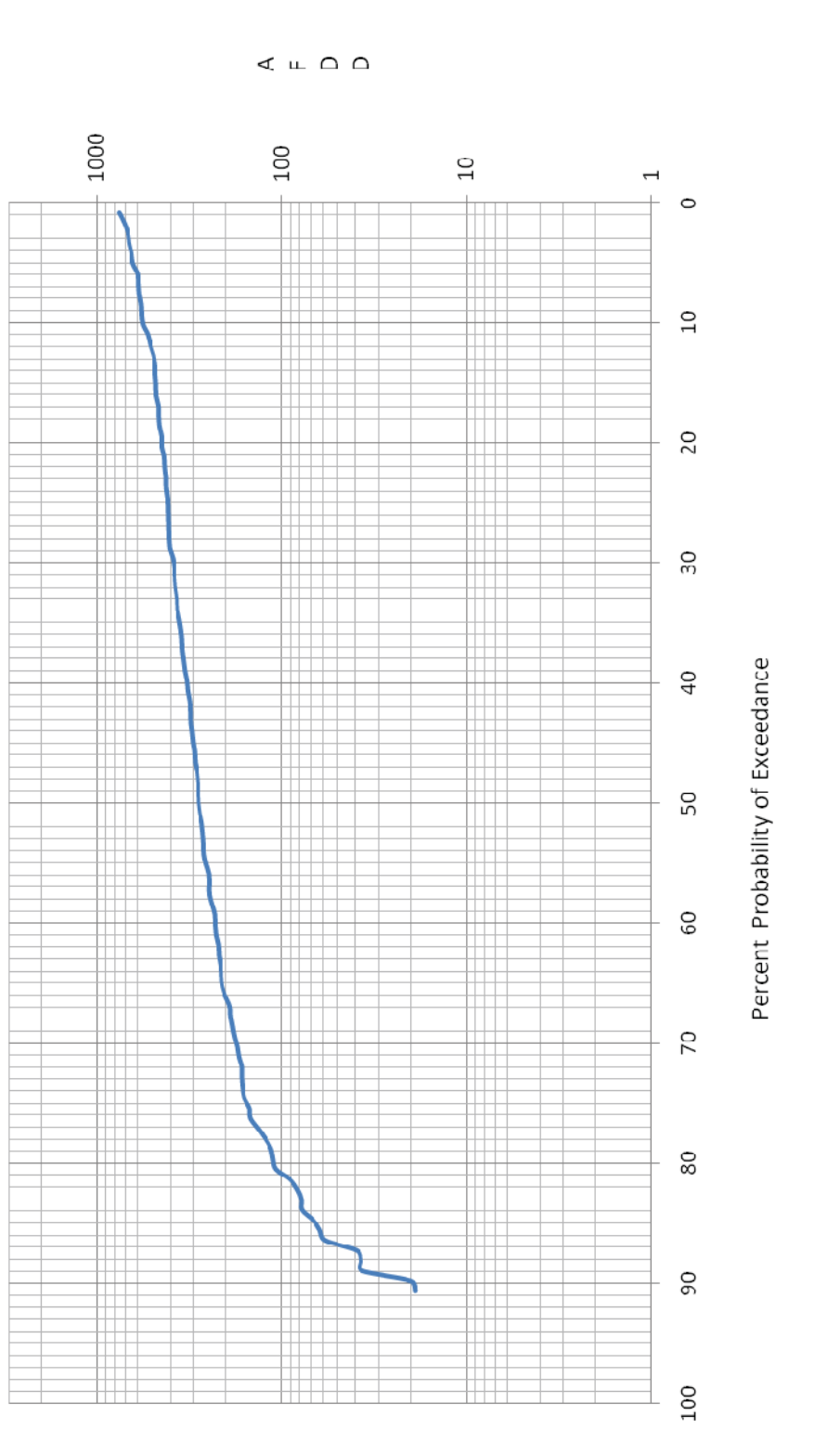
AFDD Histogram shows the occurrences of peak AFDD at Genoa during the period of record.

Figure A-2. AFDD Frequency Analysis - Genoa



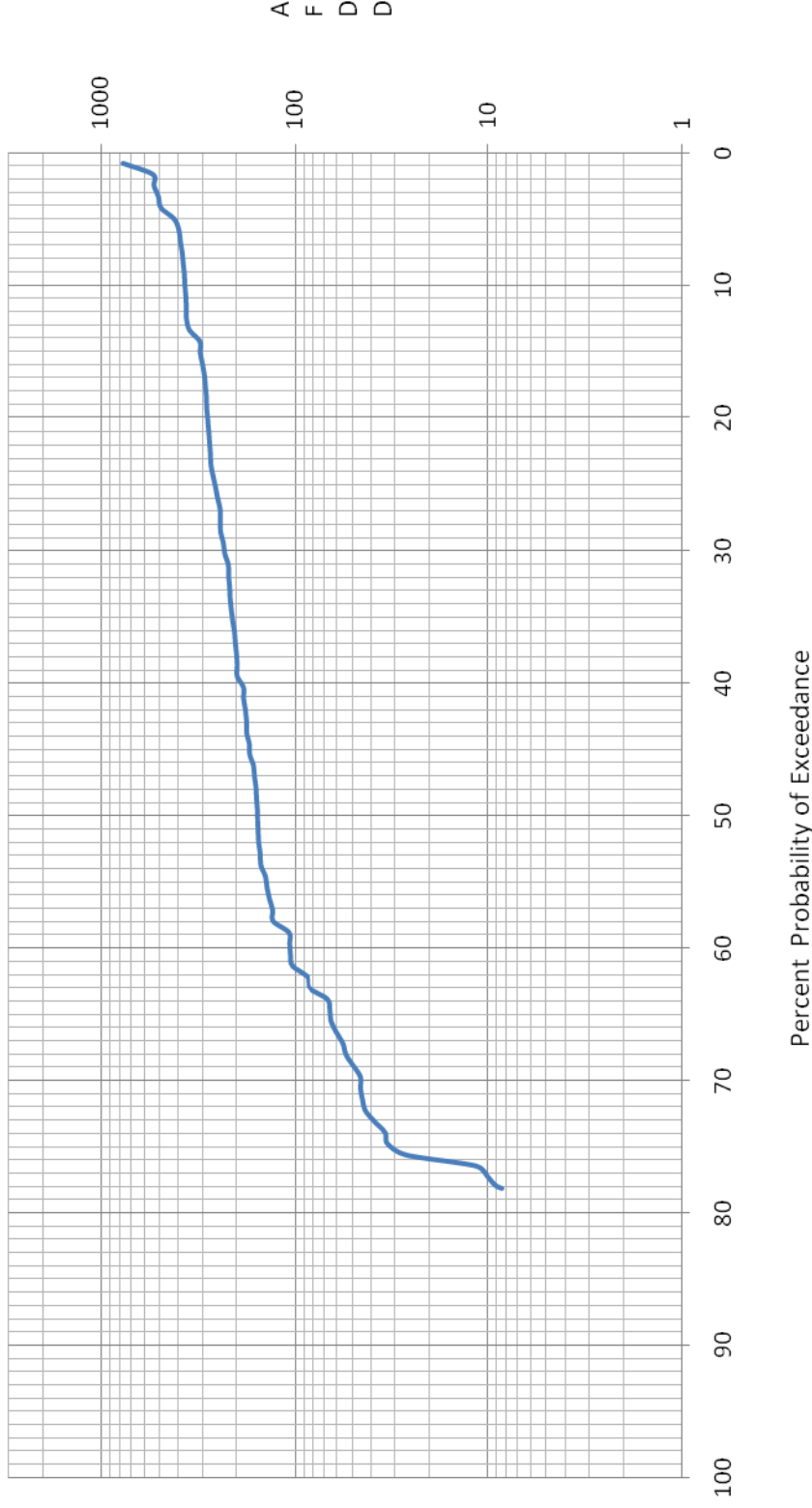
AFDD Frequency Analysis shows the probability of meeting or exceeding an AFDD value at Genoa based on the period of record. The results were plotted using a lognormal scale.

**Fig. A-3. Change in AFDD Dec 31-Jan31
Frequency Analysis - Genoa**



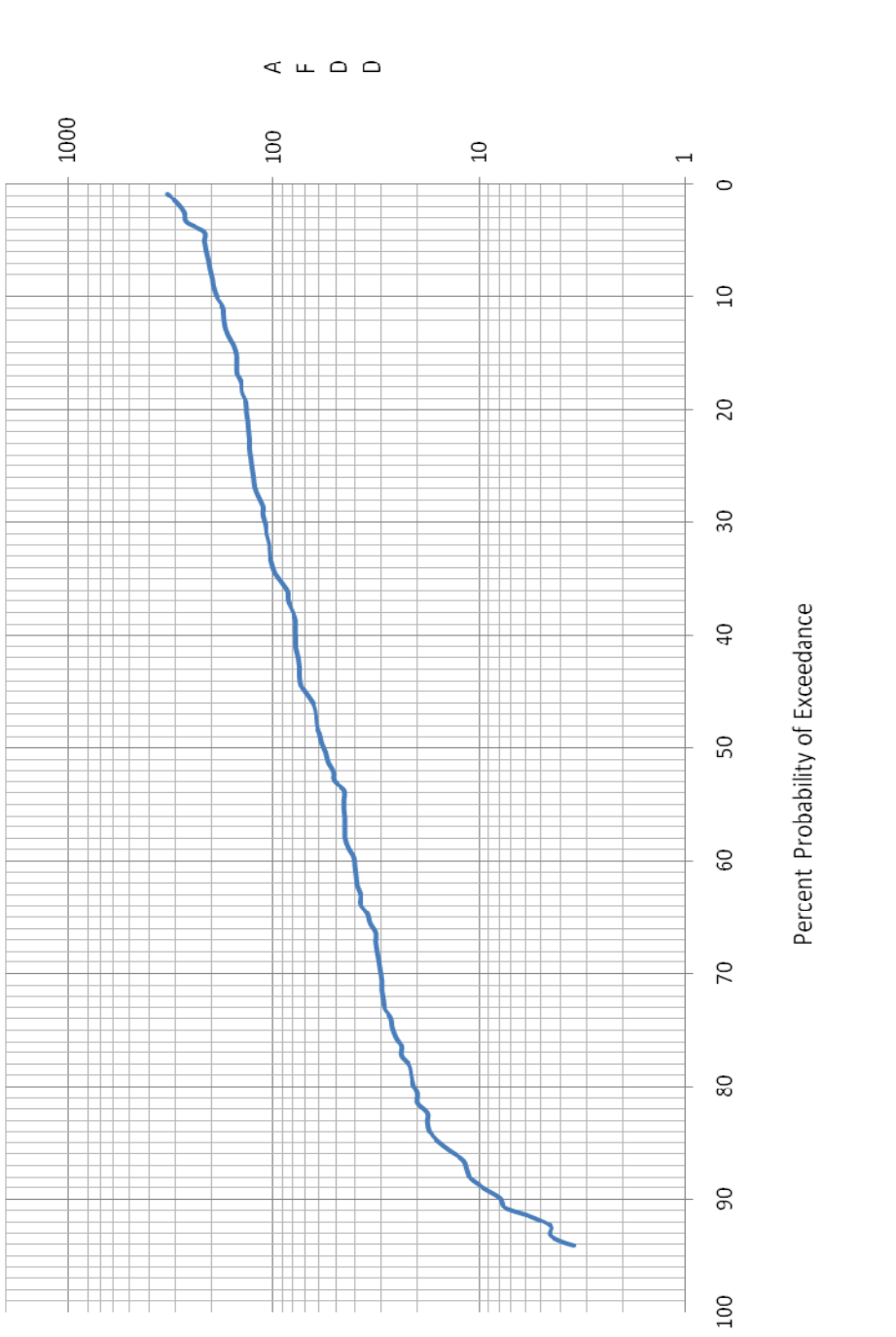
Change in AFDD Dec 31 – Jan 31 Frequency Analysis shows the probability of meeting or exceeding an accumulation of AFDD from Dec 31st through Jan 31st at Genoa based on the period of record. The results were plotted using a lognormal scale. Please note this analysis does not extend to a 100% probability. Some AFDD changes from Dec 31st – Jan 31st were negative. These negative values cannot be plotted on a lognormal scale.

**Fig. A-4. Change in AFDD Jan 31-Feb 28/29
Frequency Analysis - Genoa**



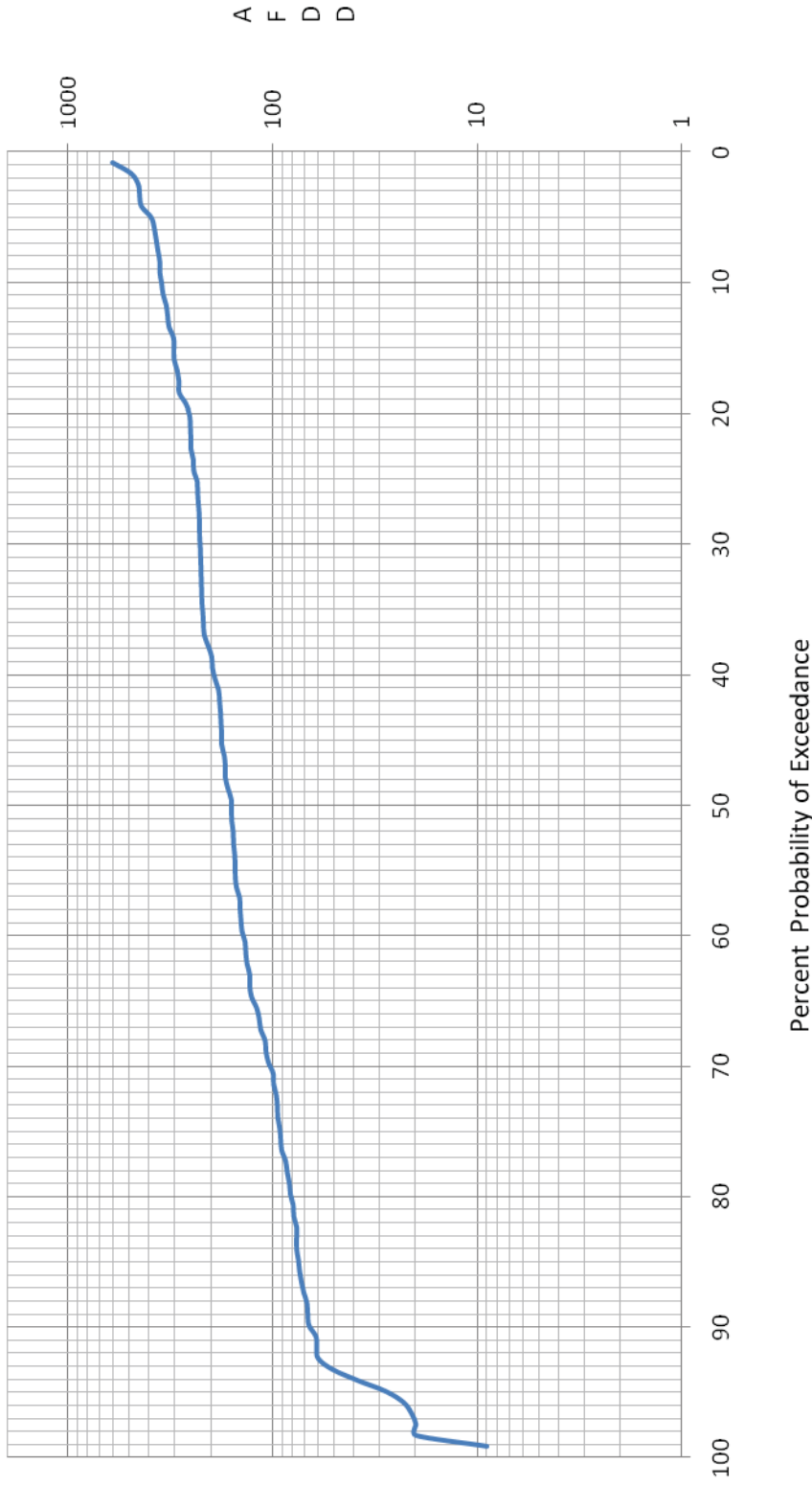
Change in AFDD Jan 31 – Feb 28/29 Frequency Analysis shows the probability of meeting or exceeding an accumulation of AFDD from Jan 31st through Feb 28th/29th at Genoa based on the period of record. The results were plotted using a lognormal scale. Please note this analysis does not extend to a 100% probability. Some AFDD changes from Jan 31st through Feb 28th/29th were negative. These negative values cannot be plotted on a lognormal scale.

**Figure A-5. Difference in AFDD Peak-Feb28/29
Frequency Analysis - Genoa**



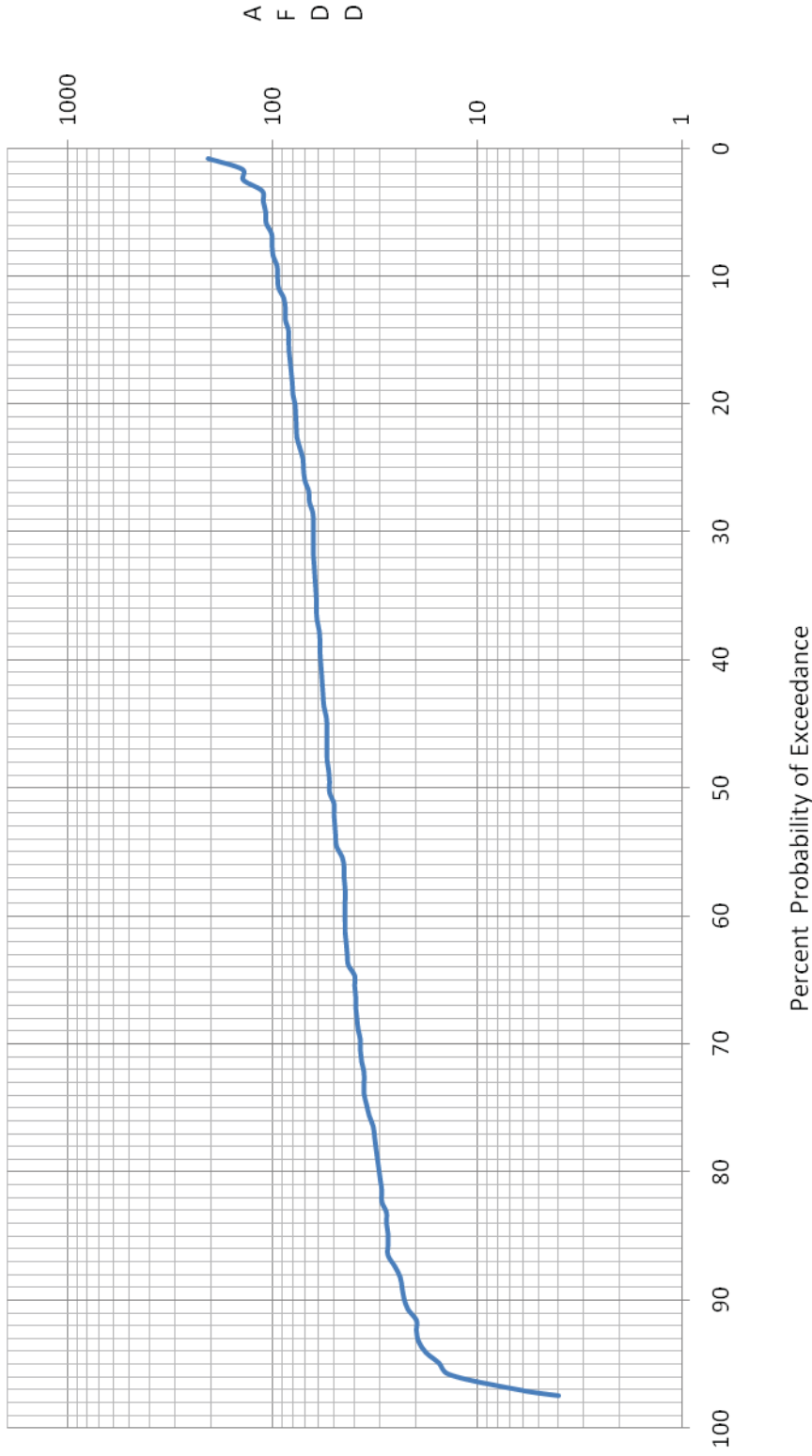
Change in AFDD Peak – Feb 28/29 Frequency Analysis shows the probability of meeting or exceeding an accumulation of AFDD from Feb 28th/29th to the peak AFDD value at Genoa based on the period of record. The results were plotted using a lognormal scale. Please note this analysis does not extend to a 100% probability. Some AFDD changes from Feb 28/29th to the peak AFDD were negative. These negative values cannot be plotted on a lognormal scale.

**Figure A-6. AFDD₋₂₁
Frequency Analysis - Genoa**



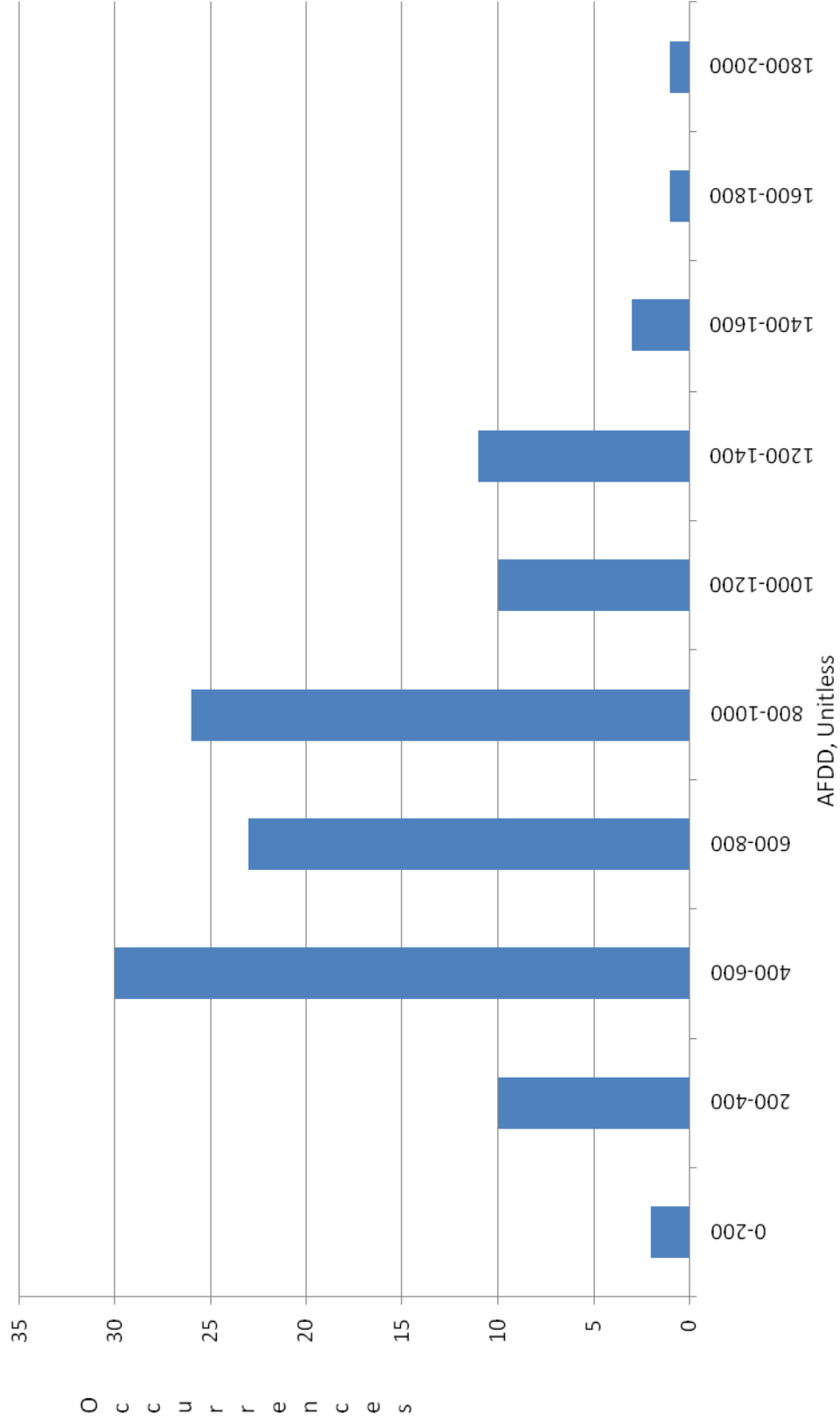
AFDD₋₂₁ Frequency Analysis shows the probability of meeting or exceeding an accumulation of AFDD during the 21 days prior to the peak AFDD value at Genoa based on the period of record. The results were plotted using a lognormal scale.

**Figure A-7. AFDD₊₇
Frequency Analysis - Genoa**



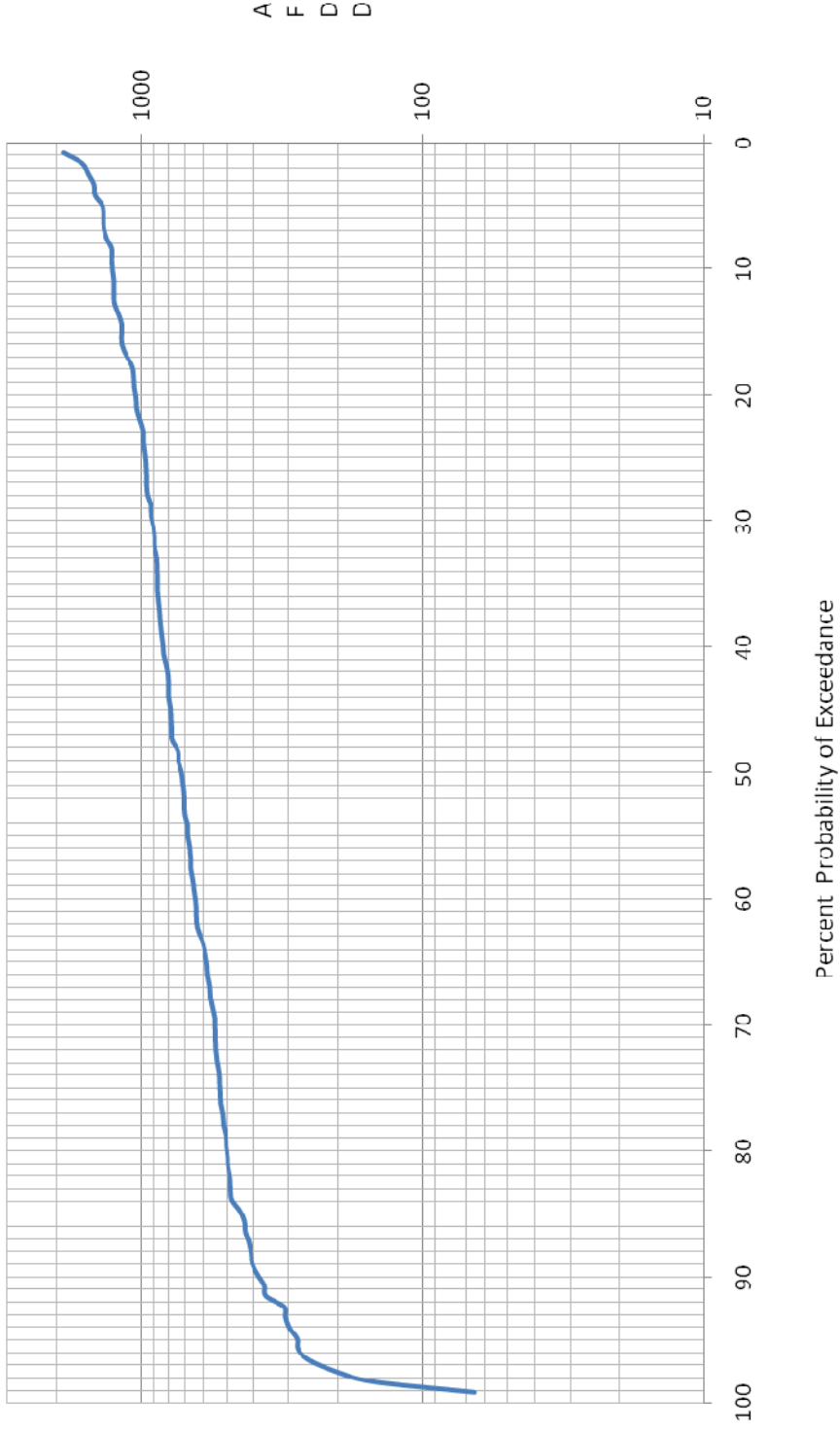
AFDD₊₇ Frequency Analysis shows the probability of meeting or exceeding a depletion of AFDD during the 7 days after the peak AFDD value at Genoa based on the period of record. The results were plotted using a lognormal scale.

Figure A-8. AFDD Histogram - Columbus



AFDD Histogram shows the occurrences of peak AFDD at Columbus during the period of record.

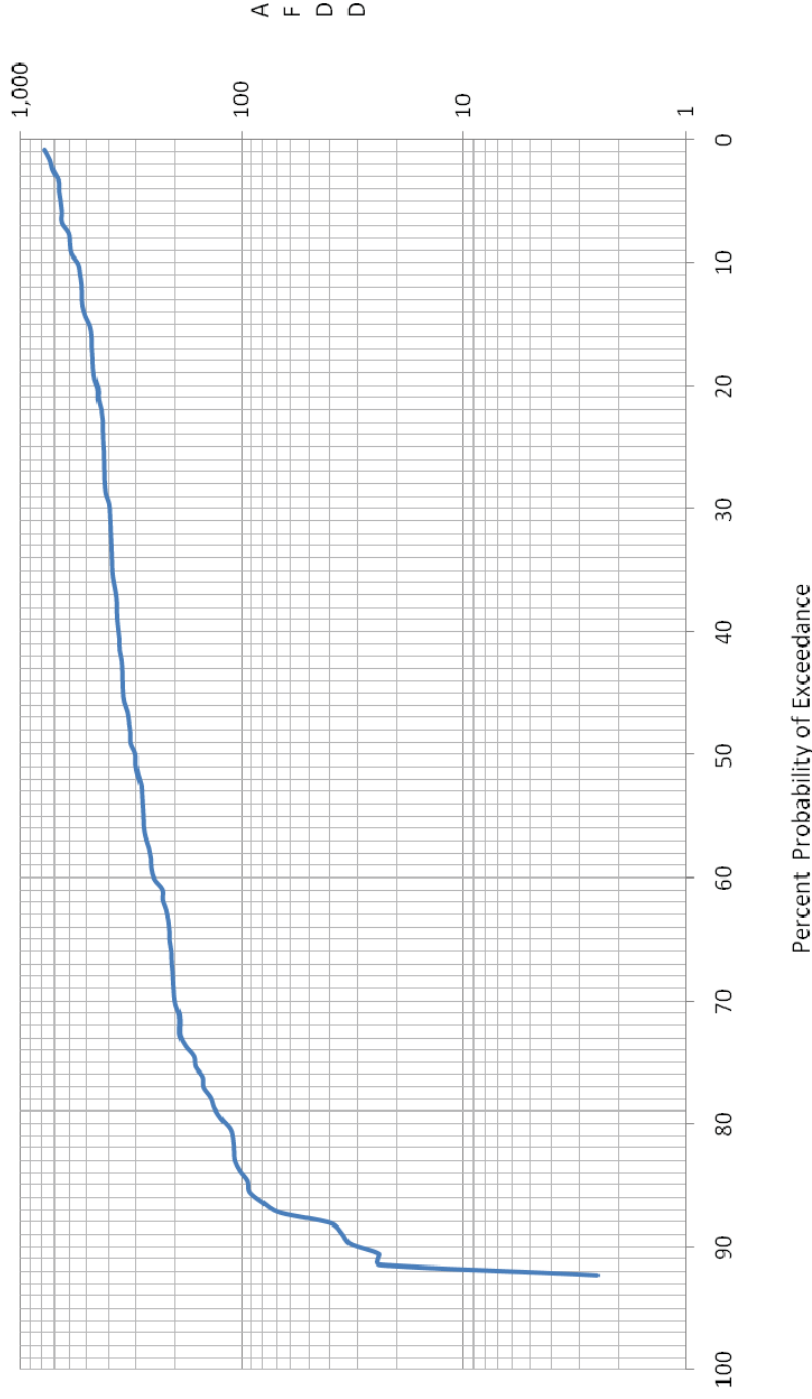
Figure A-9.
AFDD Frequency Analysis - Columbus



A
F
D
D

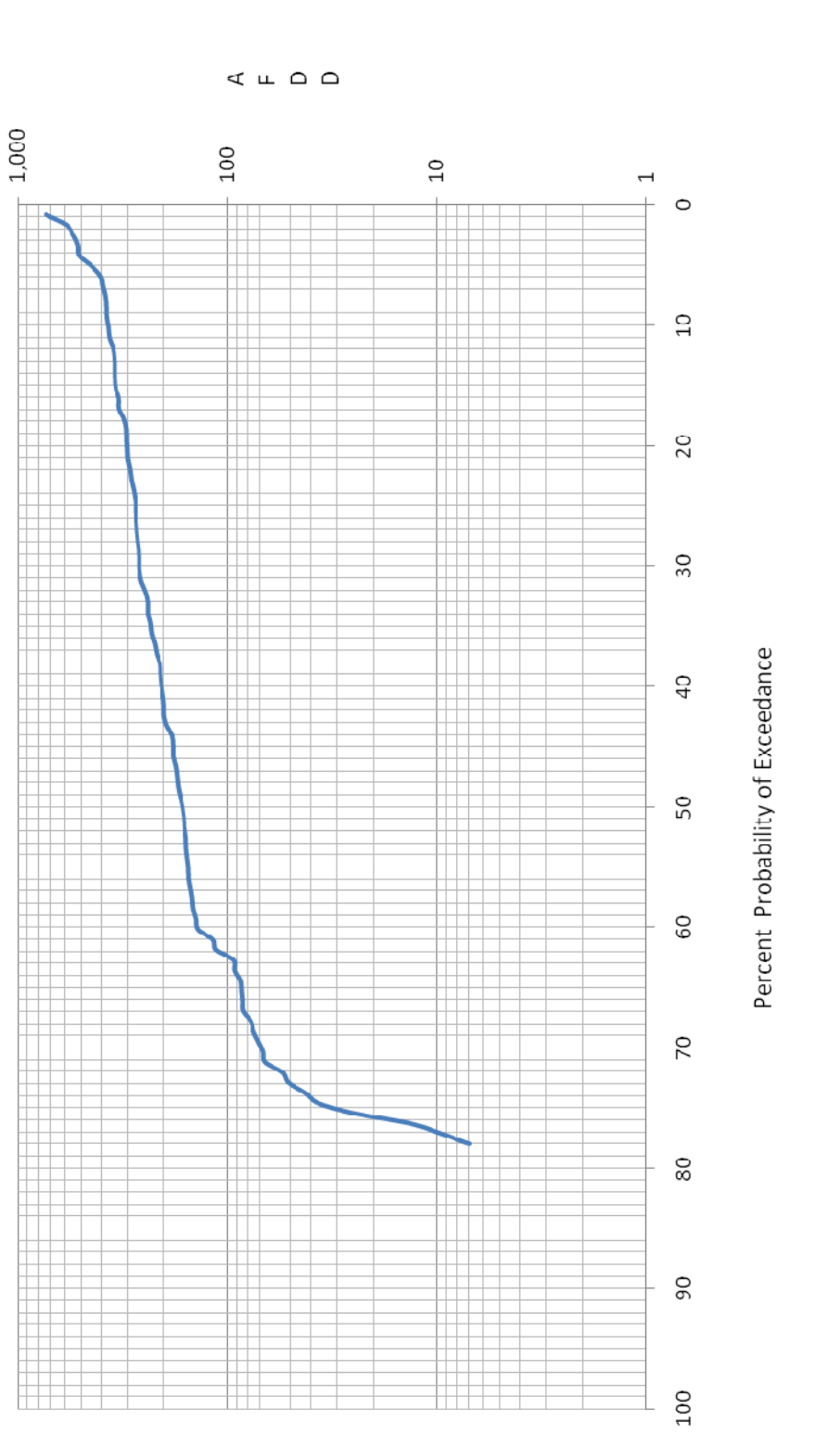
AFDD Frequency Analysis shows the probability of meeting or exceeding an AFDD value at Columbus based on the period of record. The results were plotted using a lognormal scale.

**Figure A-10. Change in AFDD Dec31-Jan31
Frequency Analysis - Columbus**



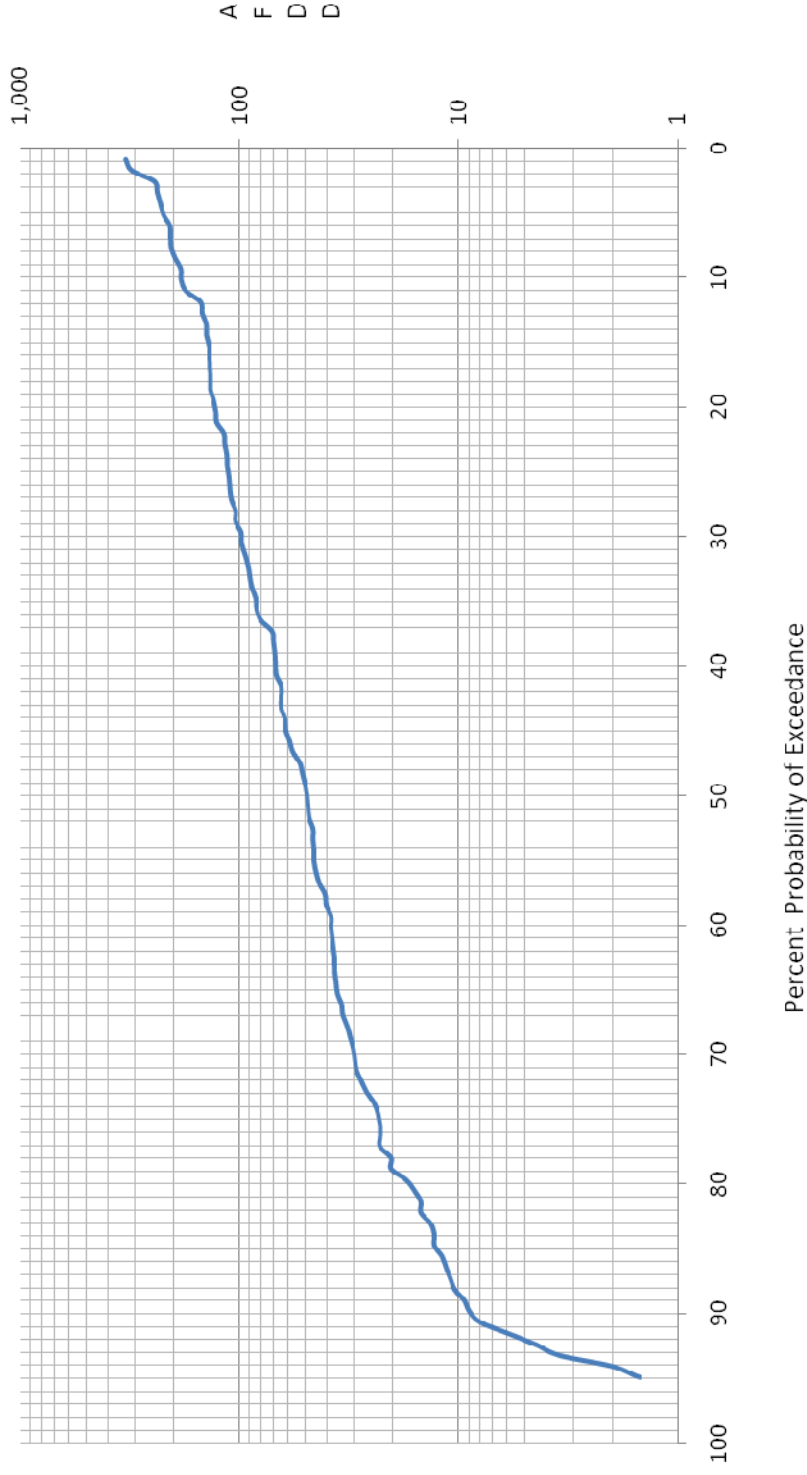
Change in AFDD Dec 31 – Jan 31 Frequency Analysis shows the probability of meeting or exceeding an accumulation of AFDD from Dec 31st through Jan 31st at Columbus based on the period of record. The results were plotted using a lognormal scale. Please note this analysis does not extend to a 100% probability. Some AFDD changes from Dec 31st – Jan 31st were negative. These negative values cannot be plotted on a lognormal scale.

**Figure A-11. Change in AFDD Jan 31-Feb 28/29
Frequency Analysis - Columbus**



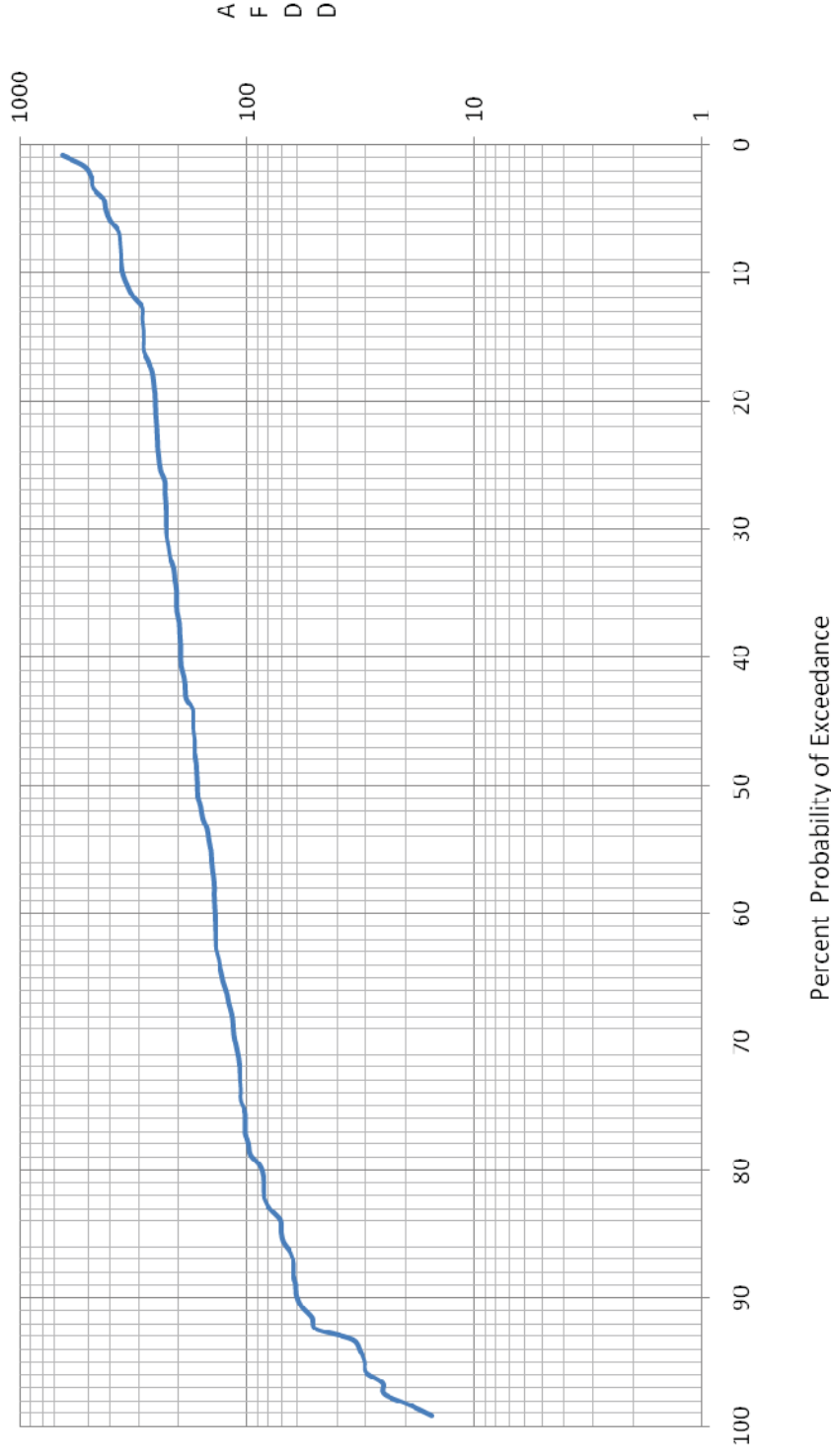
Change in AFDD Jan 31 – Feb 28/29 Frequency Analysis shows the probability of meeting or exceeding an accumulation of AFDD from Jan 31st through Feb 28th/29th at Columbus based on the period of record. The results were plotted using a lognormal scale. Please note this analysis does not extend to a 100% probability. Some AFDD changes from Jan 31st through Feb 28th/29th were negative. These negative values cannot be plotted on a lognormal scale.

**Figure A-12. Difference in AFDD Peak-Feb28/29
Frequency Analysis - Columbus**



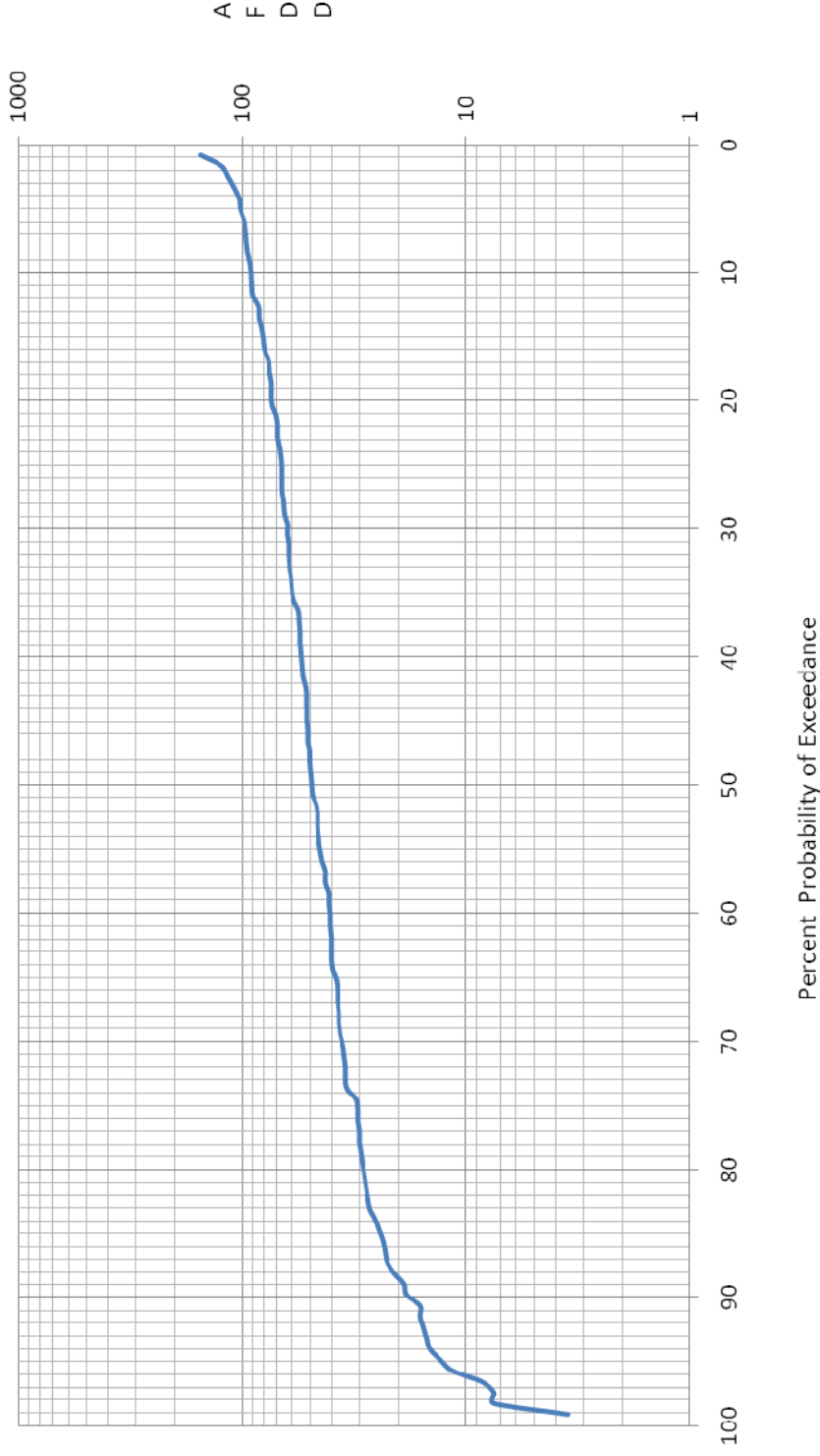
Change in AFDD Peak – Feb 28/29 Frequency Analysis shows the probability of meeting or exceeding an accumulation of AFDD from Feb 28th/29th to the peak AFDD value at Columbus based on the period of record. The results were plotted using a lognormal scale. Please note this analysis does not extend to a 100% probability. Some AFDD changes from Feb 28/29th to the peak AFDD were negative. These negative values cannot be plotted on a lognormal scale.

**Figure A-13. AFDD₋₂₁
Frequency Analysis - Columbus**



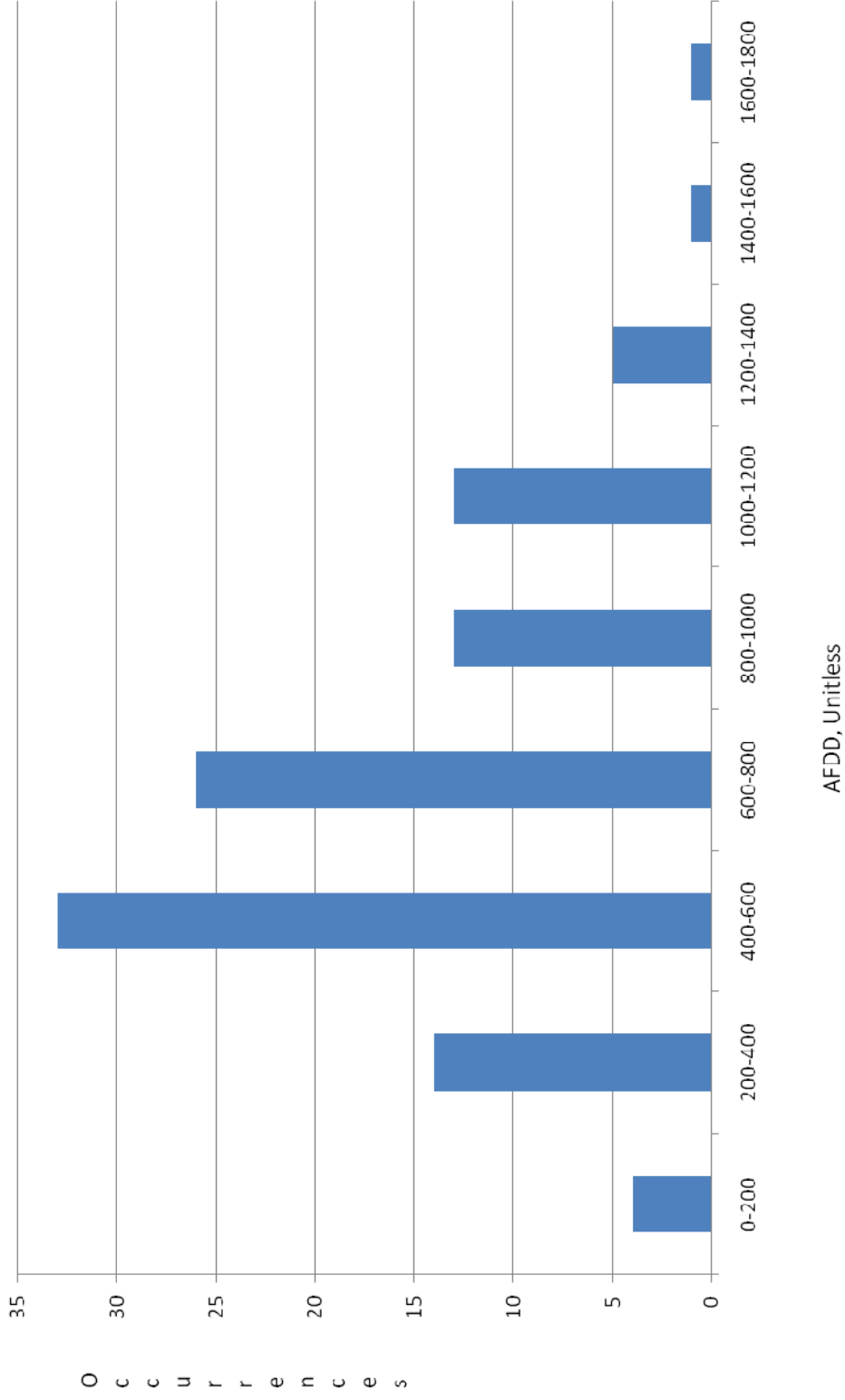
AFDD₋₂₁ Frequency Analysis shows the probability of meeting or exceeding an accumulation of AFDD during the 21 days prior to the peak AFDD value at Columbus based on the period of record. The results were plotted using a lognormal scale.

**Figure A-14. AFDD₊₇
Frequency Analysis - Columbus**



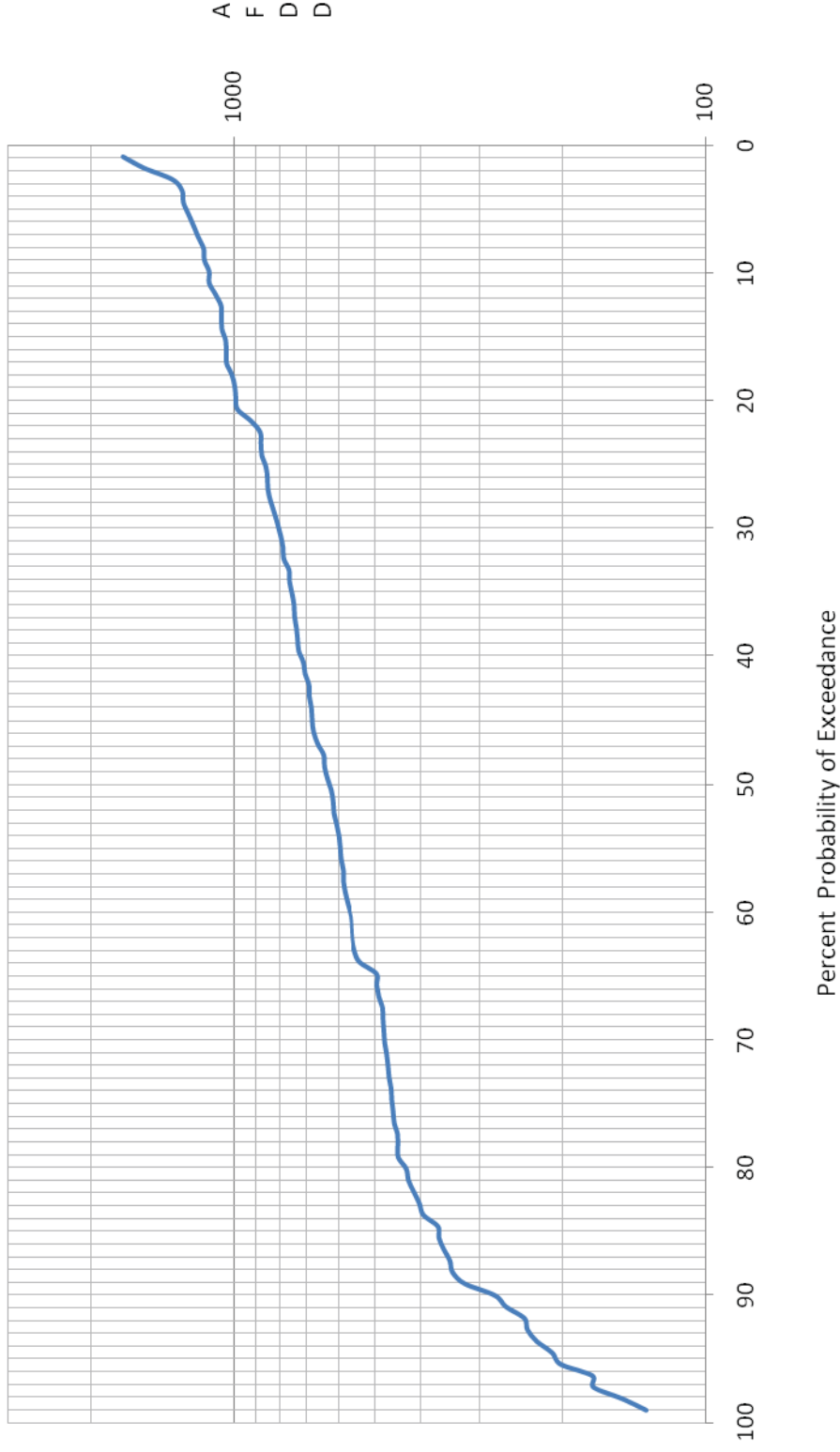
AFDD₊₇ Frequency Analysis shows the probability of meeting or exceeding a depletion of AFDD during the 7 days after the peak AFDD value at Columbus based on the period of record. The results were plotted using a lognormal scale.

Figure A-15.
AFDD Histogram - St. Paul



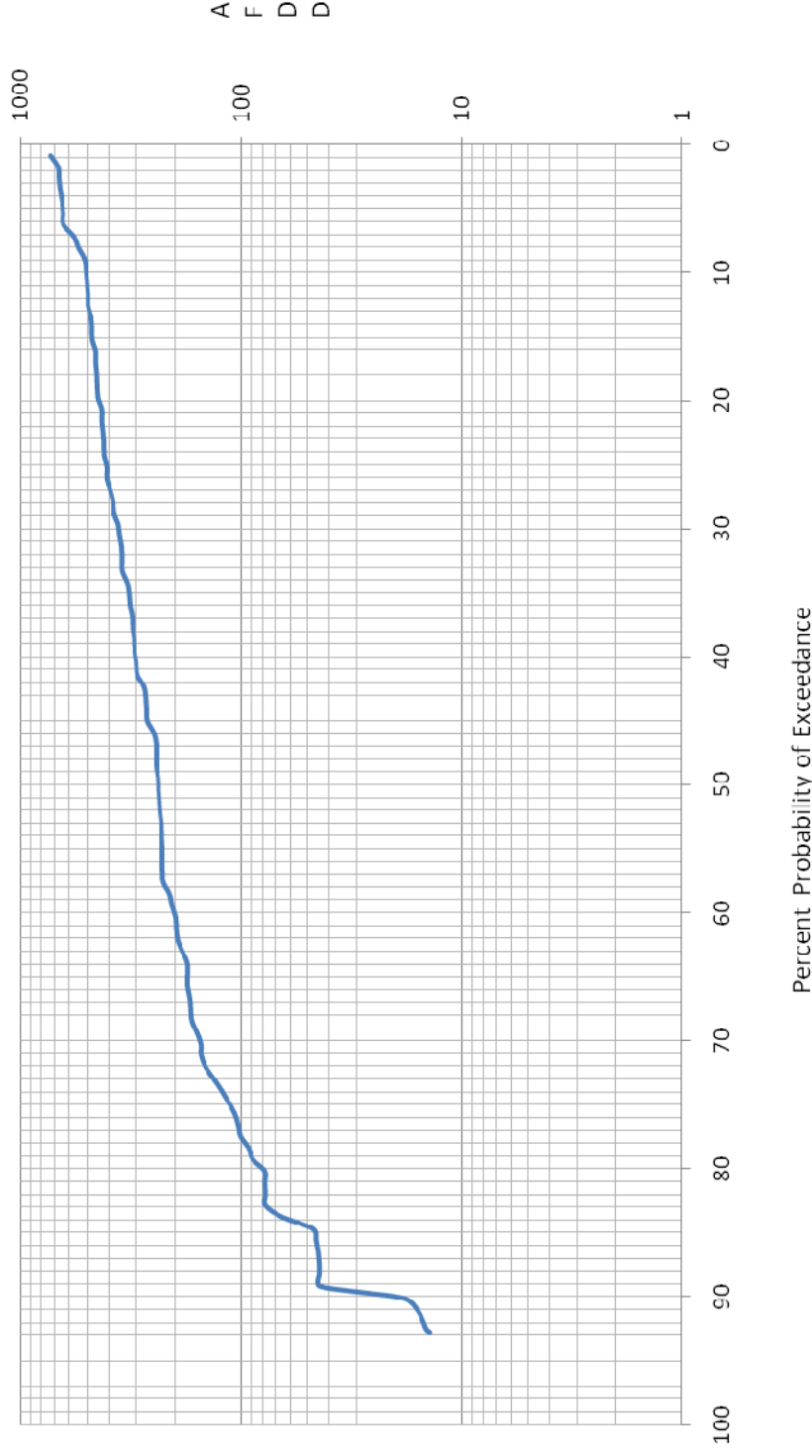
AFDD Histogram shows the occurrences of peak AFDD at St. Paul during the period of record.

Figure A-16.
AFDD Frequency Analysis - St. Paul



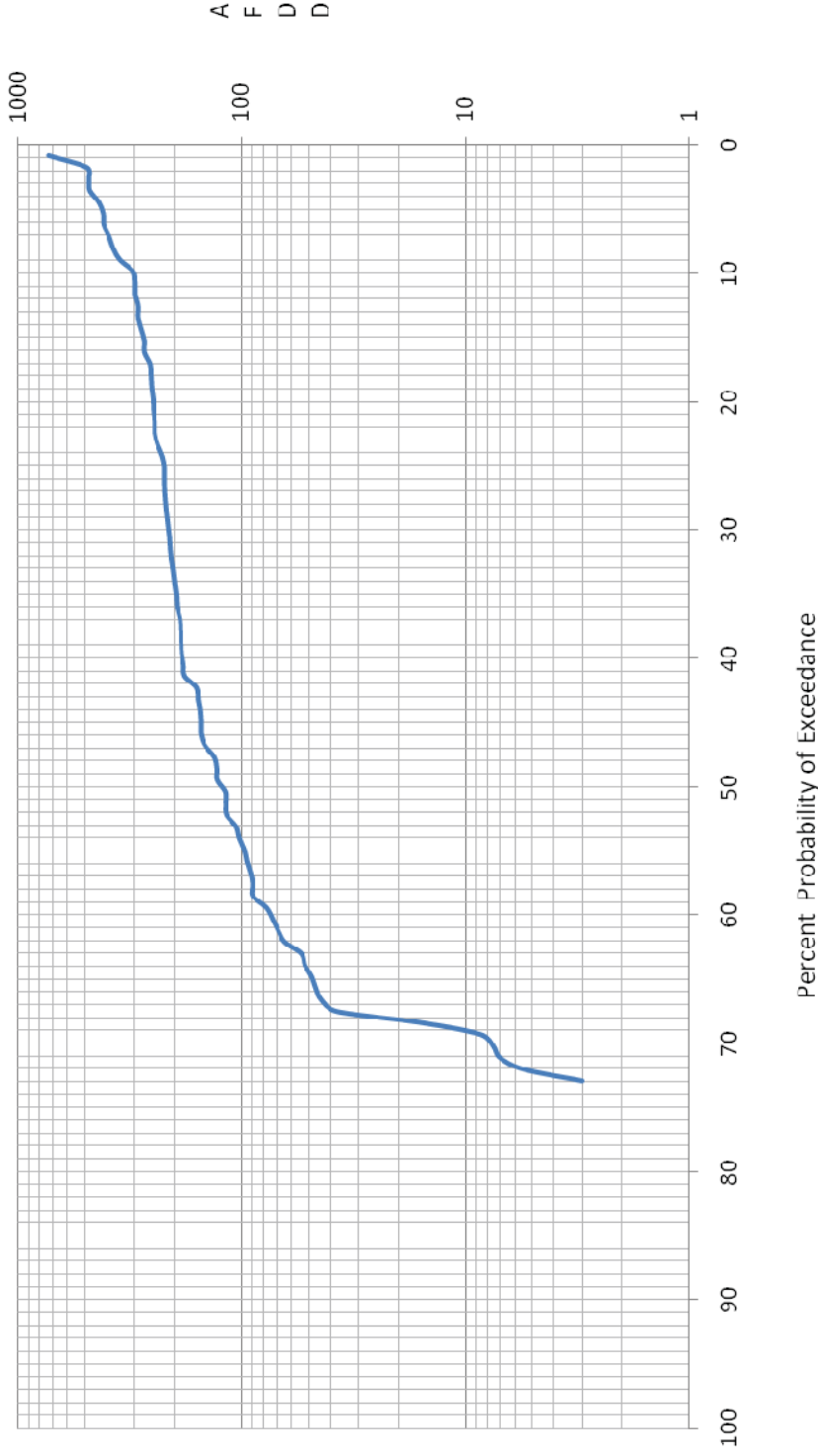
AFDD Frequency Analysis shows the probability of meeting or exceeding an AFDD value at St. Paul based on the period of record. The results were plotted using a lognormal scale.

**Figure A-17. Change in AFDD Dec 31-Jan31
Frequency Analysis - St. Paul**



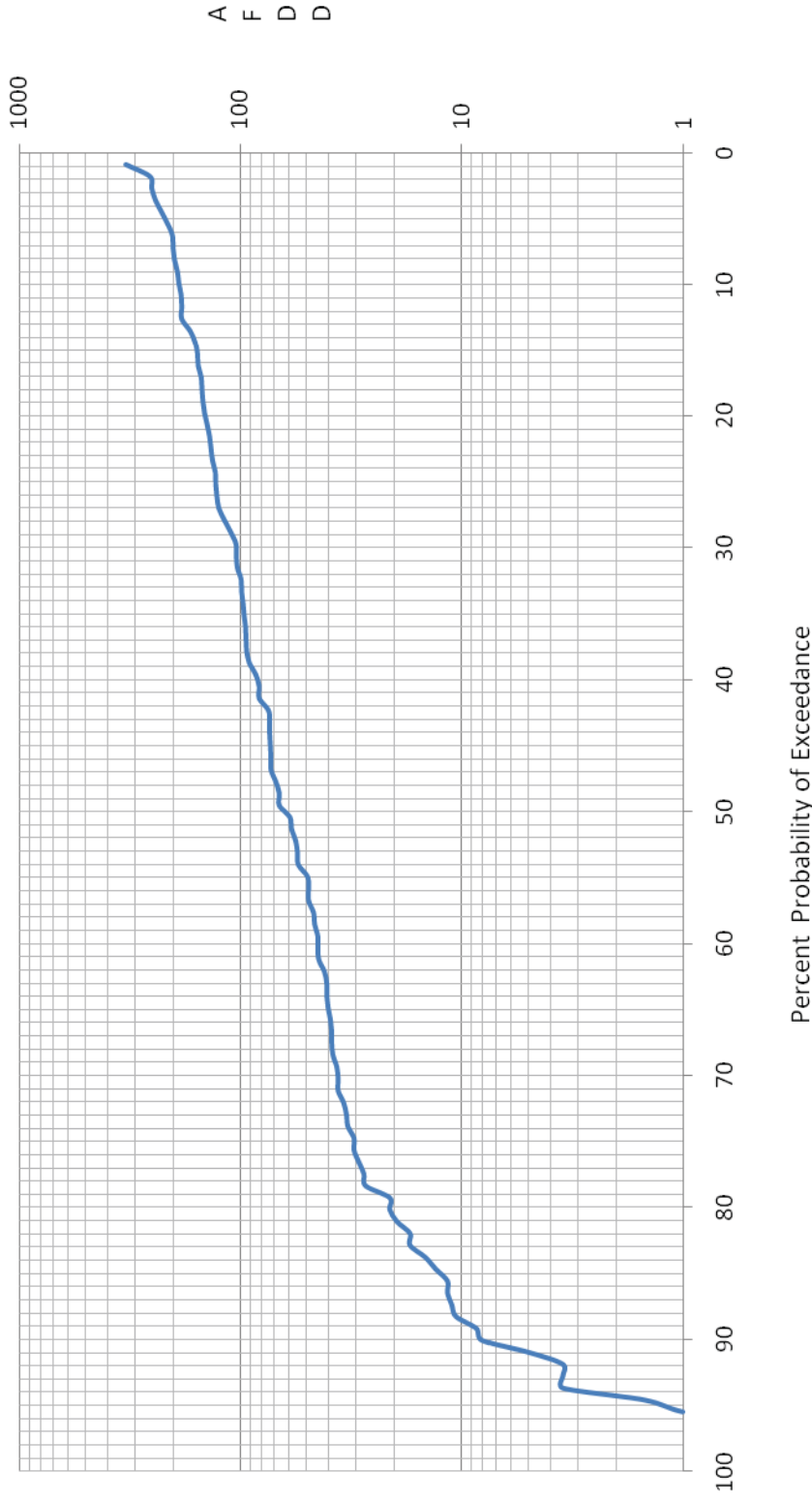
Change in AFDD Dec 31 – Jan 31 Frequency Analysis shows the probability of meeting or exceeding an accumulation of AFDD from Dec 31st through Jan 31st at St. Paul based on the period of record. The results were plotted using a lognormal scale. Please note this analysis does not extend to a 100% probability. Some AFDD changes from Dec 31st – Jan 31st were negative. These negative values cannot be plotted on a lognormal scale.

**Figure A-18. Change in AFDD Jan31-Feb28/29
Frequency Analysis - St. Paul**



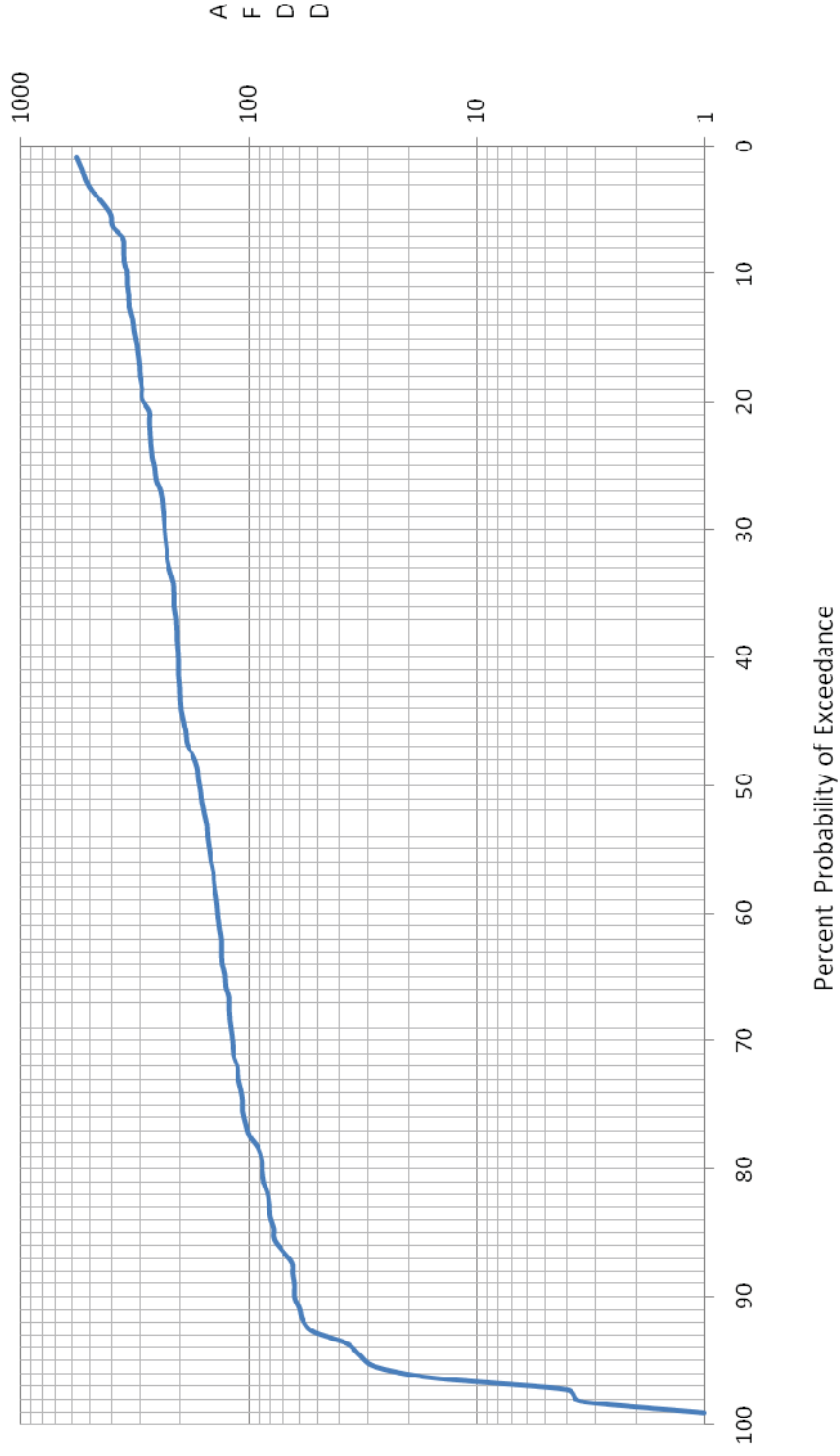
Change in AFDD Jan 31 – Feb 28/29 Frequency Analysis shows the probability of meeting or exceeding an accumulation of AFDD from Jan 31st through Feb 28th/29th at St. Paul based on the period of record. The results were plotted using a lognormal scale. Please note this analysis does not extend to a 100% probability. Some AFDD changes from Jan 31st through Feb 28th/29th were negative. These negative values cannot be plotted on a lognormal scale.

**Figure A-19. Difference in AFDD Peak-Feb28/29
Frequency Analysis - St. Paul**



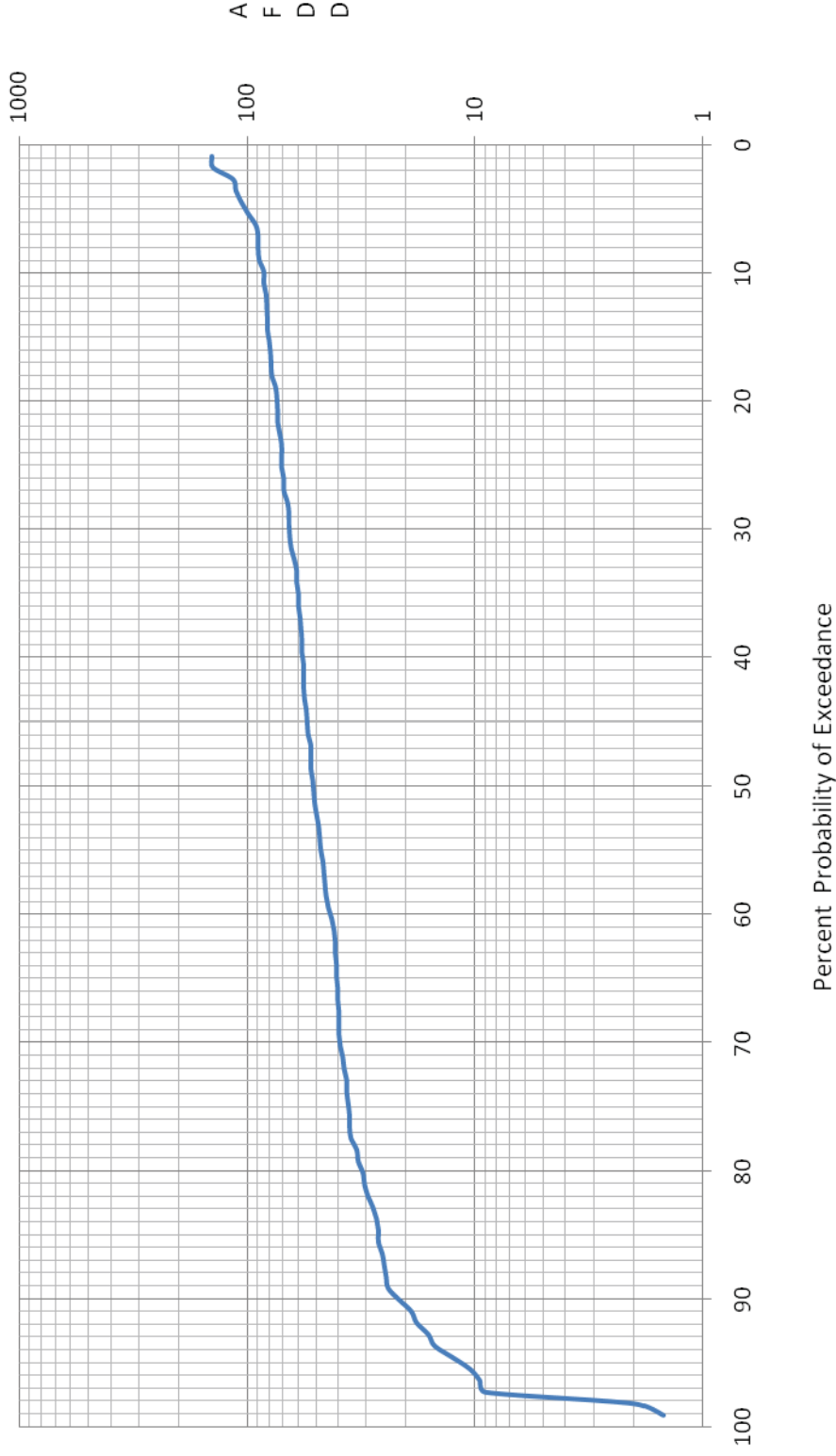
Change in AFDD Peak – Feb 28/29 Frequency Analysis shows the probability of meeting or exceeding an accumulation of AFDD from Feb 28th/29th to the peak AFDD value at St. Paul based on the period of record. The results were plotted using a lognormal scale. Please note this analysis does not extend to a 100% probability. Some AFDD changes from Feb 28/29th to the peak AFDD were negative. These negative values cannot be plotted on a lognormal scale.

**Figure A-20. AFDD₋₂₁
Frequency Analysis - St. Paul**



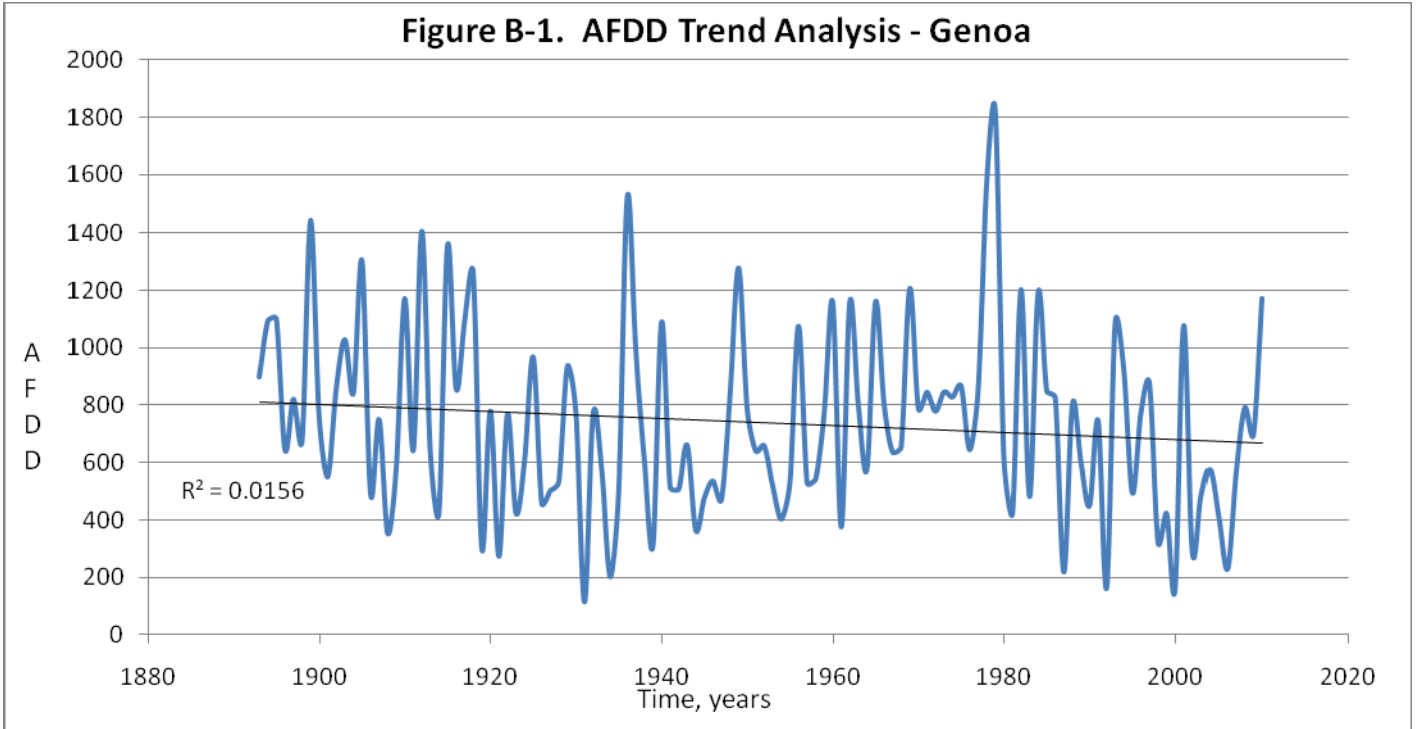
AFDD₋₂₁ Frequency Analysis shows the probability of meeting or exceeding an accumulation of AFDD during the 21 days prior to the peak AFDD value at St. Paul based on the period of record. The results were plotted using a lognormal scale.

**Figure A-21. AFDD₊₇
Frequency Analysis - St. Paul**

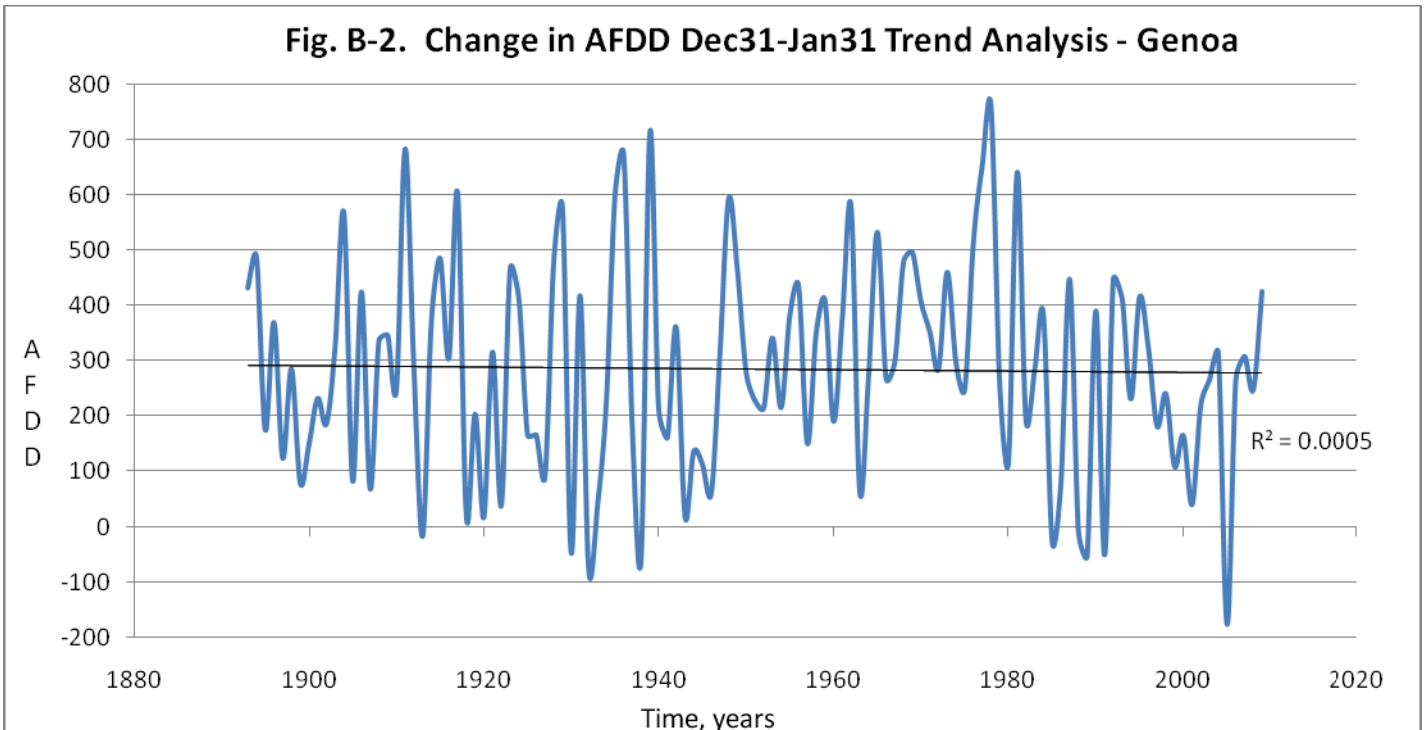


AFDD₊₇ Frequency Analysis shows the probability of meeting or exceeding a depletion of AFDD during the 7 days after the peak AFDD value at St. Paul based on the period of record. The results were plotted using a lognormal scale.

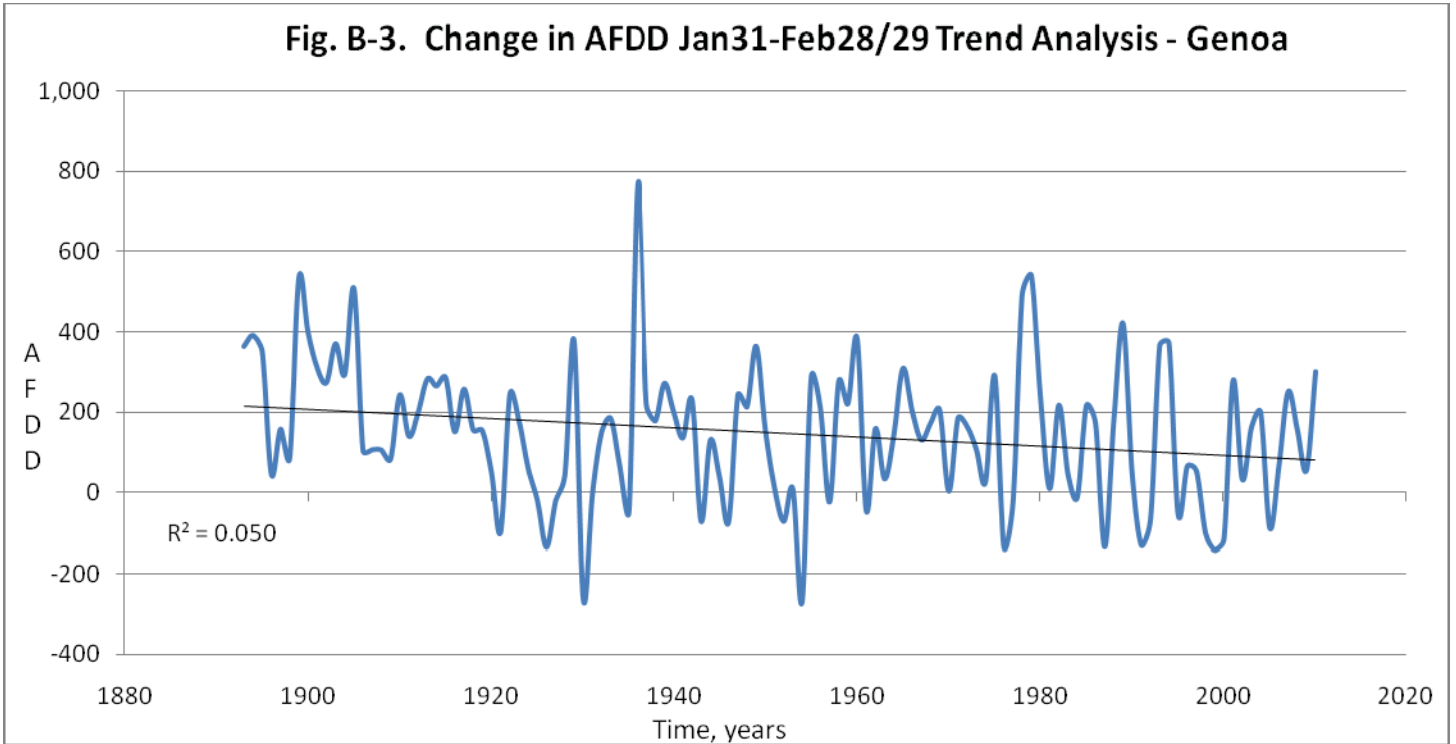
ATTACHMENT B
TREND ANALYSIS



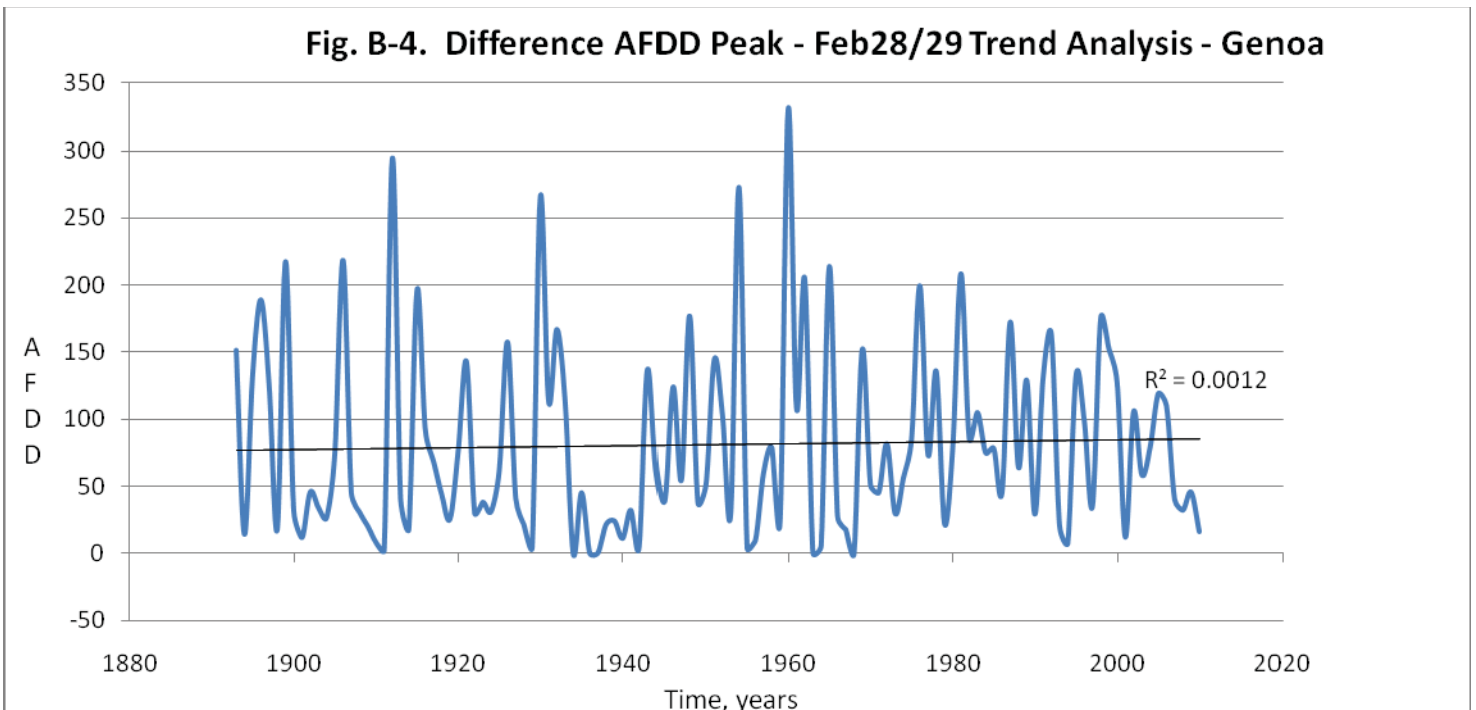
AFDD Trend Analysis shows peak AFDD relative to time at Genoa.



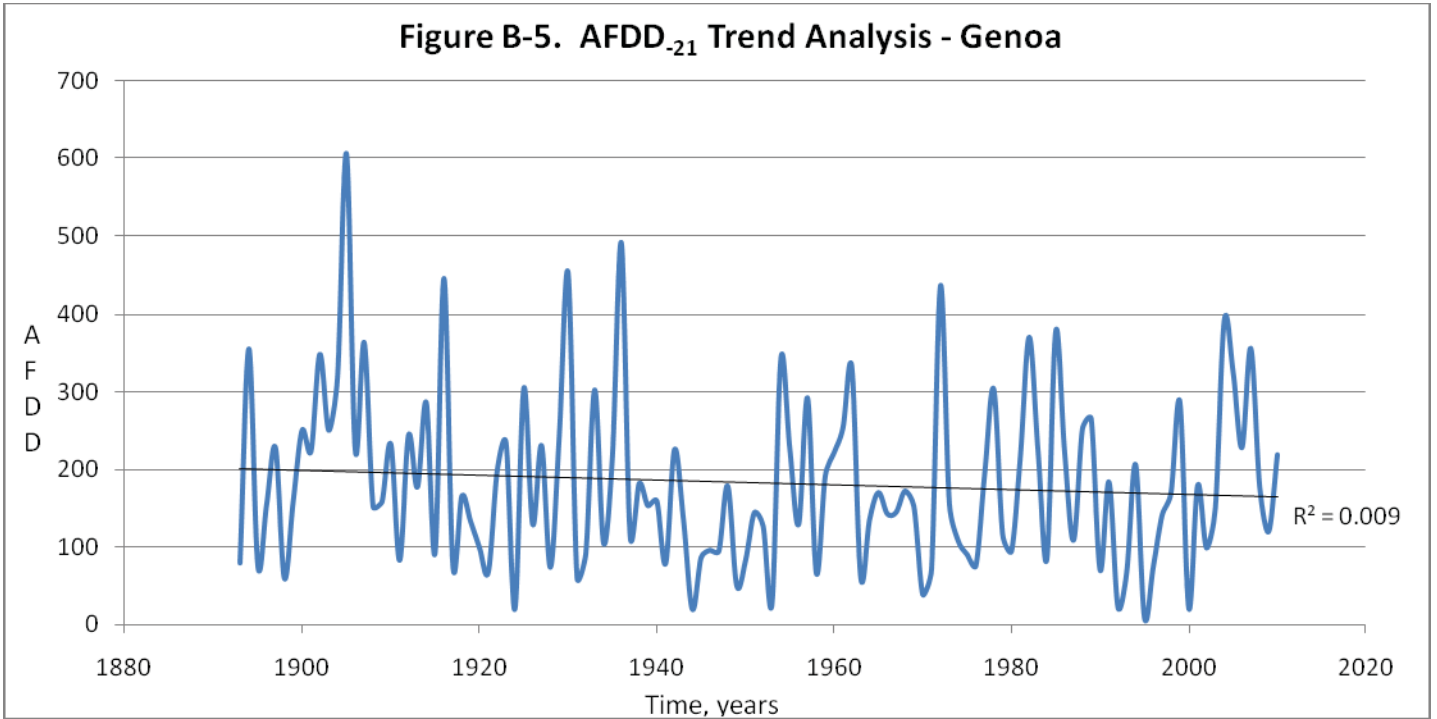
Change in AFDD Dec 31 – Jan 31 Trend Analysis shows the change in AFDD from Dec 31st through Jan 31st over time at Genoa.



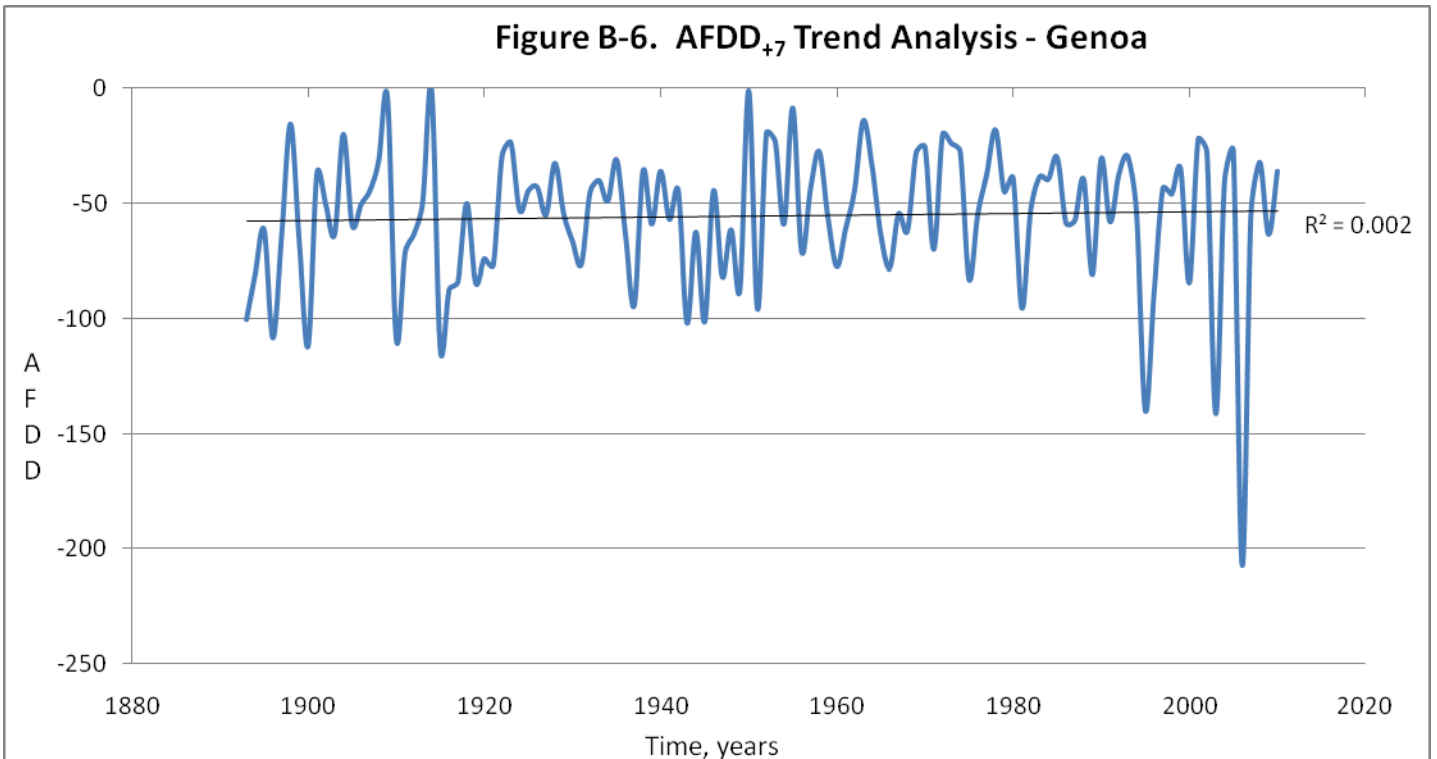
Change in AFDD Jan 31 – Feb 28/29 Trend Analysis shows the change in AFDD from Jan 31st – Feb 28th/29th over time at Genoa.



Difference AFDD Peak – Feb 28/29 Trend Analysis shows the difference between peak AFDD and Feb 28th/29th AFDD value over time at Genoa.



AFDD₋₂₁ Trend Analysis shows the change in AFDD during the 21 days before peak AFDD at Genoa.



AFDD₊₇ Trend Analysis shows the change in AFDD during the 7 days after peak AFDD over time at Genoa.

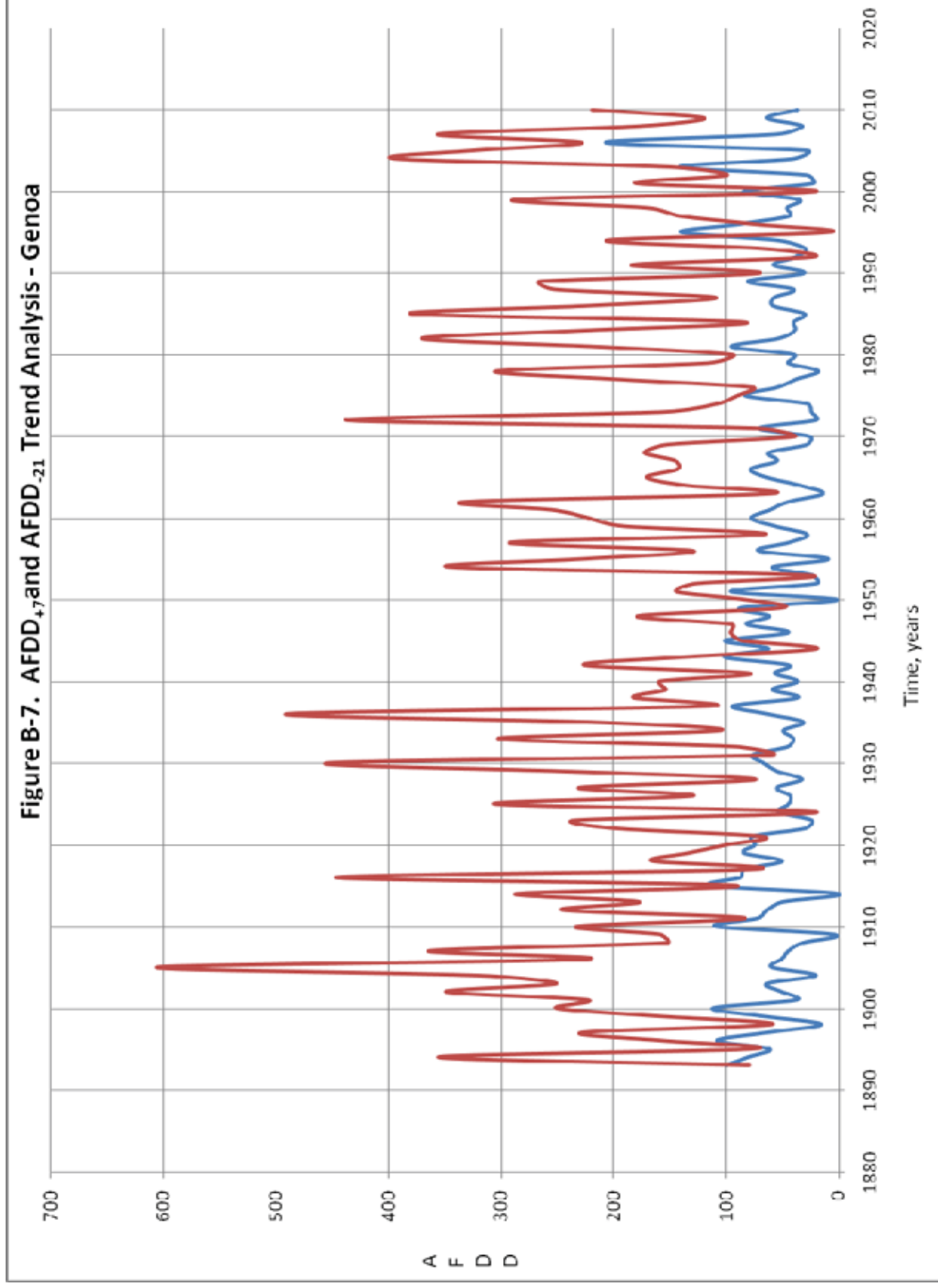
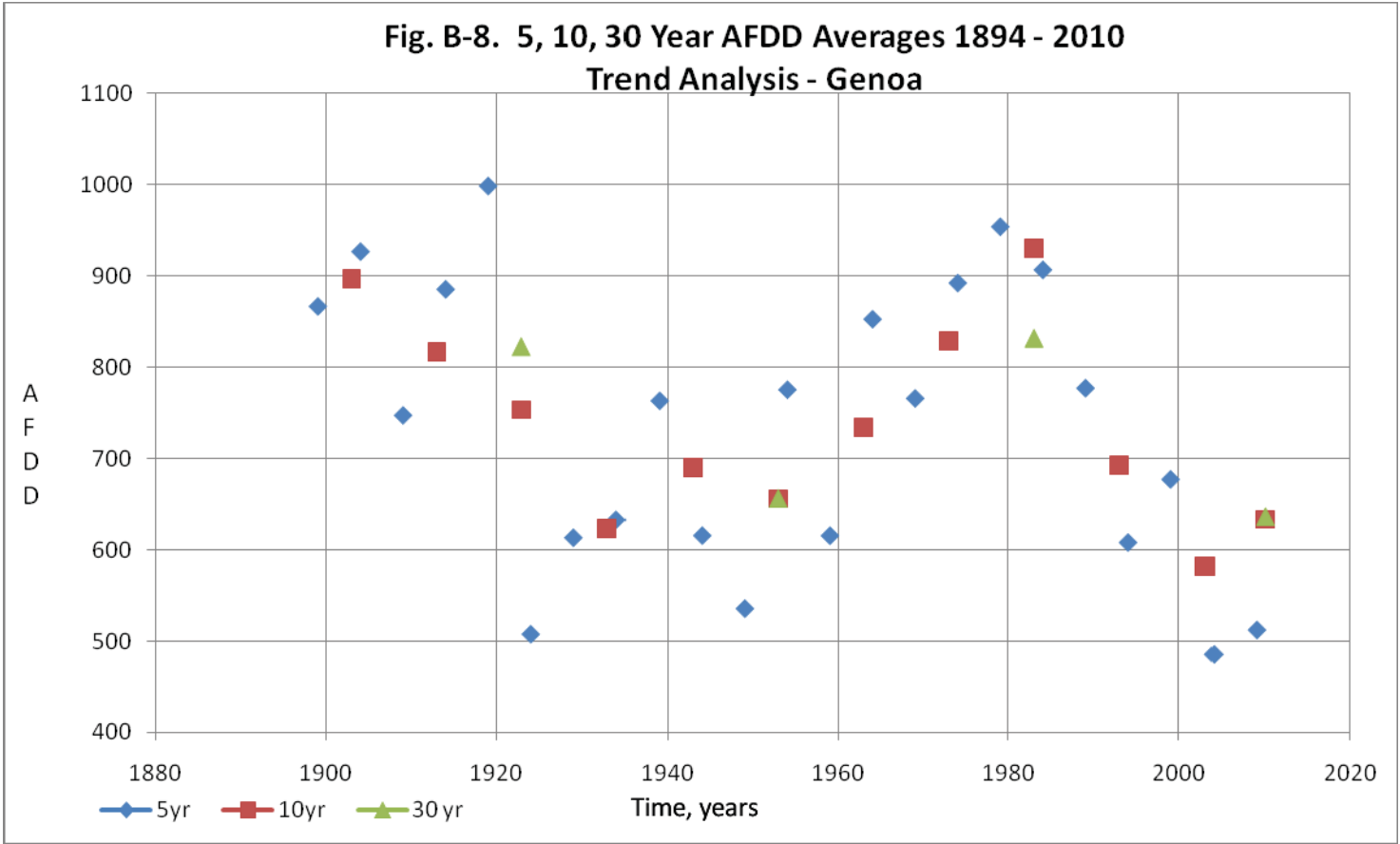
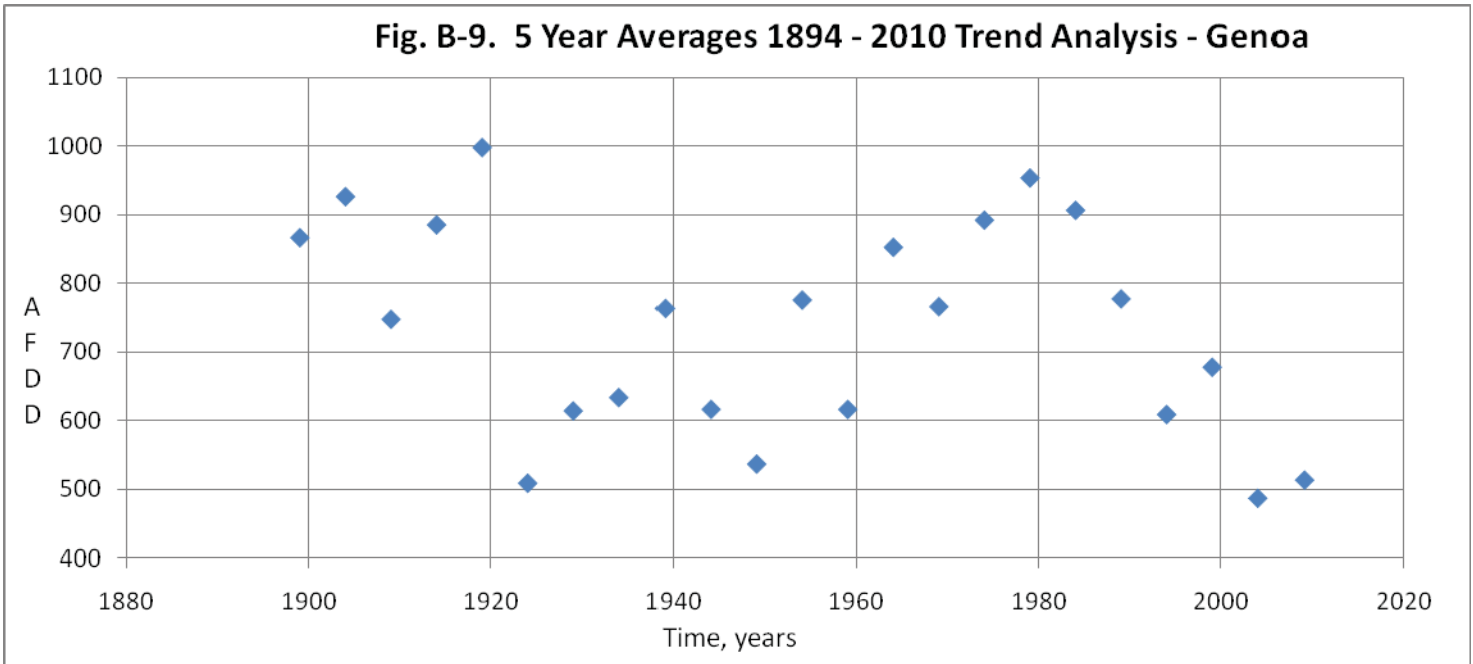


Figure B-7. AFDD₊₇ and AFDD₋₂₁ Trend Analysis - Genoa

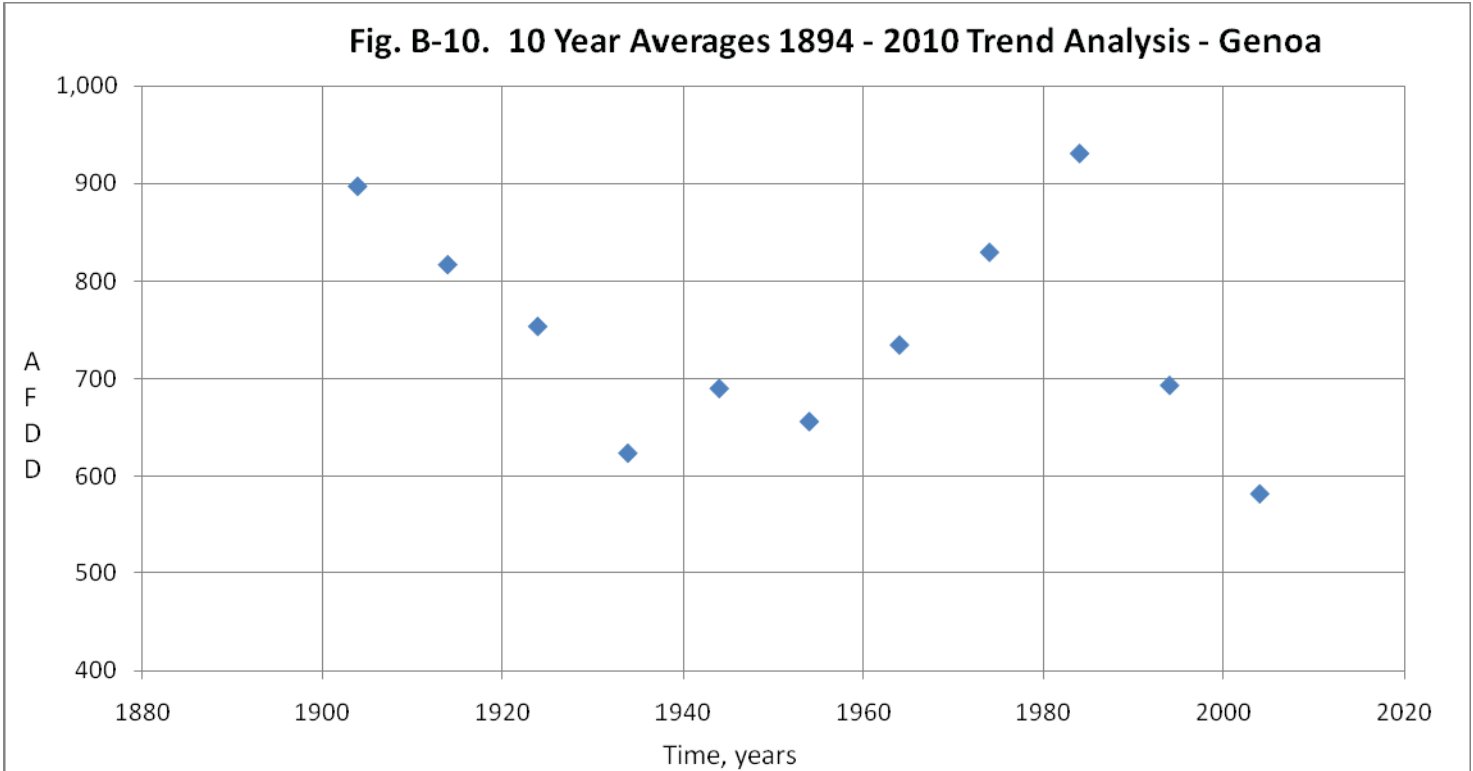
AFDD₊₇ and AFDD₋₂₁ Trend Analysis plots the difference in peak AFDD and AFDD 21 days before peak AFDD along with the difference in peak AFDD and AFDD 7 days after peak AFDD over time at Genoa.



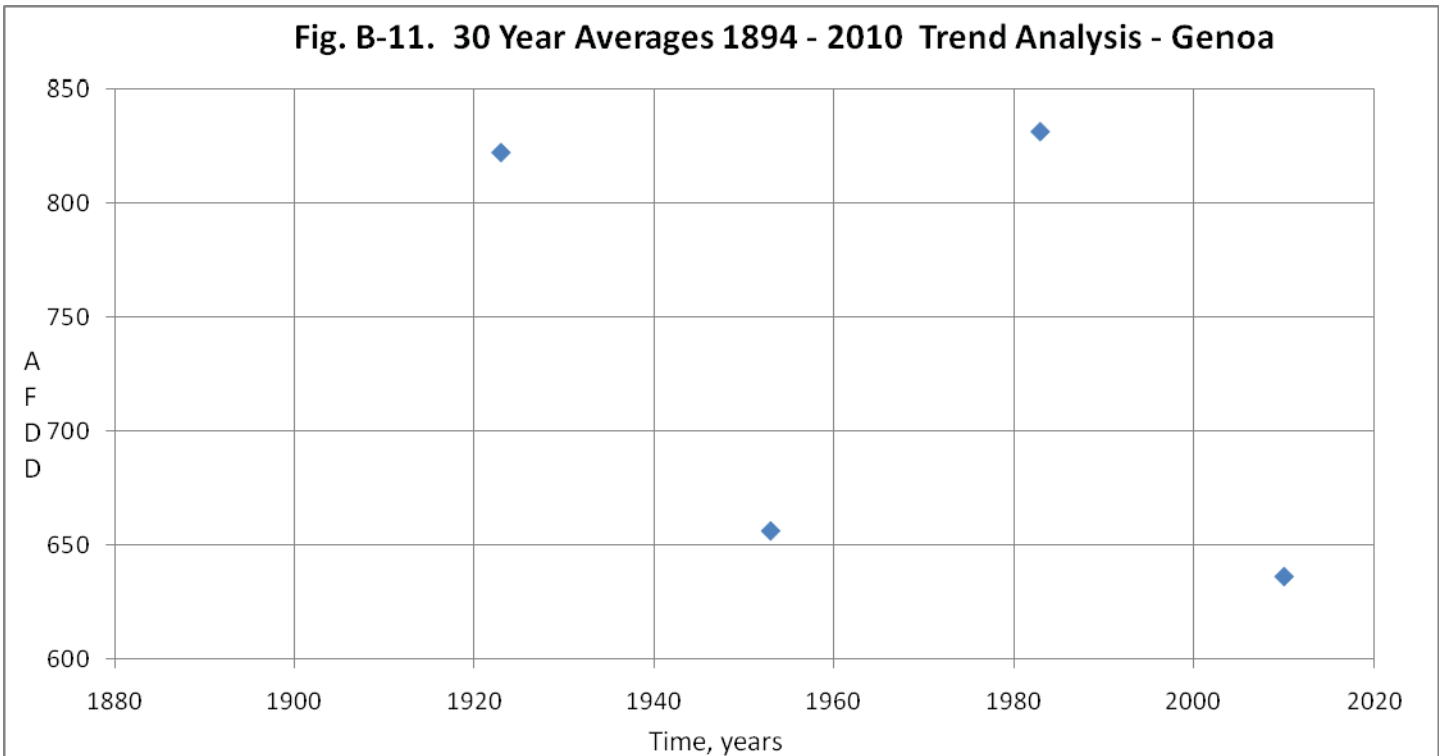
5, 10 and 30 Year AFDD Averages 1900 – 2010 Trend Analyses at Genoa.



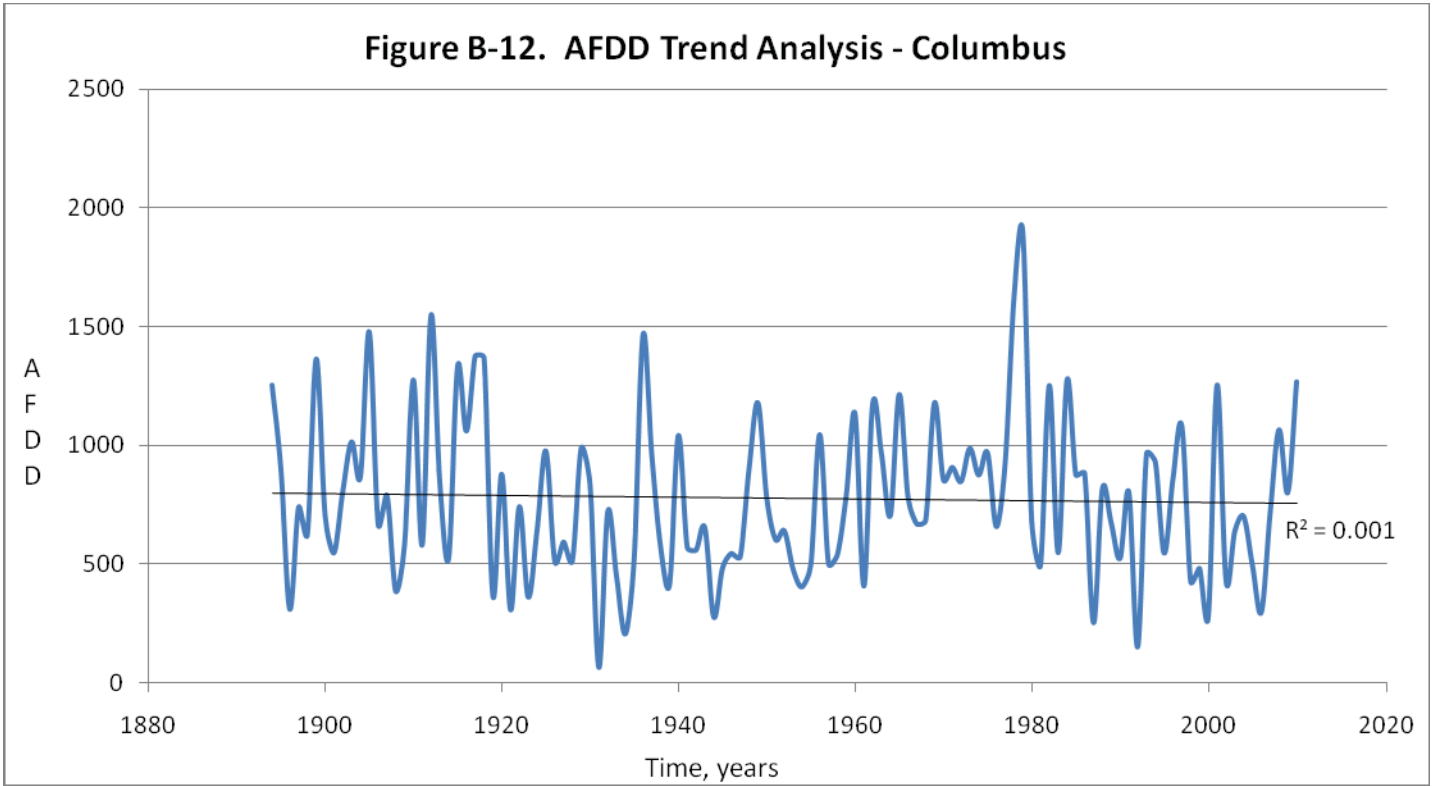
5 Year Averages 1894 – 2010 Trend Analysis shows the 5 year averages over time at Genoa.



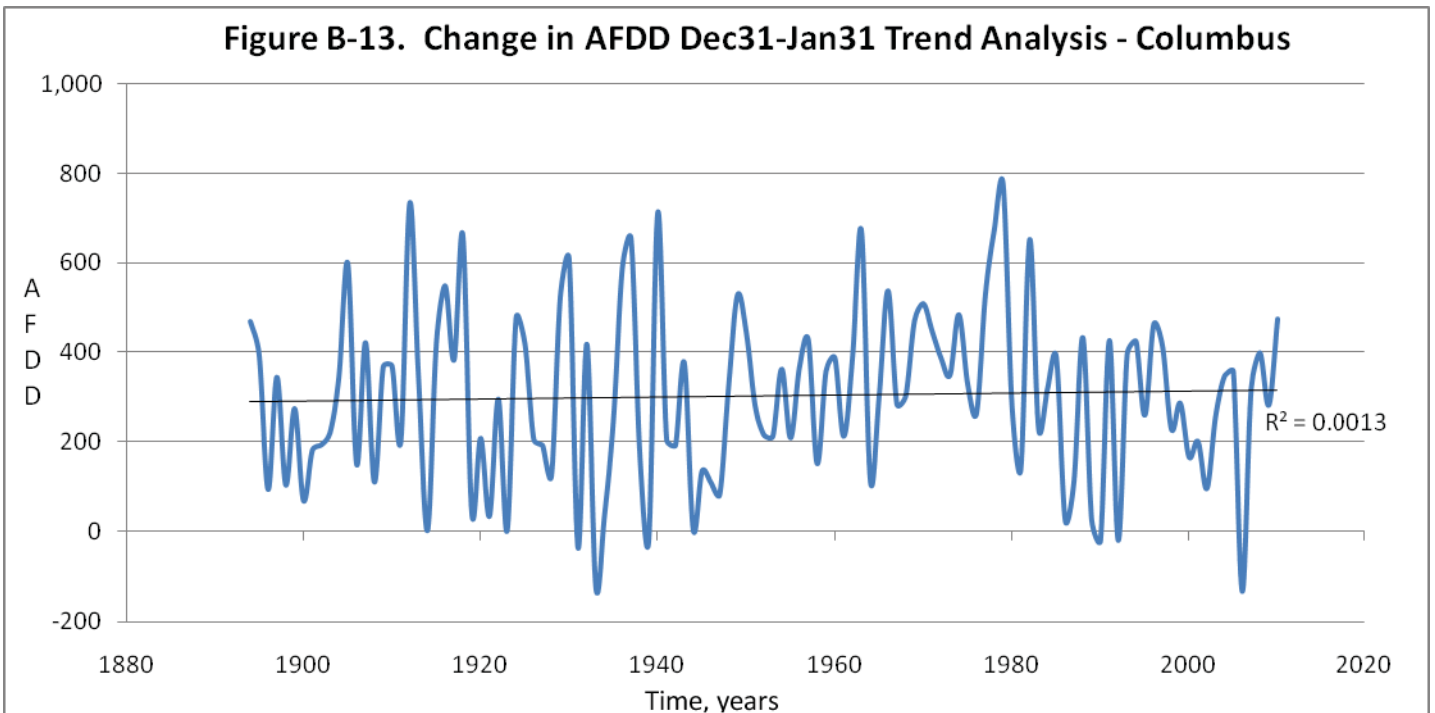
10 Year Averages 1894 – 2010 Trend Analysis shows the 10 year averages over time at Genoa.



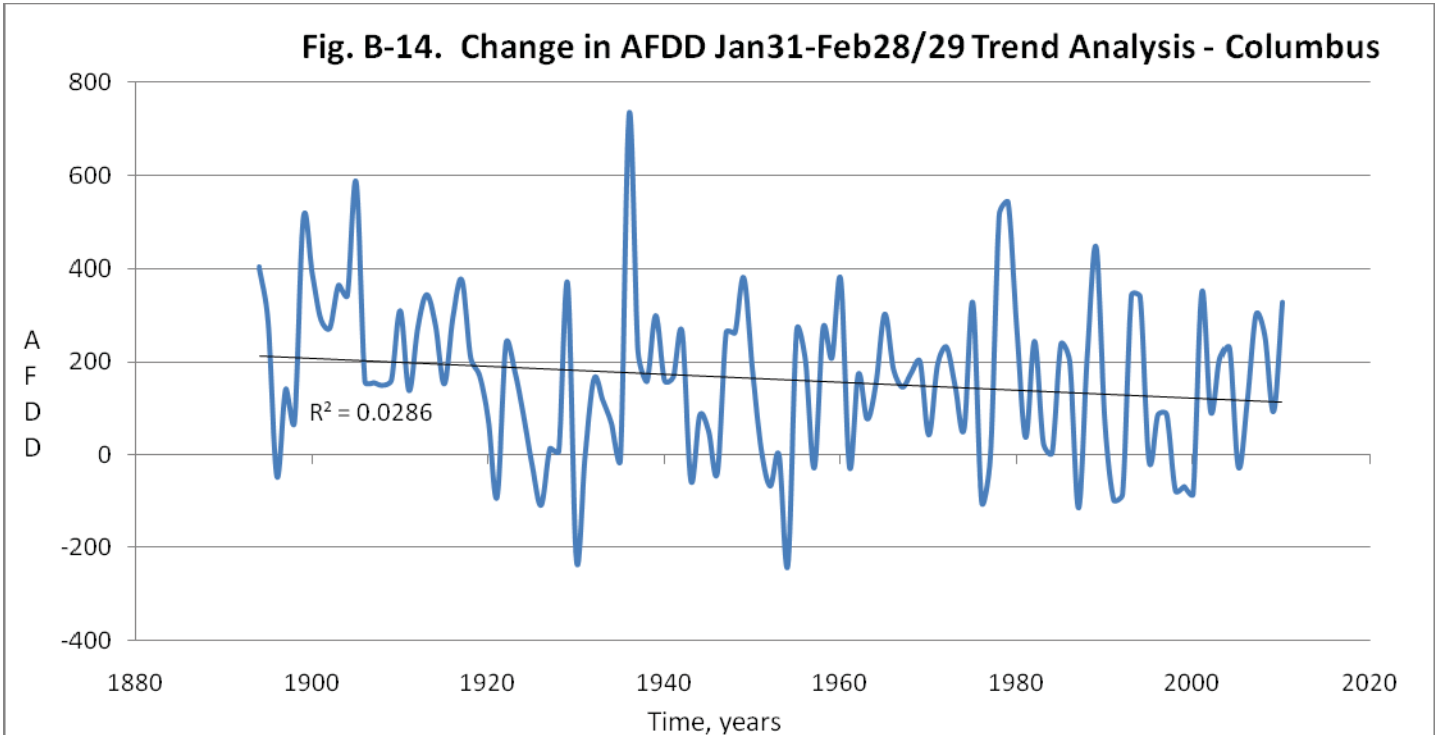
30 Year Averages 1894 – 2010 Trend Analysis shows the 30 year averages over time at Genoa.



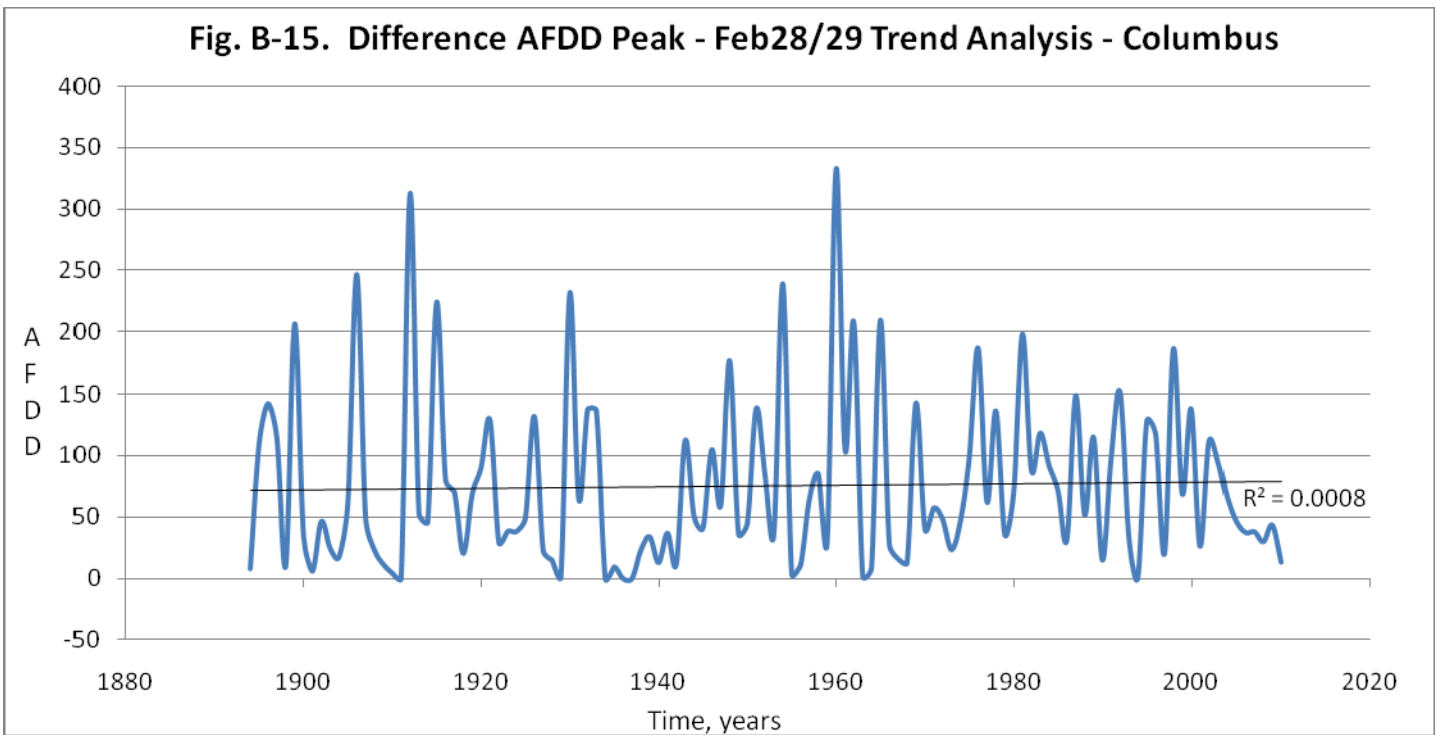
AFDD Trend Analysis shows peak AFDD over time at Columbus.



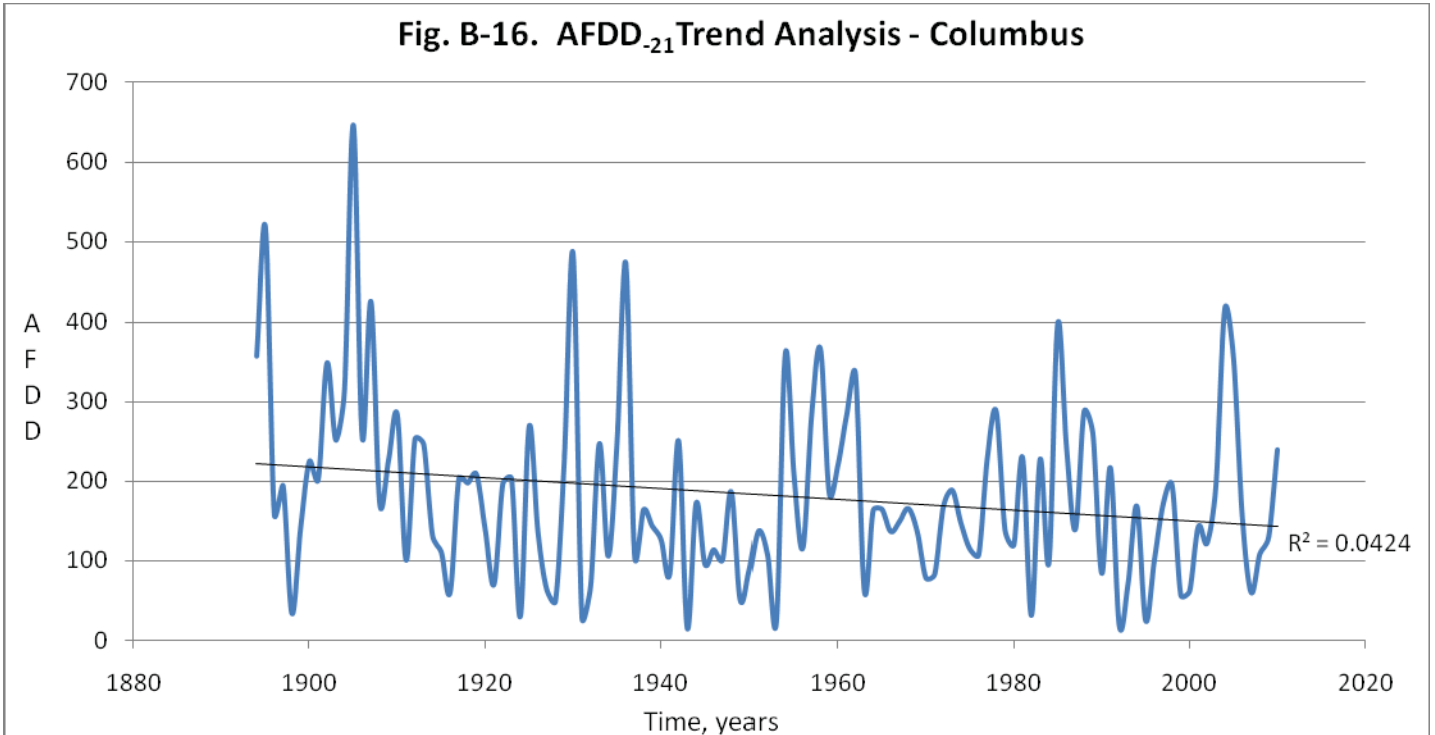
Change in AFDD Dec 31 – Jan 31 Trend Analysis shows the change in AFDD from Dec 31st through Jan 31st over time at Columbus.



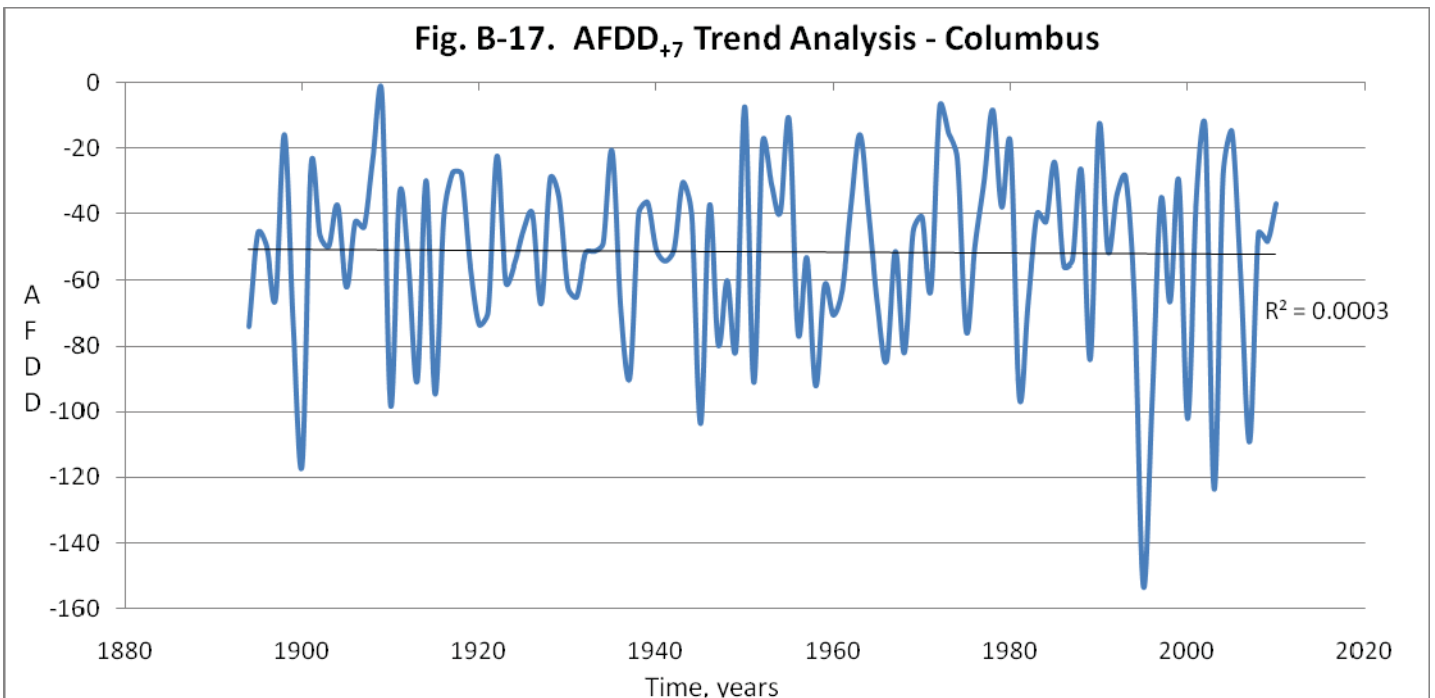
Change in AFDD Jan 31 – Feb 28/29 Trend Analysis shows the change in AFDD from Jan 31st – Feb 28th/29th over time at Columbus.



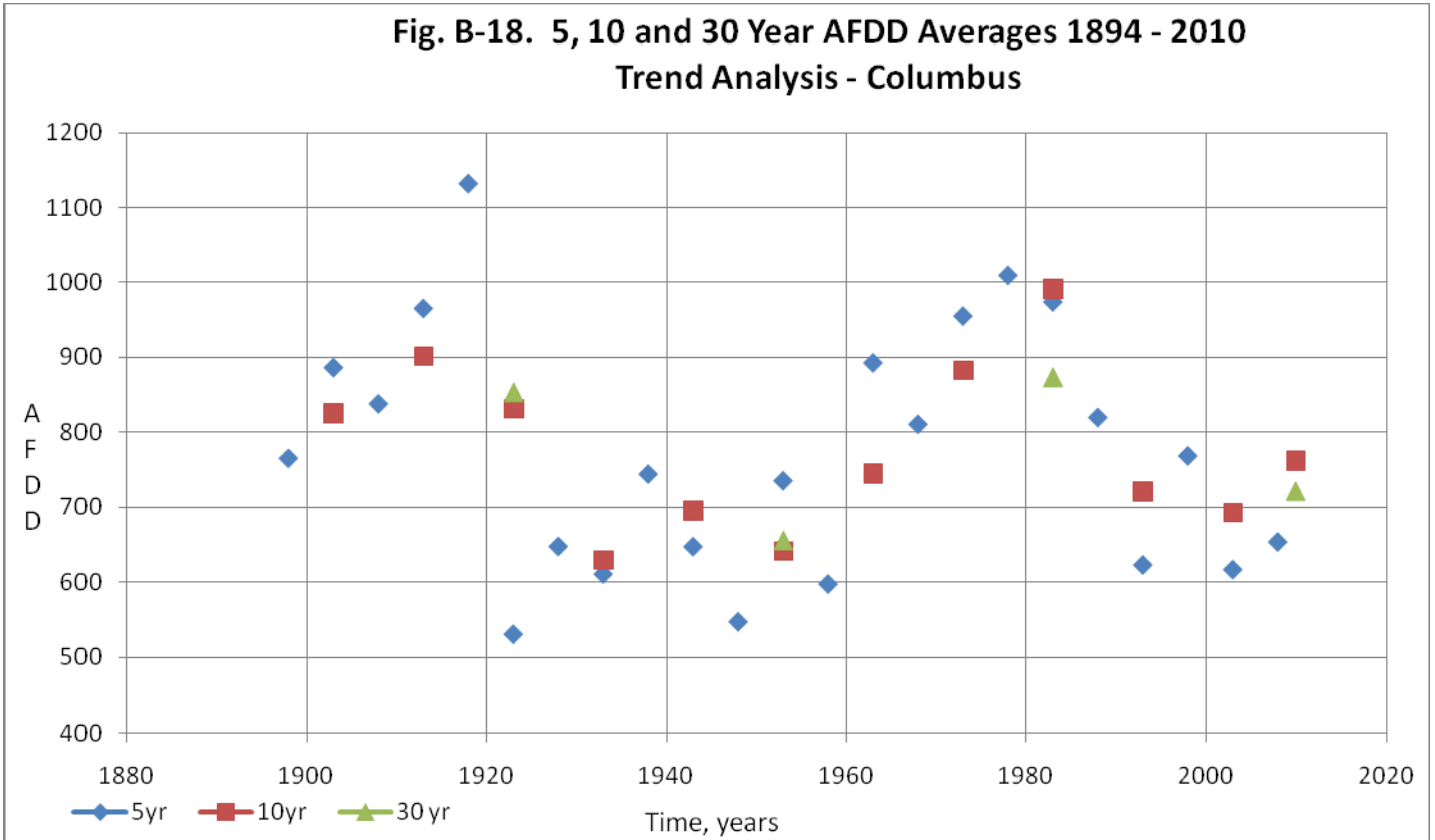
Difference AFDD Peak – Feb 28/29 Trend Analysis shows the difference between peak AFDD and Feb 28th/29th AFDD value over time at Columbus.



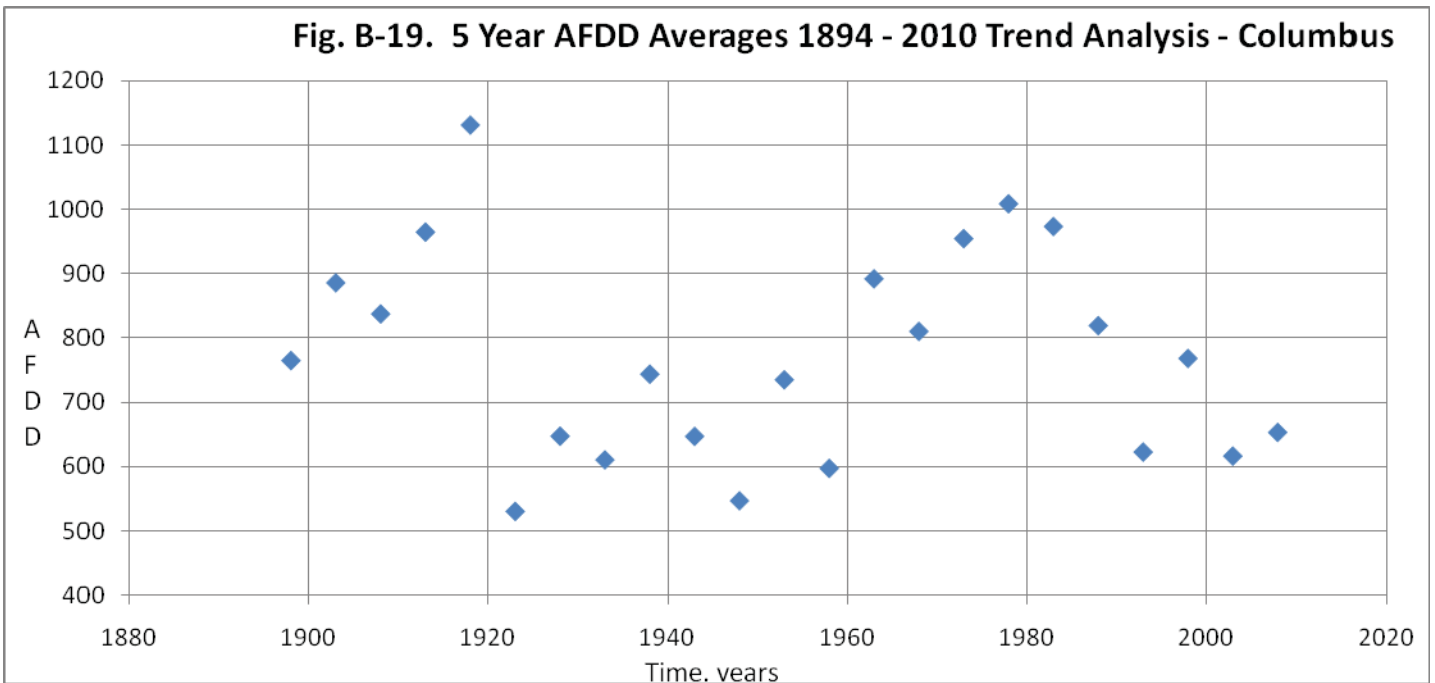
AFDD₋₂₁ Trend Analysis shows the change in AFDD during the 21 days before peak AFDD over time at Columbus.



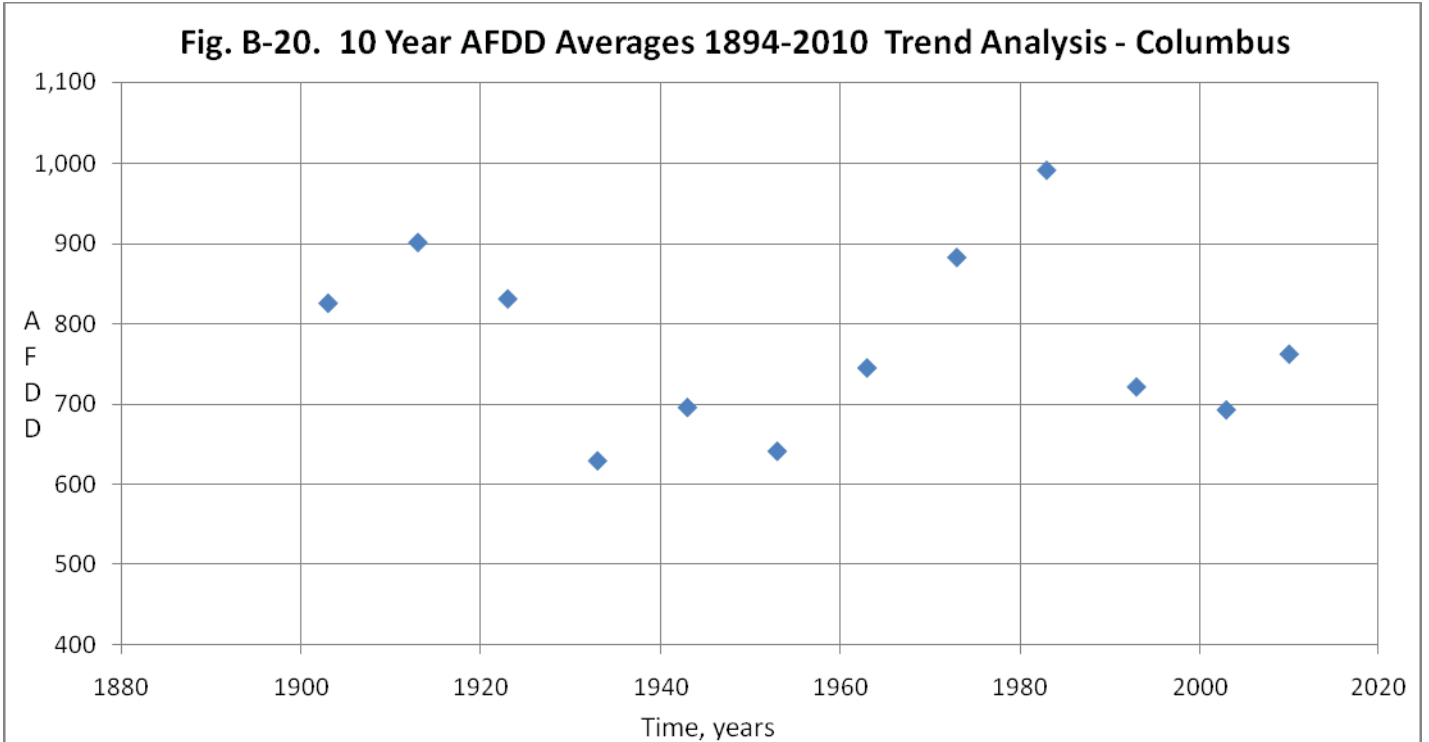
AFDD₊₇ Trend Analysis shows the change in AFDD during the 7 days after peak AFDD over time at Columbus.



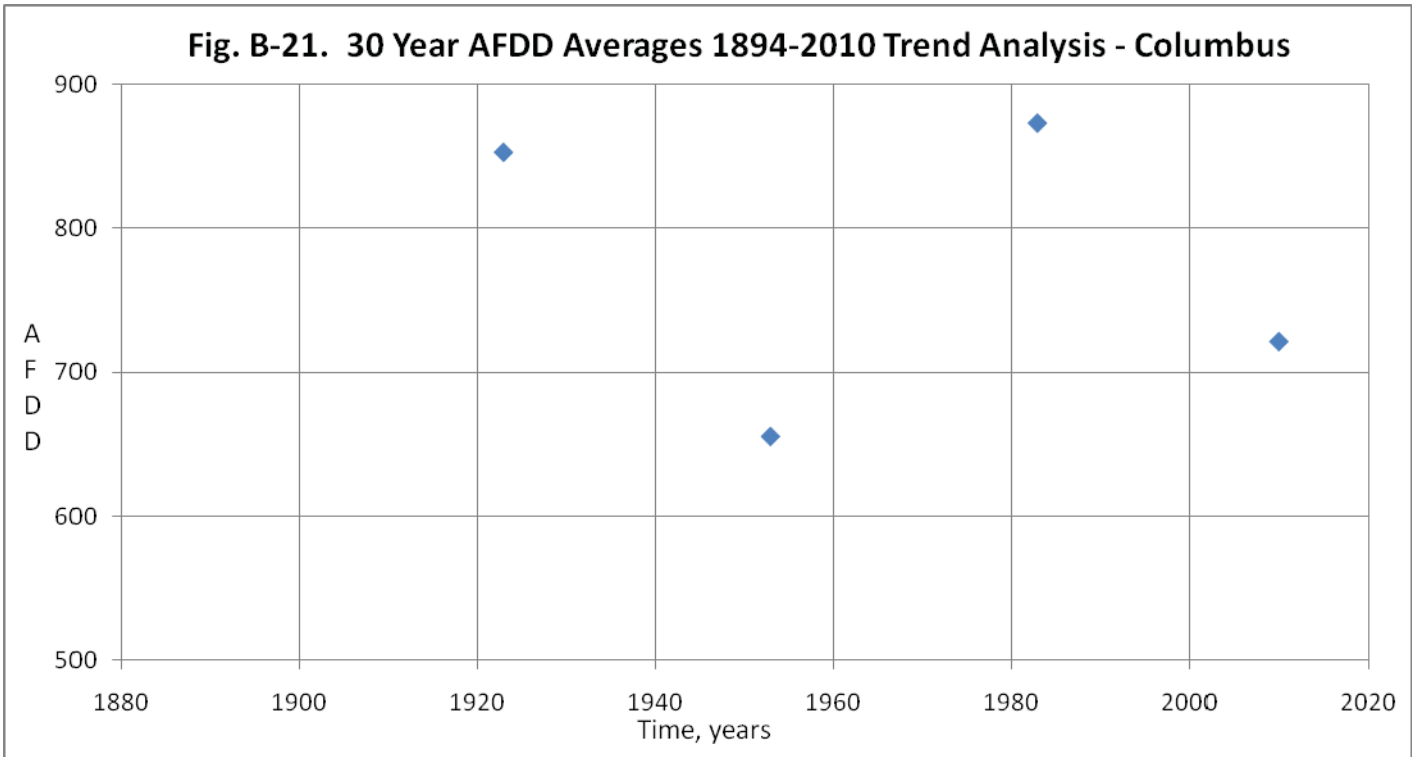
5, 10 and 30 Year AFDD Averages 1900 – 2010 Trend Analyses at Columbus.



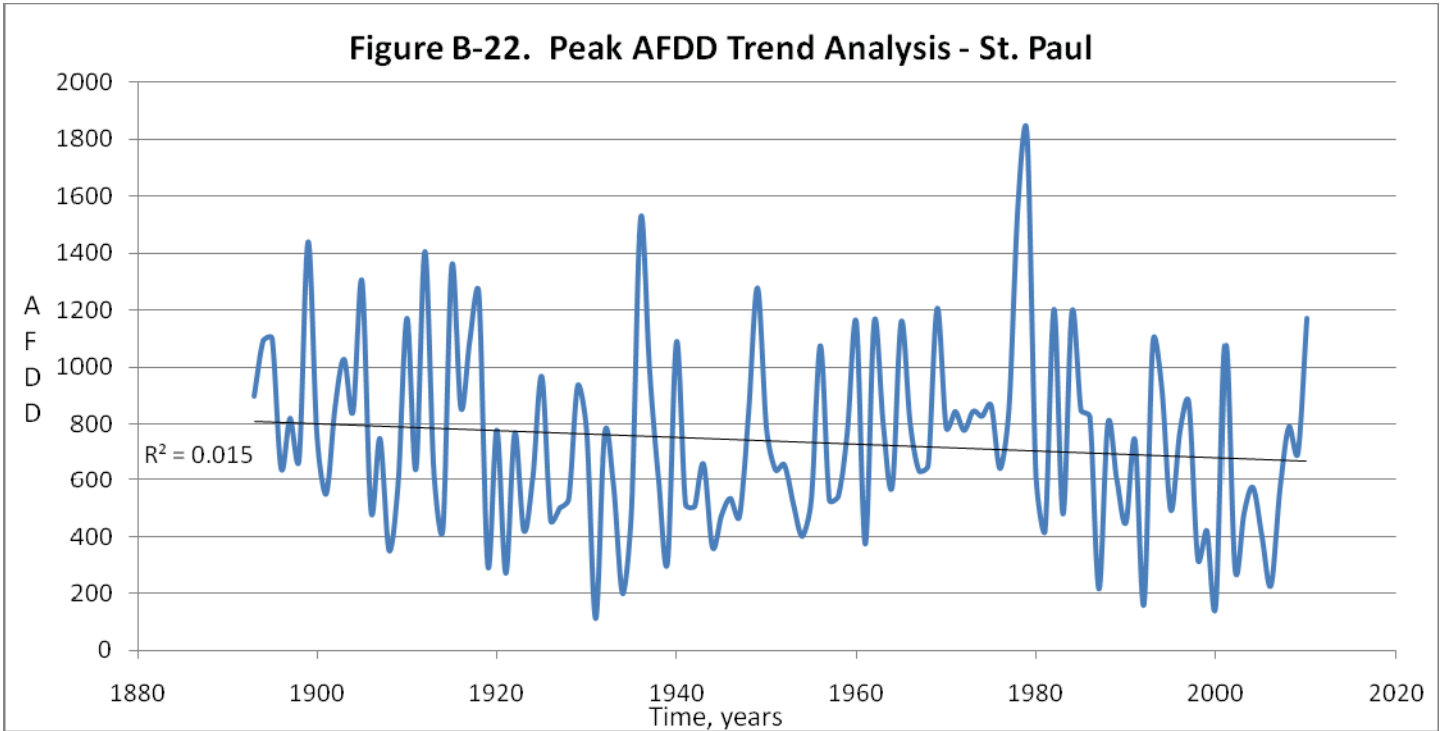
5 Year Averages 1894 – 2010 Trend Analysis shows the 5 year averages over time at Columbus.



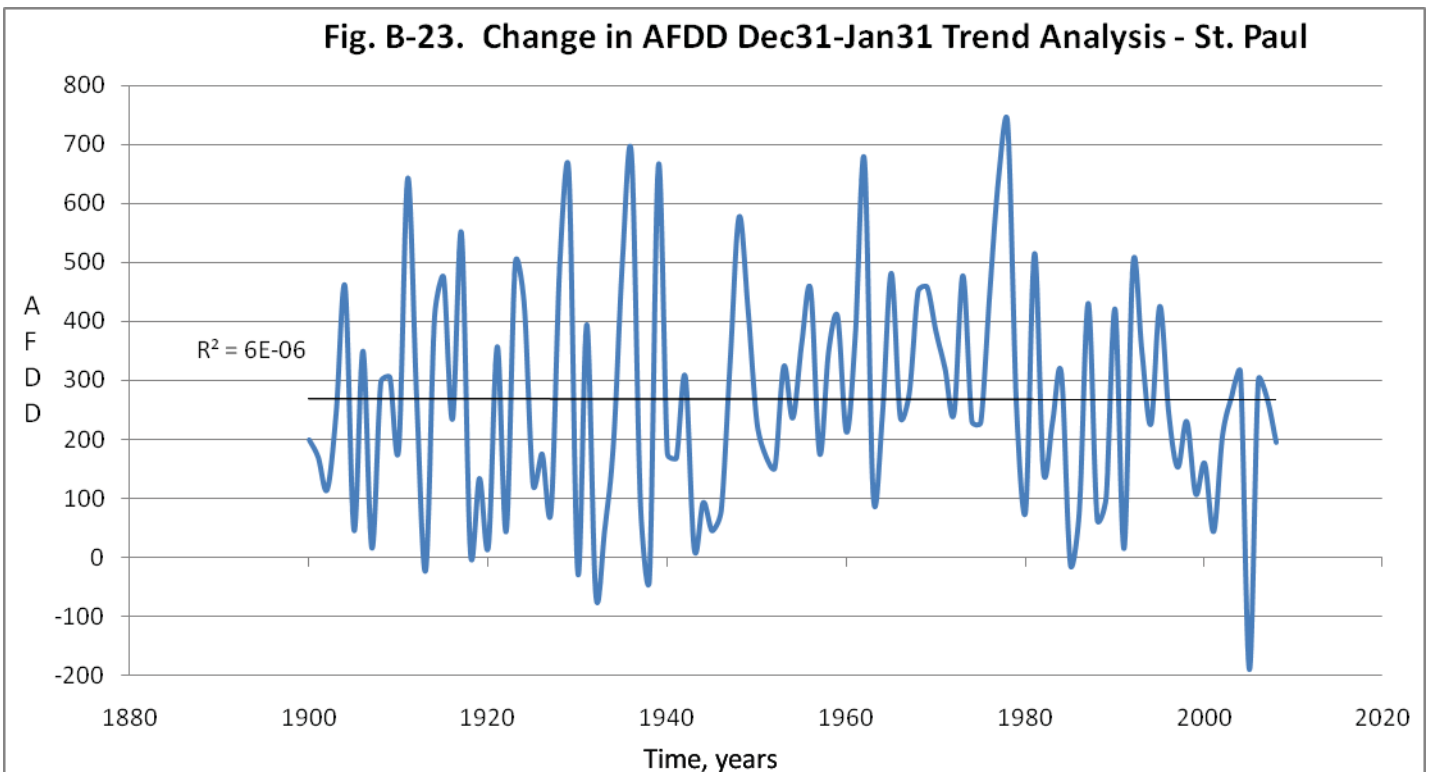
10 Year Averages 1894 – 2010 Trend Analysis shows the 10 year averages over time at Columbus.



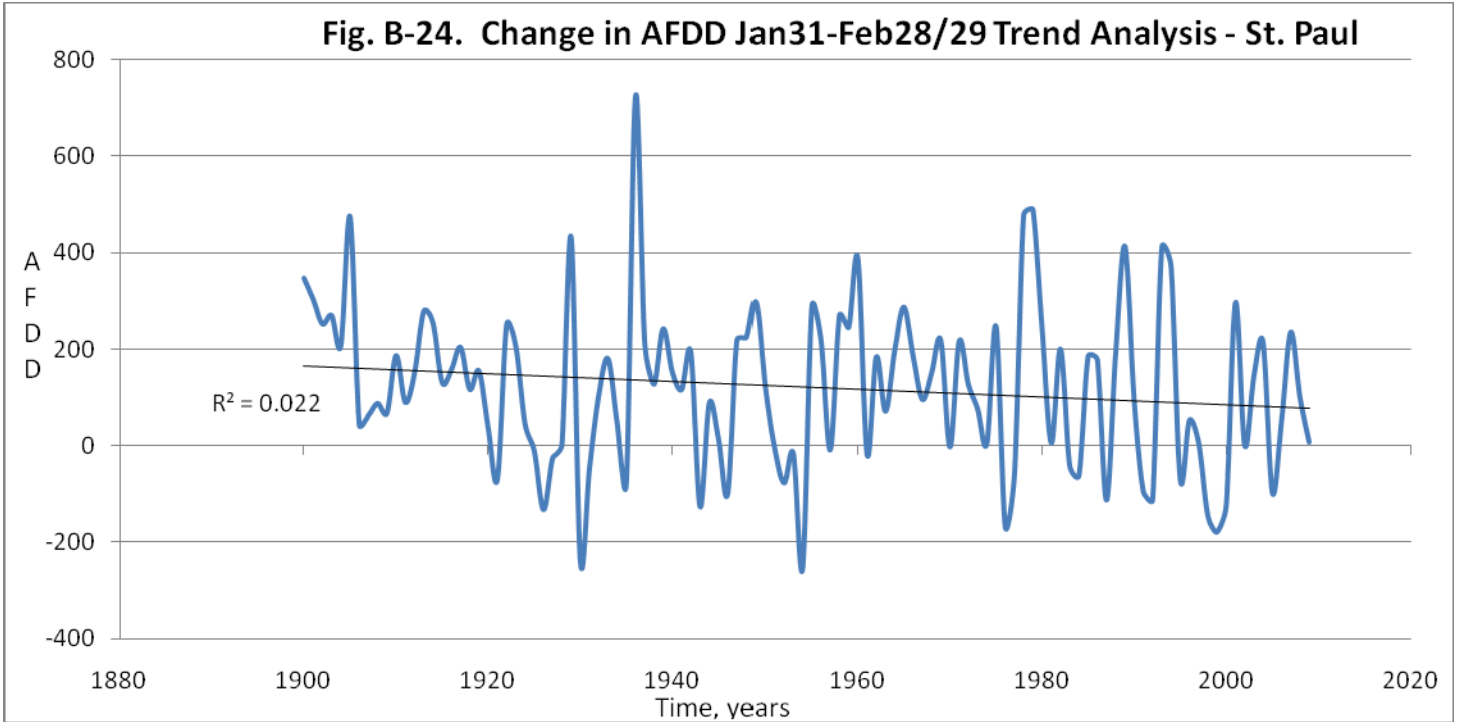
30 Year Averages 1894 – 2010 Trend Analysis shows the 30 year averages over time at Columbus.



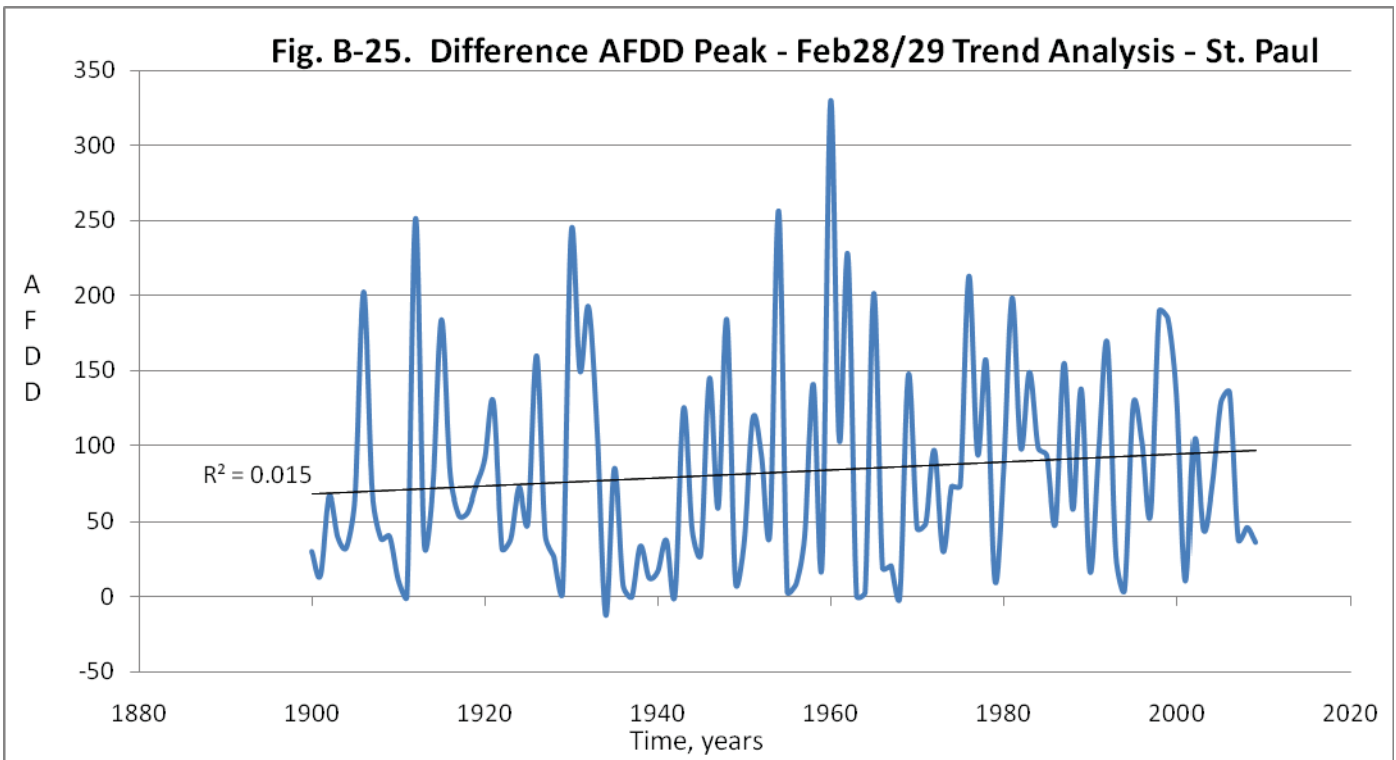
AFDD Trend Analysis shows peak AFDD over time at St. Paul.



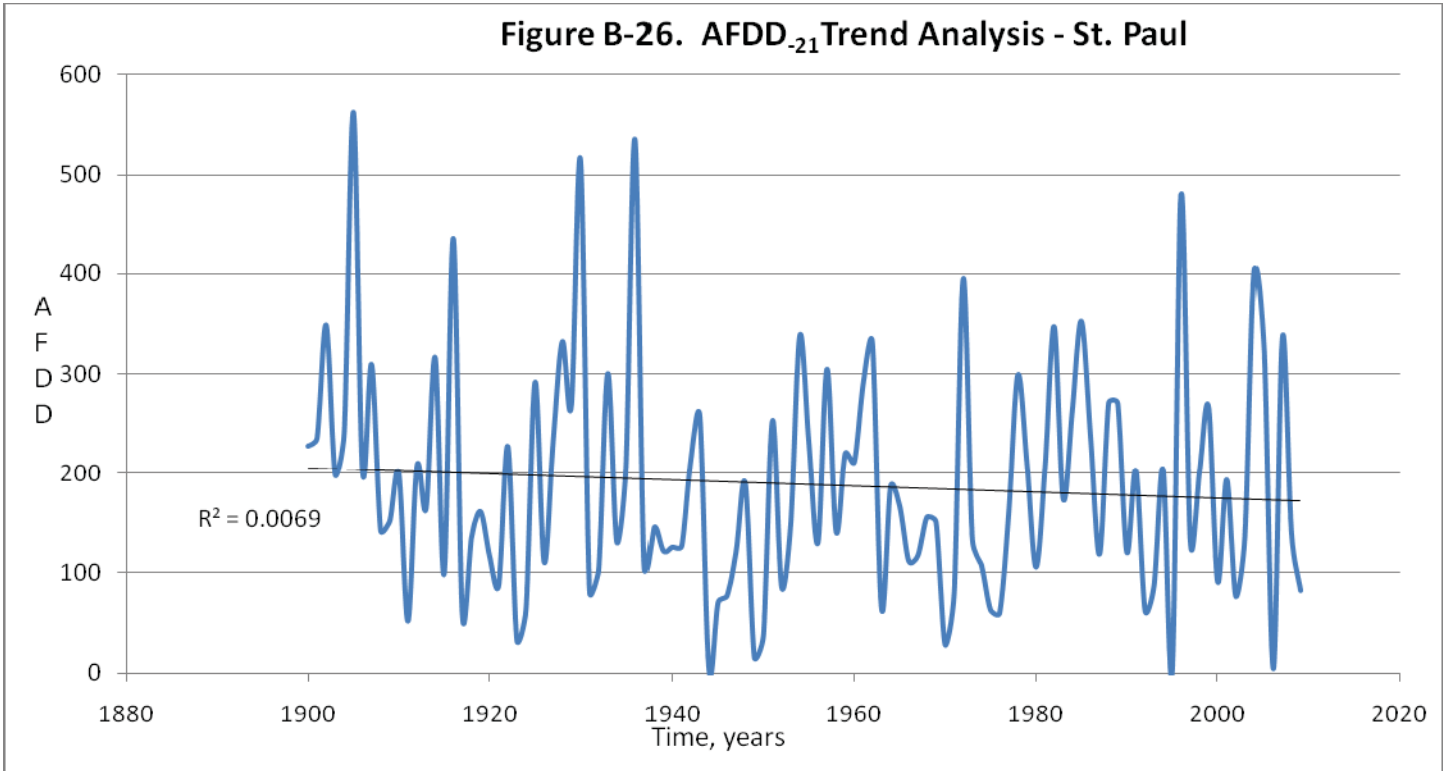
Change in AFDD Dec 31 – Jan 31 Trend Analysis shows the change in AFDD from Dec 31st through Jan 31st over time at St. Paul.



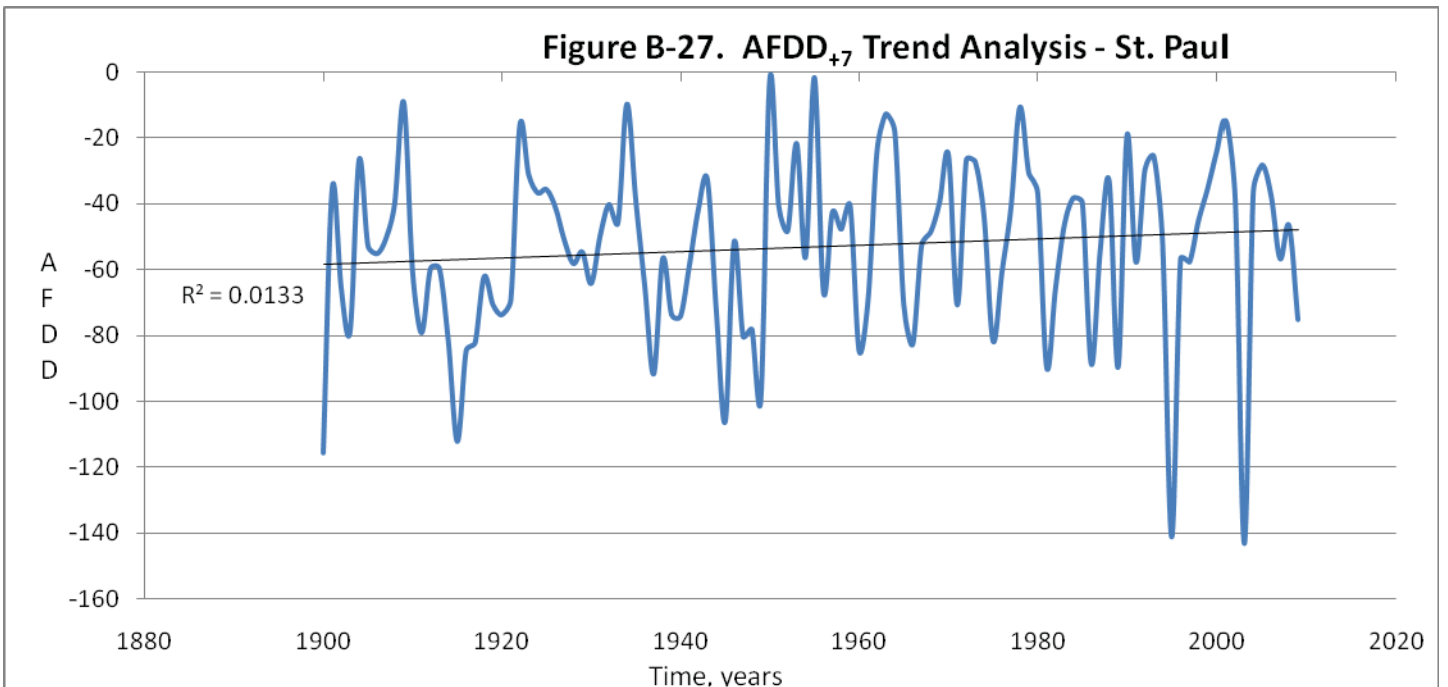
Change in AFDD Jan 31 – Feb 28/29 Trend Analysis shows the change in AFDD from Jan 31st – Feb 28th/29th over time at St. Paul.



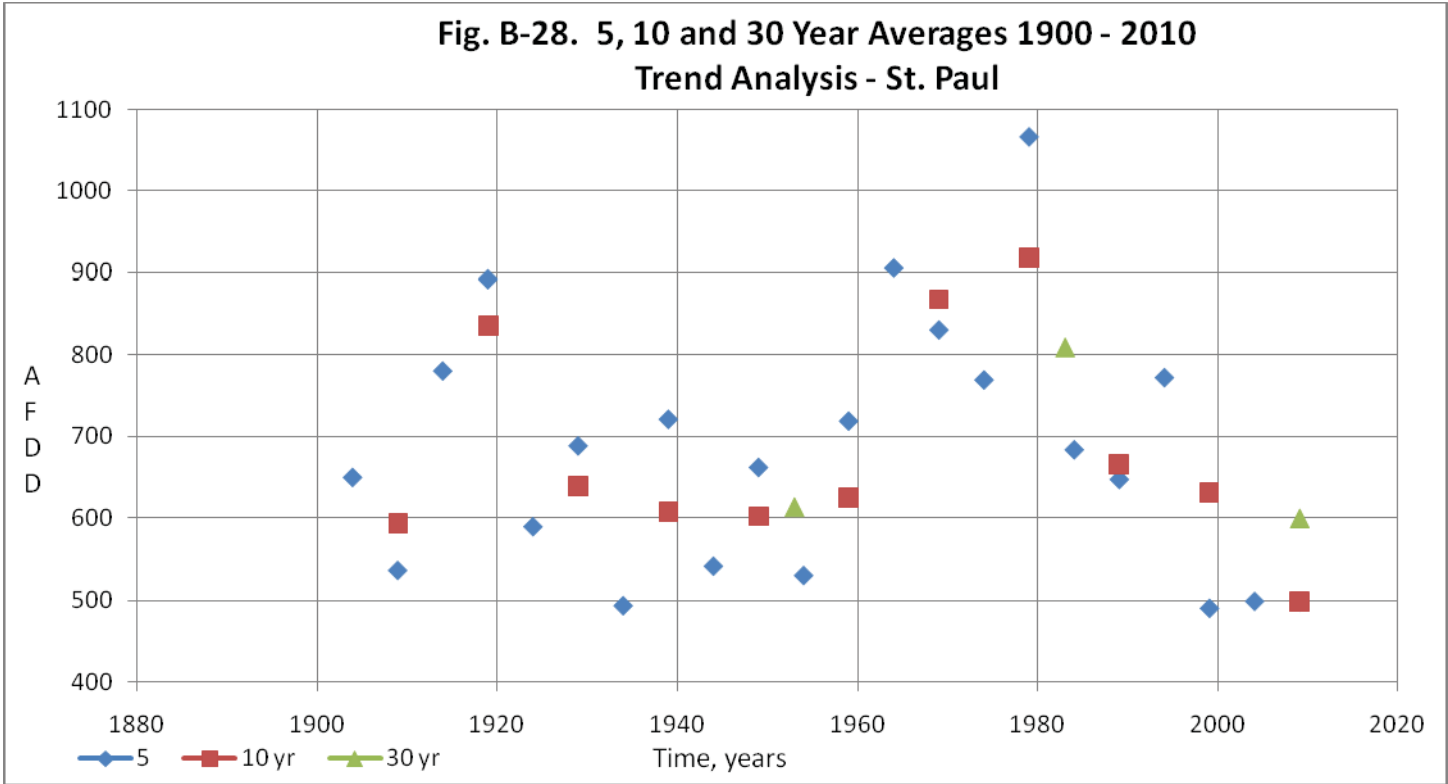
Difference AFDD Peak – Feb 28/29 Trend Analysis shows the difference between peak AFDD and Feb 28th/29th AFDD value over time at St. Paul.



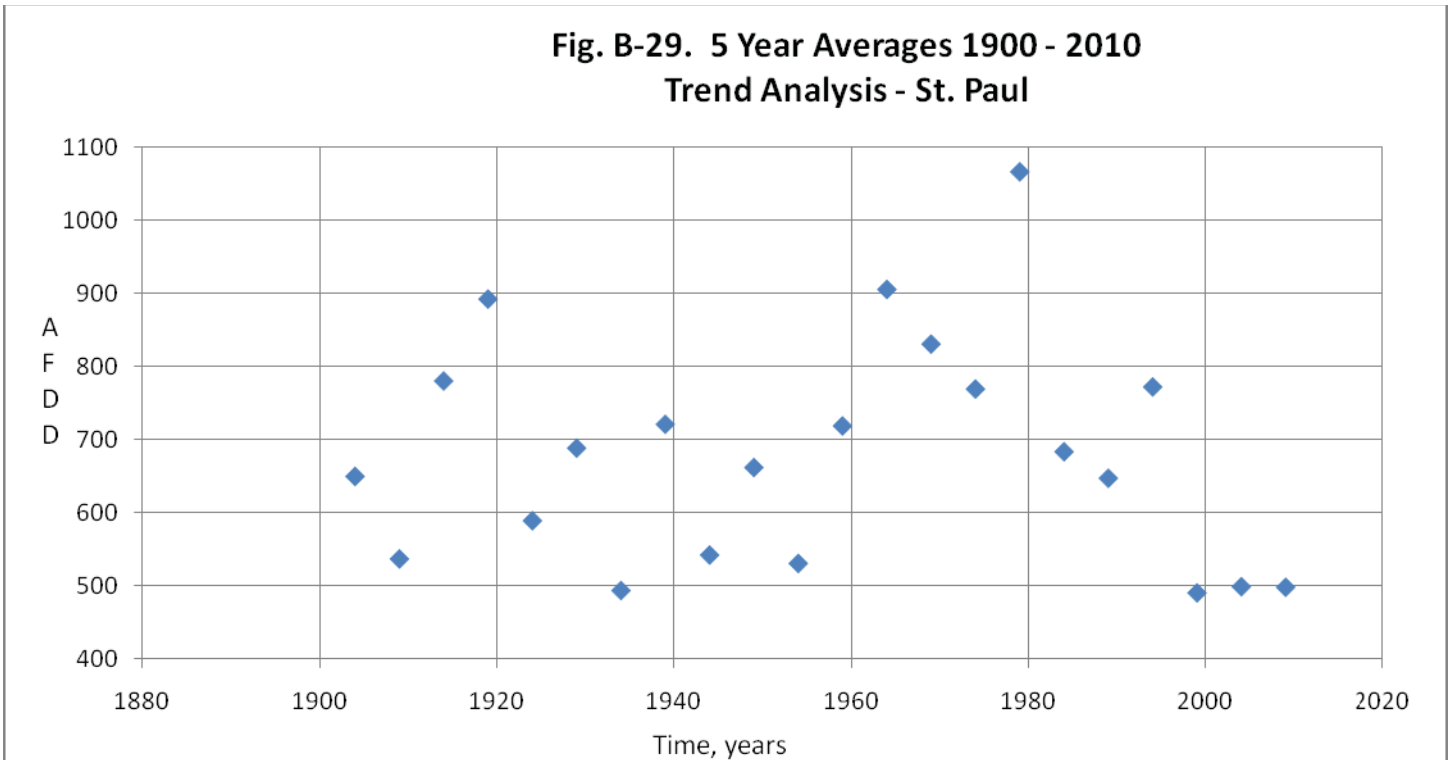
AFDD₋₂₁ Trend Analysis shows the change in AFDD during the 21 days before peak AFDD over time at St. Paul.



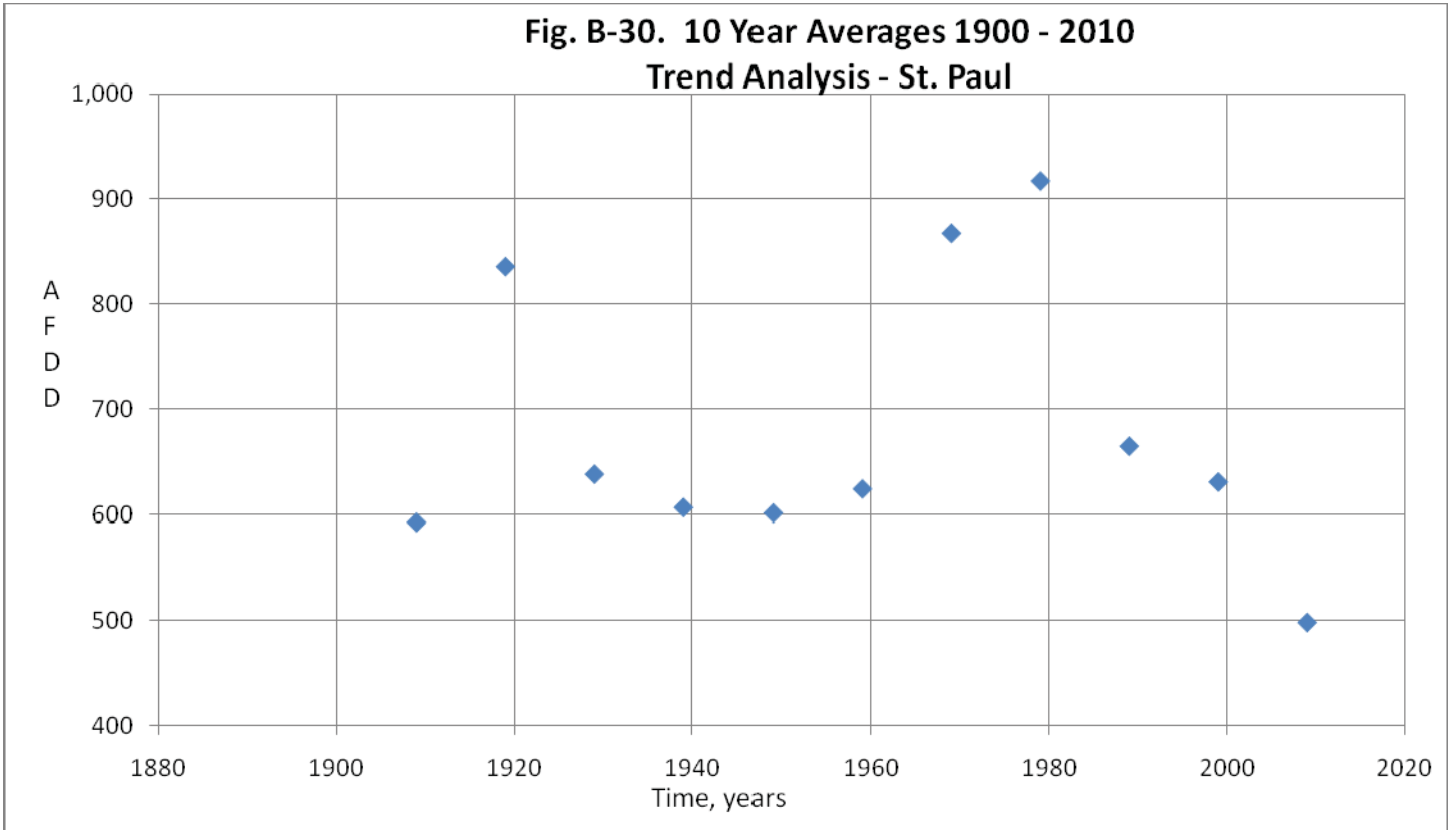
AFDD₊₇ Trend Analysis shows the change in AFDD during the 7 days after peak AFDD over time at St. Paul.



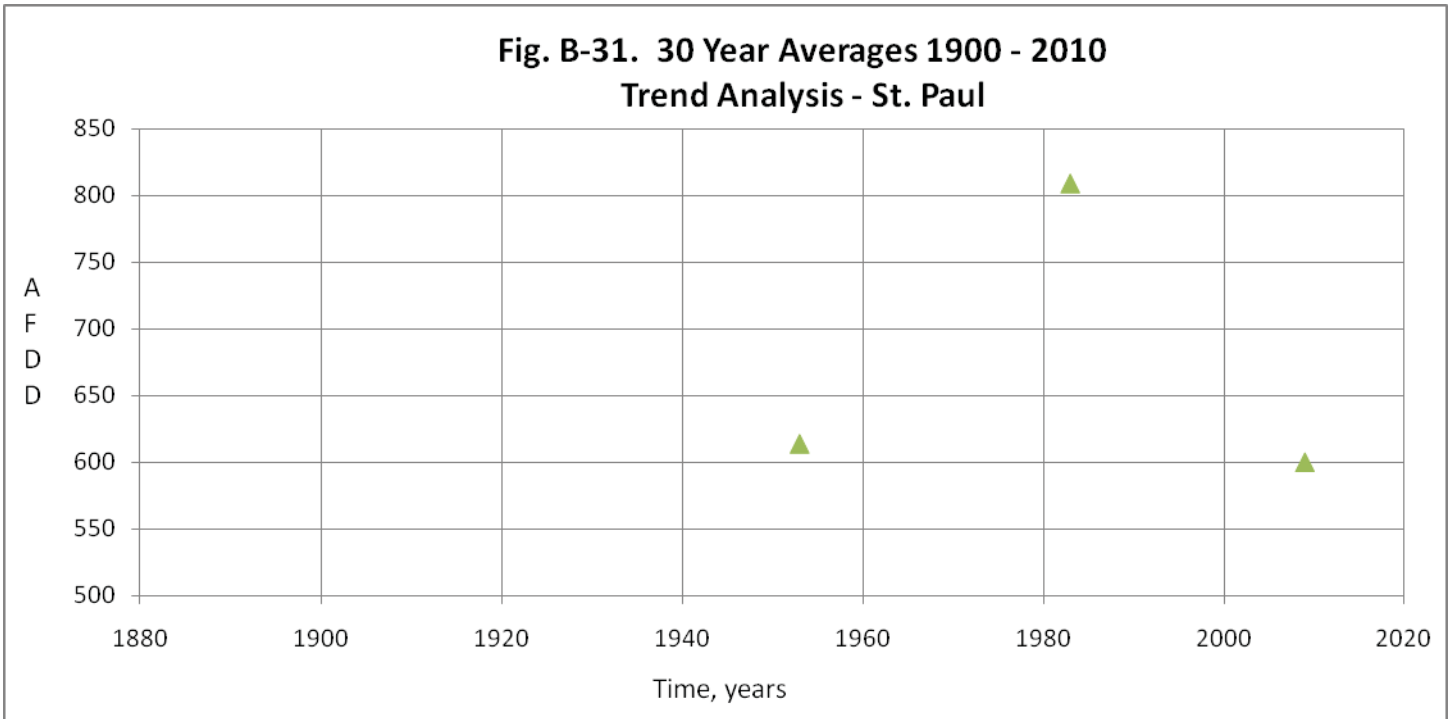
5, 10 and 30 Year AFDD Averages 1900 – 2010 Trend Analyses at St. Paul.



5 Year Averages 1894 – 2010 Trend Analysis shows the 5 year averages over time at St. Paul.

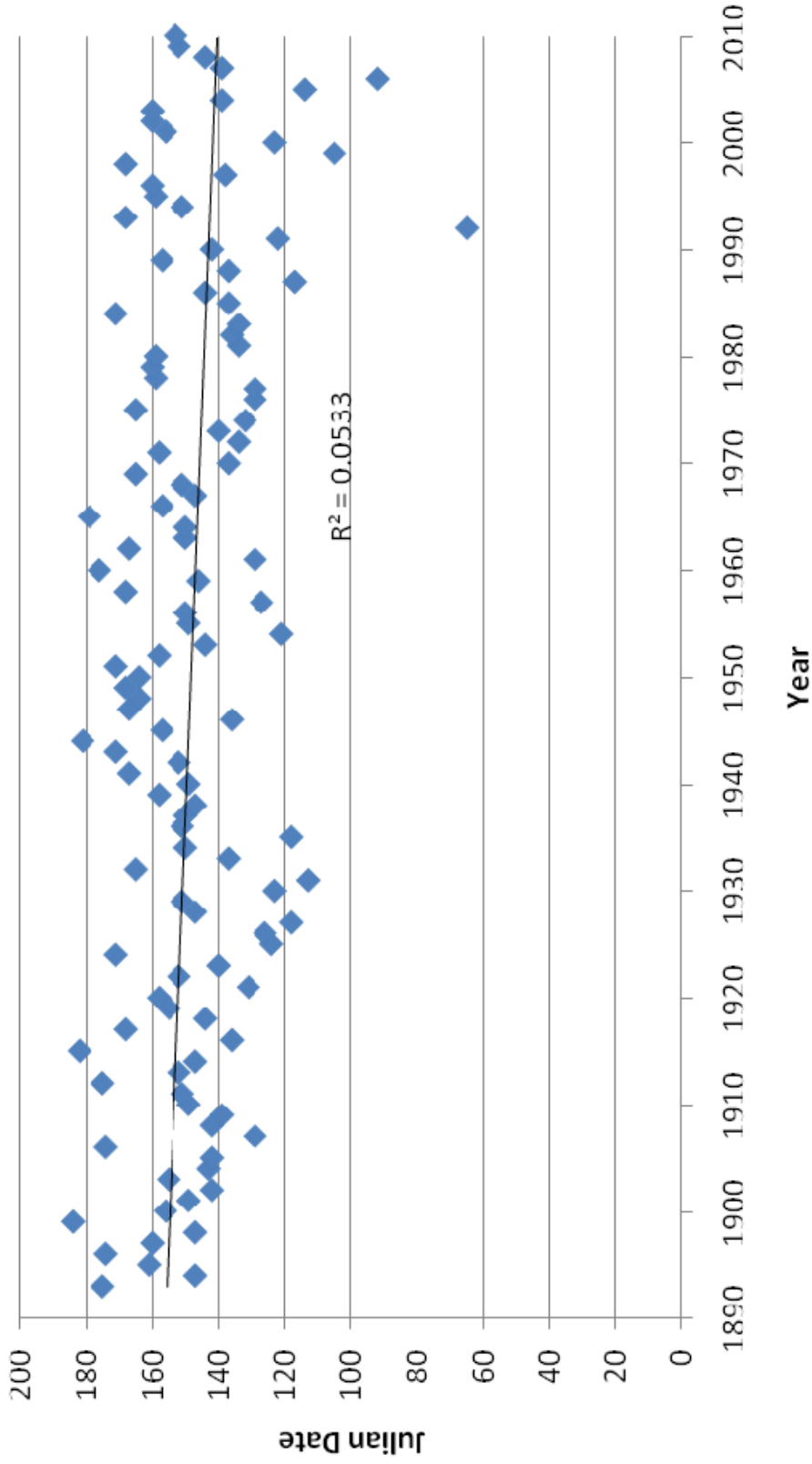


10 Year Averages 1894 – 2010 Trend Analysis shows the 10 year averages over time at St. Paul.



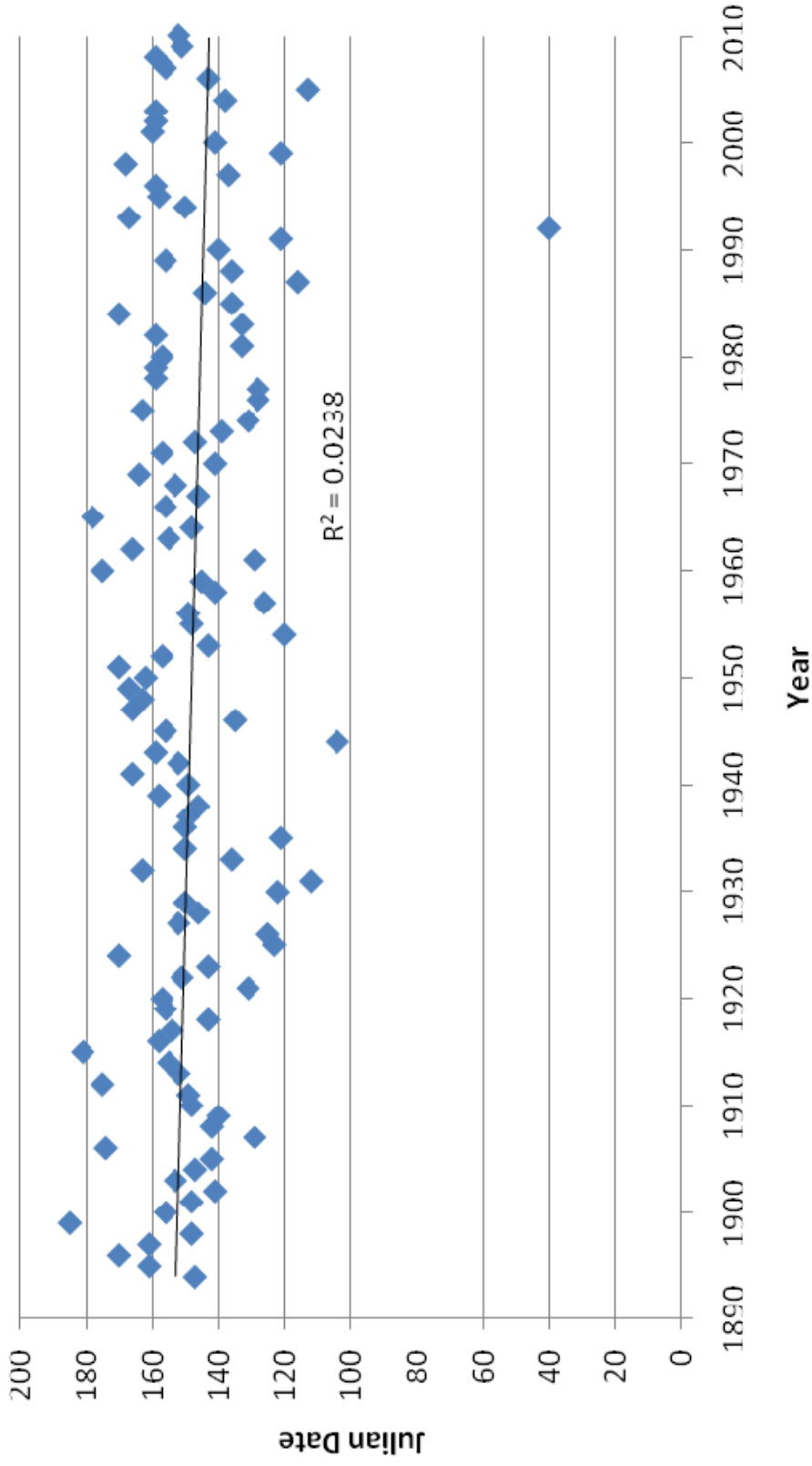
30 Year Averages 1894 – 2010 Trend Analysis shows the 30 year averages over time at St. Paul.

Figure B-32. Julian Date of AFDD_{max} vs Time



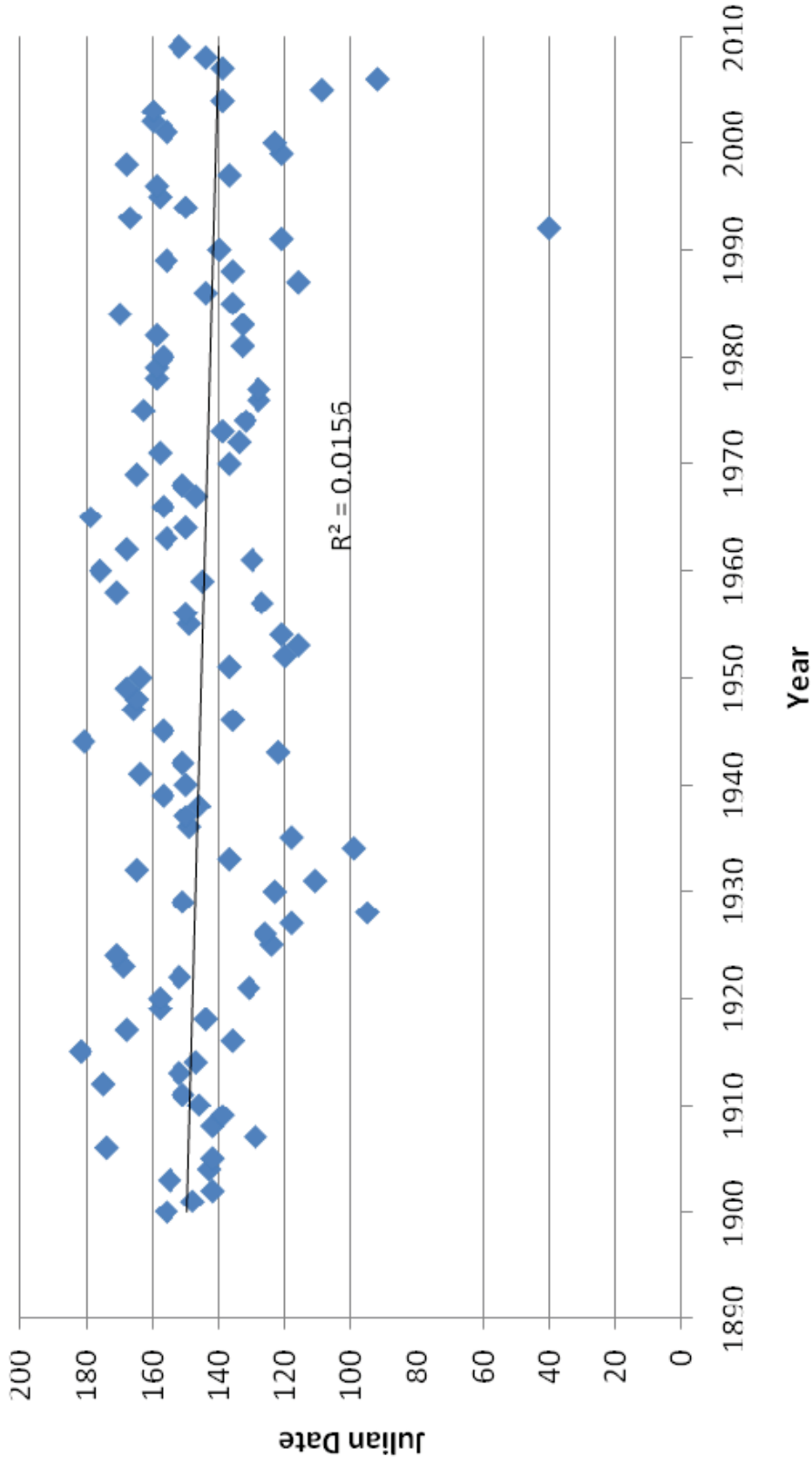
Trend of Julian Date vs. Year at Genoa

Figure B-33. Julian Date of AFDD_{max} vs Time



Trend of Julian Date vs. Year at Columbus

Figure B-34. Julian Date of AFDD_{max} vs Time



Trend of Julian Date vs. Year at St. Paul

ATTACHMENT C

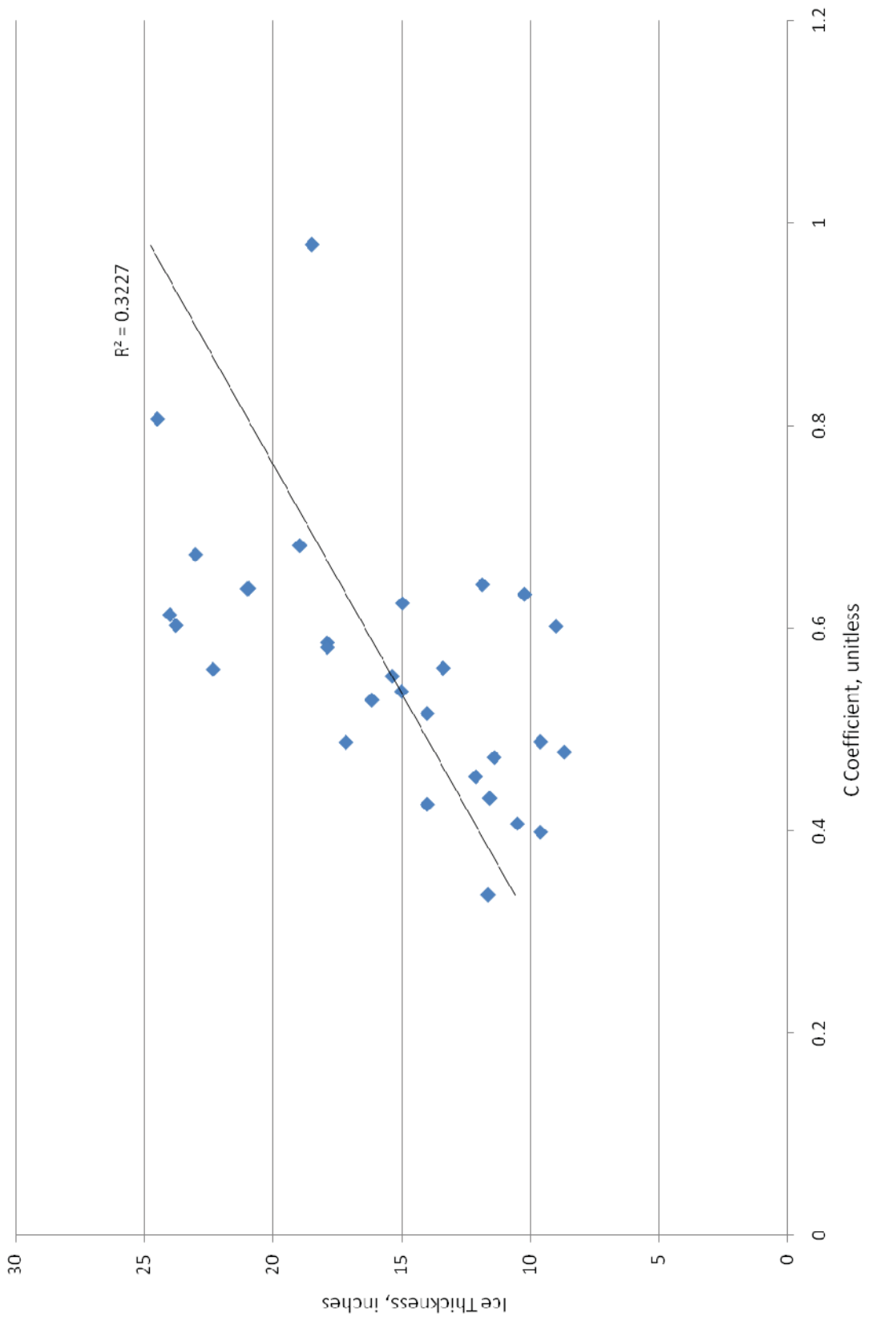
ICE THICKNESS

Table C-1. Measured Ice Thickness and Calculated C values

Date	Thickness, in	AFDD	C	Location
2/17/1948	12.1	716	0.45	Columbus
2/2/1966	13.4	571	0.56	Columbus
12/27/1968	9.0	224	0.60	Genoa
12/30/1968	10.2	261	0.63	Columbus
1/14/1969	9.6	581	0.40	Genoa
1/17/1969	15.0	575	0.62	Columbus
1/30/1969	15.4	774	0.55	Columbus
2/11/1969	16.2	934	0.53	Columbus
2/11/1969	17.9	934	0.59	Columbus
2/12/1969	17.9	948	0.58	Columbus
3/5/1969	20.9	1074	0.64	Genoa
1/4/1978	11.9	341	0.64	Columbus
1/5/1978	18.5	357	0.98	Columbus
1/24/1978	15.0	780	0.54	Columbus
1/25/1978	19.0	775	0.68	Columbus
2/15/1978	11.6	1197	0.34	Columbus
2/16/1978	17.2	1243	0.49	Columbus
3/6/1978	24.0	1534	0.61	Genoa
3/8/1978	22.3	1595	0.56	Genoa
12/19/1978	8.7	331	0.48	Genoa
1/17/1979	24.5	923	0.81	Genoa
2/13/1979	23.8	1557	0.60	Genoa
2/3/1988	11.4	584	0.47	Genoa
2/10/1988	11.6	720	0.43	Genoa
1/4/2001	9.6	388	0.49	St. Paul
3/2/2001	14.0	1082	0.43	St. Paul
3/2/2001	21.0	1082	0.64	Genoa
1/7/2009	10.5	667	0.41	Genoa
1/14/2010	14.0	738	0.52	Genoa
3/3/2010	23.0	1171	0.67	Genoa
			0.56	Average
			0.13	St. Dev
			0.56	Median

This table contains ice measurement data collected by the USGS. Corresponding AFDD values were used to calculate a C value for each measurement.

Figure C-1. Ice thickness Vs. C



The table above plots measured ice thickness versus the calculated C values.

Table C-2. Estimated Ice Thickness - Genoa

Year	Peak AFDD Date	Peak AFDD	Ice Thickness at Peak AFDD w/ C=0.4	Ice Thickness at Peak AFDD w/ C=0.6	Year	Peak AFDD Date	Peak AFDD	Ice Thickness at Peak AFDD w/ C=0.4	Ice Thickness at Peak AFDD w/ C=0.6
1892 - 93	3/25/1893	898	12.0	18.0	1917 - 18	2/22/1918	1258	14.2	21.3
1893 - 94	2/25/1894	1093	13.2	19.8	1918 - 19	3/5/1919	299	6.9	10.4
1894 - 95	3/16/1895	1100	13.3	19.9	1919 - 20	3/7/1920	779	11.2	16.7
1895 - 96	3/23/1896	645	10.2	15.2	1920 - 21	2/9/1921	273	6.6	9.9
1896 - 97	3/15/1897	821	11.5	17.2	1921 - 22	3/2/1922	768	11.1	16.6
1897 - 98	2/25/1898	676	10.4	15.6	1922 - 23	2/18/1923	423	8.2	12.3
1898 - 99	4/3/1899	1440	15.2	22.8	1923 - 24	3/20/1924	610	9.9	14.8
1899 - 1900	3/6/1900	757	11.0	16.5	1924 - 25	2/2/1925	967	12.4	18.7
1900 - 01	2/27/1901	550	9.4	14.1	1925 - 26	2/4/1926	458	8.6	12.8
1901 - 02	2/20/1902	859	11.7	17.6	1926 - 27	1/27/1927	502	9.0	13.4
1902 - 03	3/5/1903	1028	12.8	19.2	1927 - 28	2/25/1928	533	9.2	13.9
1903 - 04	2/21/1904	843	11.6	17.4	1928 - 29	3/1/1929	935	12.2	18.3
1904 - 05	2/20/1905	1302	14.4	21.6	1929 - 30	2/1/1930	773	11.1	16.7
1905 - 06	3/24/1906	492	8.9	13.3	1930 - 31	1/22/1931	114	4.3	6.4
1906 - 07	2/7/1907	749	10.9	16.4	1931 - 32	3/14/1932	768	11.1	16.6
1907 - 08	2/20/1908	353	7.5	11.3	1932 - 33	2/15/1933	578	9.6	14.4
1908 - 09	2/17/1909	580	9.6	14.4	1933 - 34	2/28/1934	201	5.7	8.5
1909 - 10	2/27/1910	1171	13.7	20.5	1934 - 35	1/27/1935	503	9.0	13.5
1910 - 11	3/1/1911	642	10.1	15.2	1935 - 36	2/29/1936	1522	15.6	23.4
1911 - 12	3/24/1912	1406	15.0	22.5	1936 - 37	2/28/1937	989	12.6	18.9
1912 - 13	3/2/1913	630	10.0	15.1	1937 - 38	2/25/1938	603	9.8	14.7
1913 - 14	2/25/1914	427	8.3	12.4	1938 - 39	3/8/1939	312	7.1	10.6
1914 - 15	4/1/1915	1356	14.7	22.1	1939 - 40	2/27/1940	1089	13.2	19.8
1915 - 16	2/14/1916	857	11.7	17.6	1940 - 41	3/17/1941	514	9.1	13.6
1916 - 17	3/18/1917	1095	13.2	19.8	1941 - 42	3/2/1942	506	9.0	13.5

The table above shows the peak AFDD value and corresponding estimated ice thickness at Genoa.

Table C-2. Estimated Ice Thickness - Genoa

Year	Peak AFDD Date	Peak AFDD	Ice Thickness at Peak AFDD w/ C=0.4	Ice Thickness at Peak AFDD w/ C=0.6	Year	Peak AFDD Date	Peak AFDD	Ice Thickness at Peak AFDD w/ C=0.4	Ice Thickness at Peak AFDD w/ C=0.6
1942 - 43	3/21/1943	660	10.3	15.4	1967 - 68	2/29/1968	656	10.2	15.4
1943 - 44	3/30/1944	364	7.6	11.4	1968 - 69	3/15/1969	1206	13.9	20.8
1944 - 45	3/7/1945	476	8.7	13.1	1969 - 70	2/15/1970	788	11.2	16.8
1945 - 46	2/14/1946	535	9.3	13.9	1970 - 71	3/8/1971	845	11.6	17.4
1946 - 47	3/17/1947	472	8.7	13.0	1971 - 72	2/12/1972	778	11.2	16.7
1947 - 48	3/13/1948	835	11.6	17.3	1972 - 73	2/18/1973	845	11.6	17.4
1948 - 49	3/18/1949	1278	14.3	21.4	1973 - 74	2/10/1974	828	11.5	17.3
1949 - 50	3/14/1950	788	11.2	16.8	1974 - 75	3/15/1975	866	11.8	17.7
1950 - 51	3/21/1951	640	10.1	15.2	1975 - 76	2/7/1976	644	10.2	15.2
1951 - 52	3/7/1952	657	10.3	15.4	1976 - 77	2/7/1977	858	11.7	17.6
1952 - 53	2/22/1953	515	9.1	13.6	1977 - 78	3/9/1978	1575	15.9	23.8
1953 - 54	1/30/1954	402	8.0	12.0	1978 - 79	3/10/1979	1815	17.0	25.6
1954 - 55	2/27/1955	532	9.2	13.8	1979 - 80	3/8/1980	614	9.9	14.9
1955 - 56	2/28/1956	1075	13.1	19.7	1980 - 81	2/12/1981	422	8.2	12.3
1956 - 57	2/5/1957	529	9.2	13.8	1981 - 82	2/14/1982	1203	13.9	20.8
1957 - 58	3/18/1958	542	9.3	14.0	1982 - 83	2/12/1983	481	8.8	13.2
1958 - 59	2/24/1959	774	11.1	16.7	1983 - 84	3/20/1984	1194	13.8	20.7
1959 - 60	3/25/1960	1158	13.6	20.4	1984 - 85	2/15/1985	849	11.7	17.5
1960 - 61	2/7/1961	375	7.7	11.6	1985 - 86	2/22/1986	824	11.5	17.2
1961 - 62	3/17/1962	1160	13.6	20.4	1986 - 87	1/26/1987	218	5.9	8.8
1962 - 63	2/28/1963	798	11.3	16.9	1987 - 88	2/15/1988	803	11.3	17.0
1963 - 64	2/28/1964	578	9.6	14.4	1988 - 89	3/7/1989	600	9.8	14.7
1964 - 65	3/29/1965	1159	13.6	20.4	1989 - 90	2/20/1990	450	8.5	12.7
1965 - 66	3/7/1966	803	11.3	17.0	1990 - 91	1/31/1991	745	10.9	16.4
1966 - 67	2/25/1967	635	10.1	15.1	1991 - 92	12/5/1991	163	5.1	7.7

The table above shows the peak AFDD value and corresponding estimated ice thickness at Genoa.

Table C-2. Estimated Ice Thickness - Genoa

Year	Peak AFDD Date	Peak AFDD	Ice Thickness at Peak AFDD w/ C=0.4	Ice Thickness at Peak AFDD w/ C=0.6
1992 - 93	3/18/1993	1086	13.2	19.8
1993 - 94	3/1/1994	925	12.2	18.2
1994 - 95	3/9/1995	494	8.9	13.3
1995 - 96	3/9/1996	772	11.1	16.7
1996 - 97	2/16/1997	875	11.8	17.7
1997 - 98	3/18/1998	323	7.2	10.8
1998 - 99	1/14/1999	422	8.2	12.3
1999 - 2000	2/1/2000	161	5.1	7.6
2000 - 01	3/6/2001	1077	13.1	19.7
2001 - 02	3/10/2002	289	6.8	10.2
2002 - 03	3/10/2003	483	8.8	13.2
2003 - 04	2/17/2004	573	9.6	14.4
2004 - 05	1/23/2005	401	8.0	12.0
2005 - 06	1/1/2006	230	6.1	9.1
2006 - 07	2/17/2007	569	9.5	14.3
2007 - 08	2/22/2008	791	11.2	16.9
2008 - 09	3/2/2009	699	10.6	15.9
2009 - 10	3/3/2010	1172	13.7	20.5

The table above shows the peak AFDD value and corresponding estimated ice thickness at Genoa.

Table C-3 Estimated Ice Thickness - Columbus

Year	Peak AFDD Date	Peak AFDD	Ice Thickness at Ice Thickness at Peak AFDD w/ C=0.4	Ice Thickness at Ice Thickness at Peak AFDD w/ C=0.6	Year	Peak AFDD Date	Peak AFDD	Ice Thickness at Ice Thickness at Peak AFDD w/ C=0.4	Ice Thickness at Ice Thickness at Peak AFDD w/ C=0.6
1893 - 94	2/25/1894	1253	14.2	21.2	1918 - 19	3/6/1919	366	7.6	11.5
1894 - 95	2/16/1895	897	12.0	18.0	1919 - 20	3/6/1920	878	11.8	17.8
1895 - 96	3/19/1896	311	7.0	10.6	1920 - 21	2/9/1921	307	7.0	10.5
1896 - 97	3/16/1897	739	10.9	16.3	1921 - 22	3/1/1922	742	10.9	16.3
1897 - 98	2/26/1898	627	10.0	15.0	1922 - 23	2/21/1923	361	7.6	11.4
1898 - 99	4/4/1899	1363	14.8	22.1	1923 - 24	3/19/1924	643	10.1	15.2
1899 - 1900	3/6/1900	703	10.6	15.9	1924 - 25	2/1/1925	976	12.5	18.7
1900 - 01	2/26/1901	547	9.4	14.0	1925 - 26	2/3/1926	512	9.0	13.6
1901 - 02	2/19/1902	804	11.3	17.0	1926 - 27	3/2/1927	593	9.7	14.6
1902 - 03	3/3/1903	1014	12.7	19.1	1927 - 28	2/24/1928	515	9.1	13.6
1903 - 04	2/25/1904	868	11.8	17.7	1928 - 29	2/28/1929	988	12.6	18.9
1904 - 05	2/20/1905	1477	15.4	23.1	1929 - 30	1/31/1930	833	11.5	17.3
1905 - 06	3/24/1906	669	10.3	15.5	1930 - 31	1/21/1931	65	3.2	4.8
1906 - 07	2/7/1907	789	11.2	16.9	1931 - 32	3/12/1932	720	10.7	16.1
1907 - 08	2/20/1908	386	7.9	11.8	1932 - 33	2/14/1933	448	8.5	12.7
1908 - 09	2/18/1909	585	9.7	14.5	1933 - 34	2/28/1934	206	5.7	8.6
1909 - 10	2/26/1910	1275	14.3	21.4	1934 - 35	1/30/1935	528	9.2	13.8
1910 - 11	2/27/1911	581	9.6	14.5	1935 - 36	2/28/1936	1464	15.3	23.0
1911 - 12	3/24/1912	1547	15.7	23.6	1936 - 37	2/27/1937	955	12.4	18.5
1912 - 13	3/2/1913	838	11.6	17.4	1937 - 38	2/24/1938	568	9.5	14.3
1913 - 14	3/5/1914	526	9.2	13.8	1938 - 39	3/8/1939	415	8.1	12.2
1914 - 15	3/31/1915	1331	14.6	21.9	1939 - 40	2/27/1940	1040	12.9	19.3
1915 - 16	3/7/1916	1060	13.0	19.5	1940 - 41	3/16/1941	571	9.6	14.3
1916 - 17	3/4/1917	1376	14.8	22.3	1941 - 42	3/2/1942	559	9.5	14.2
1917 - 18	2/21/1918	1367	14.8	22.2	1942 - 43	3/9/1943	652	10.2	15.3

The table above shows the peak AFDD value and corresponding estimated ice thickness at Columbus.

Table C-3. Estimated Ice Thickness - Columbus

Year	Peak AFDD Date	Peak AFDD	Ice Thickness at Ice Thickness at Peak AFDD w/ C=0.4	Ice Thickness at Ice Thickness at Peak AFDD w/ C=0.6	Year	Peak AFDD Date	Peak AFDD	Ice Thickness at Ice Thickness at Peak AFDD w/ C=0.4	Ice Thickness at Ice Thickness at Peak AFDD w/ C=0.6
1943 - 44	1/13/1944	277	6.7	10.0	1968 - 69	3/14/1969	1179	13.7	20.6
1944 - 45	3/6/1945	484	8.8	13.2	1969 - 70	2/19/1970	855	11.7	17.5
1945 - 46	2/13/1946	545	9.3	14.0	1970 - 71	3/7/1971	907	12.0	18.1
1946 - 47	3/16/1947	531	9.2	13.8	1971 - 72	2/25/1972	847	11.6	17.5
1947 - 48	3/12/1948	899	12.0	18.0	1972 - 73	2/17/1973	987	12.6	18.8
1948 - 49	3/17/1949	1179	13.7	20.6	1973 - 74	2/9/1974	875	11.8	17.7
1949 - 50	3/12/1950	779	11.2	16.7	1974 - 75	3/13/1975	968	12.4	18.7
1950 - 51	3/20/1951	603	9.8	14.7	1975 - 76	2/6/1976	658	10.3	15.4
1951 - 52	3/6/1952	639	10.1	15.2	1976 - 77	2/6/1977	926	12.2	18.3
1952 - 53	2/21/1953	477	8.7	13.1	1977 - 78	3/9/1978	1620	16.1	24.1
1953 - 54	1/29/1954	404	8.0	12.1	1978 - 79	3/9/1979	1892	17.4	26.1
1954 - 55	2/26/1955	499	8.9	13.4	1979 - 80	3/6/1980	684	10.5	15.7
1955 - 56	2/27/1956	1044	12.9	19.4	1980 - 81	2/11/1981	494	8.9	13.3
1956 - 57	2/4/1957	501	9.0	13.4	1981 - 82	3/9/1982	1251	14.1	21.2
1957 - 58	2/19/1958	539	9.3	13.9	1982 - 83	2/11/1983	548	9.4	14.0
1958 - 59	2/23/1959	786	11.2	16.8	1983 - 84	3/19/1984	1275	14.3	21.4
1959 - 60	3/24/1960	1132	13.5	20.2	1984 - 85	2/14/1985	875	11.8	17.7
1960 - 61	2/7/1961	408	8.1	12.1	1985 - 86	2/22/1986	881	11.9	17.8
1961 - 62	3/16/1962	1174	13.7	20.6	1986 - 87	1/25/1987	253	6.4	9.5
1962 - 63	3/5/1963	963	12.4	18.6	1987 - 88	2/14/1988	815	11.4	17.1
1963 - 64	2/26/1964	705	10.6	15.9	1988 - 89	3/6/1989	674	10.4	15.6
1964 - 65	3/28/1965	1213	13.9	20.9	1989 - 90	2/18/1990	524	9.2	13.7
1965 - 66	3/6/1966	782	11.2	16.8	1990 - 91	1/30/1991	801	11.3	17.0
1966 - 67	2/24/1967	668	10.3	15.5	1991 - 92	11/10/1991	152	4.9	7.4
1967 - 68	3/2/1968	685	10.5	15.7	1992 - 93	3/17/1993	964	12.4	18.6

The table above shows the peak AFDD value and corresponding estimated ice thickness at Columbus.

Table C-3. Estimated Ice Thickness - Columbus

Year	Peak AFDD Date	Peak AFDD	Ice Thickness at Peak AFDD w/ C=0.4	Ice Thickness at Peak AFDD w/ C=0.6
1993 - 94	2/28/1994	930	12.2	18.3
1994 - 95	3/8/1995	546	9.3	14.0
1995 - 96	3/8/1996	861	11.7	17.6
1996 - 97	2/15/1997	1079	13.1	19.7
1997 - 98	3/18/1998	427	8.3	12.4
1998 - 99	1/30/1999	482	8.8	13.2
1999 - 2000	2/19/2000	280	6.7	10.0
2000 - 01	3/10/2001	1253	14.2	21.2
2001 - 02	3/9/2002	431	8.3	12.4
2002 - 03	3/9/2003	638	10.1	15.2
2003 - 04	2/16/2004	701	10.6	15.9
2004 - 05	1/22/2005	492	8.9	13.3
2005 - 06	2/21/2006	298	6.9	10.3
2006 - 07	3/6/2007	713	10.7	16.0
2007 - 08	3/8/2008	1065	13.1	19.6
2008 - 09	3/1/2009	801	11.3	17.0
2009 - 10	3/2/2010	1267	14.2	21.4

The table above shows the peak AFDD value and corresponding estimated ice thickness at Columbus.

Table C-4. Estimated Ice Thickness – St. Paul

Year	Peak AFDD Date	Peak AFDD	Ice Thickness at Ice Thickness at Peak AFDD w/ C=0.4	Ice Thickness at Ice Thickness at Peak AFDD w/ C=0.6	Year	Peak AFDD Date	Peak AFDD	Ice Thickness at Ice Thickness at Peak AFDD w/ C=0.4	Ice Thickness at Ice Thickness at Peak AFDD w/ C=0.6
1899 - 1900	3/6/1900	634	10.1	15.1	1924 - 25	2/2/1925	994	12.6	18.9
1900 - 01	2/26/1901	606	9.8	14.8	1925 - 26	2/4/1926	414	8.1	12.2
1901 - 02	2/20/1902	692	10.5	15.8	1926 - 27	1/27/1927	477	8.7	13.1
1902 - 03	3/5/1903	745	10.9	16.4	1927 - 28	1/4/1928	497	8.9	13.4
1903 - 04	2/21/1904	572	9.6	14.3	1928 - 29	3/1/1929	1061	13.0	19.5
1904 - 05	2/20/1905	1126	13.4	20.1	1929 - 30	2/1/1930	807	11.4	17.0
1905 - 06	3/24/1906	343	7.4	11.1	1930 - 31	1/20/1931	150	4.9	7.3
1906 - 07	2/7/1907	564	9.5	14.2	1931 - 32	3/14/1932	753	11.0	16.5
1907 - 08	2/20/1908	228	6.0	9.0	1932 - 33	2/15/1933	586	9.7	14.5
1908 - 09	2/17/1909	425	8.2	12.4	1933 - 34	1/8/1934	173	5.3	7.9
1909 - 10	2/24/1910	1039	12.9	19.3	1934 - 35	1/27/1935	472	8.7	13.0
1910 - 11	3/1/1911	446	8.4	12.7	1935 - 36	2/27/1936	1345	14.7	22.0
1911 - 12	3/24/1912	1283	14.3	21.5	1936 - 37	2/28/1937	1008	12.7	19.0
1912 - 13	3/2/1913	642	10.1	15.2	1937 - 38	2/24/1938	458	8.6	12.8
1913 - 14	2/25/1914	491	8.9	13.3	1938 - 39	3/7/1939	323	7.2	10.8
1914 - 15	4/1/1915	1215	13.9	20.9	1939 - 40	2/28/1940	989	12.6	18.9
1915 - 16	2/14/1916	854	11.7	17.5	1940 - 41	3/14/1941	482	8.8	13.2
1916 - 17	3/18/1917	919	12.1	18.2	1941 - 42	3/1/1942	481	8.8	13.2
1917 - 18	2/22/1918	1126	13.4	20.1	1942 - 43	1/31/1943	496	8.9	13.4
1918 - 19	3/8/1919	347	7.5	11.2	1943 - 44	3/30/1944	264	6.5	9.7
1919 - 20	3/7/1920	706	10.6	15.9	1944 - 45	3/7/1945	368	7.7	11.5
1920 - 21	2/9/1921	279	6.7	10.0	1945 - 46	2/14/1946	448	8.5	12.7
1921 - 22	3/2/1922	820	11.5	17.2	1946 - 47	3/16/1947	469	8.7	13.0
1922 - 23	3/19/1923	455	8.5	12.8	1947 - 48	3/14/1948	872	11.8	17.7
1923 - 24	3/20/1924	685	10.5	15.7	1948 - 49	3/18/1949	1153	13.6	20.4

The table above shows the peak AFDD value and corresponding estimated ice thickness at St. Paul.

Table C-4. Estimated Ice Thickness – St. Paul

Year	Peak AFDD Date	Peak AFDD	Ice Thickness at Ice Thickness at Peak AFDD w/ C=0.4	Ice Thickness at Ice Thickness at Peak AFDD w/ C=0.6	Year	Peak AFDD Date	Peak AFDD	Ice Thickness at Ice Thickness at Peak AFDD w/ C=0.4	Ice Thickness at Ice Thickness at Peak AFDD w/ C=0.6
1949 - 50	3/14/1950	693	10.5	15.8	1974 - 75	3/14/1975	762	11.0	16.6
1950 - 51	2/15/1951	479	8.7	13.1	1975 - 76	2/7/1976	580	9.6	14.4
1951 - 52	1/29/1952	559	9.5	14.2	1976 - 77	2/7/1977	733	10.8	16.2
1952 - 53	1/25/1953	461	8.6	12.9	1977 - 78	3/10/1978	1545	15.7	23.6
1953 - 54	1/30/1954	462	8.6	12.9	1978 - 79	3/5/1979	1712	16.6	24.8
1954 - 55	2/27/1955	553	9.4	14.1	1979 - 80	3/8/1980	595	9.8	14.6
1955 - 56	2/28/1956	1034	12.9	19.3	1980 - 81	2/12/1981	358	7.6	11.3
1956 - 57	2/5/1957	539	9.3	13.9	1981 - 82	2/14/1982	1036	12.9	19.3
1957 - 58	3/21/1958	622	10.0	15.0	1982 - 83	2/11/1983	366	7.7	11.5
1958 - 59	2/23/1959	846	11.6	17.4	1983 - 84	1/24/1984	1062	13.0	19.6
1959 - 60	3/25/1960	1157	13.6	20.4	1984 - 85	2/15/1985	737	10.9	16.3
1960 - 61	2/8/1961	467	8.6	13.0	1985 - 86	2/24/1986	875	11.8	17.7
1961 - 62	3/18/1962	1245	14.1	21.2	1986 - 87	1/25/1987	174	5.3	7.9
1962 - 63	3/6/1963	981	12.5	18.8	1987 - 88	2/15/1988	786	11.2	16.8
1963 - 64	2/28/1964	677	10.4	15.6	1988 - 89	3/8/1989	664	10.3	15.5
1964 - 65	3/29/1965	1058	13.0	19.5	1989 - 90	2/20/1990	743	10.9	16.4
1965 - 66	3/7/1966	729	10.8	16.2	1990 - 91	2/1/1991	795	11.3	16.9
1966 - 67	2/25/1967	586	9.7	14.5	1991 - 92	1/19/1992	211	5.8	8.7
1967 - 68	2/29/1968	593	9.7	14.6	1992 - 93	3/18/1993	1276	14.3	21.4
1968 - 69	3/15/1969	1188	13.8	20.7	1993 - 94	3/1/1994	835	11.6	17.3
1969 - 70	2/15/1970	712	10.7	16.0	1994 - 95	3/9/1995	447	8.5	12.7
1970 - 71	3/8/1971	848	11.6	17.5	1995 - 96	2/5/1996	783	11.2	16.8
1971 - 72	2/12/1972	645	10.2	15.2	1996 - 97	2/15/1997	616	9.9	14.9
1972 - 73	2/17/1973	763	11.0	16.6	1997 - 98	1/24/1998	203	5.7	8.5
1973 - 74	2/10/1974	878	11.9	17.8	1998 - 99	1/14/1999	403	8.0	12.0

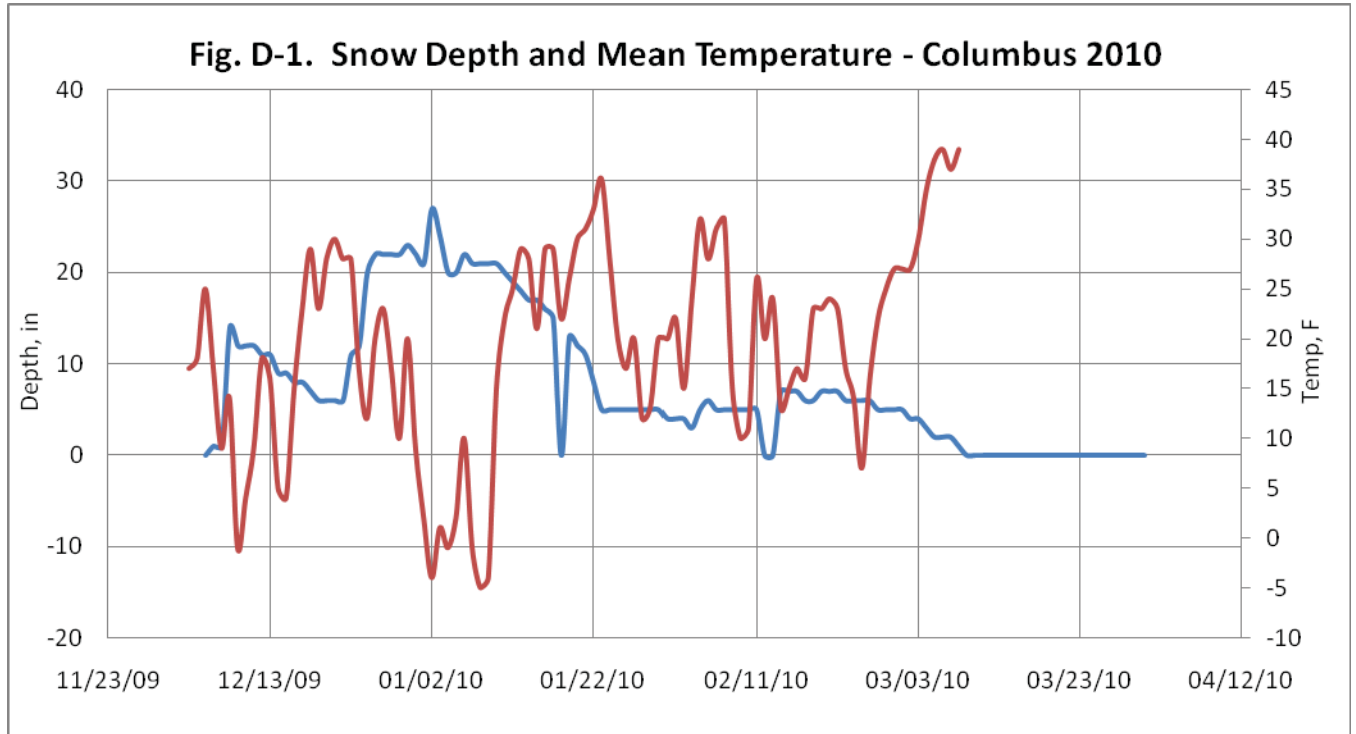
The table above shows the peak AFDD value and corresponding estimated ice thickness at St. Paul.

Table C-4. Estimated Ice Thickness – St. Paul

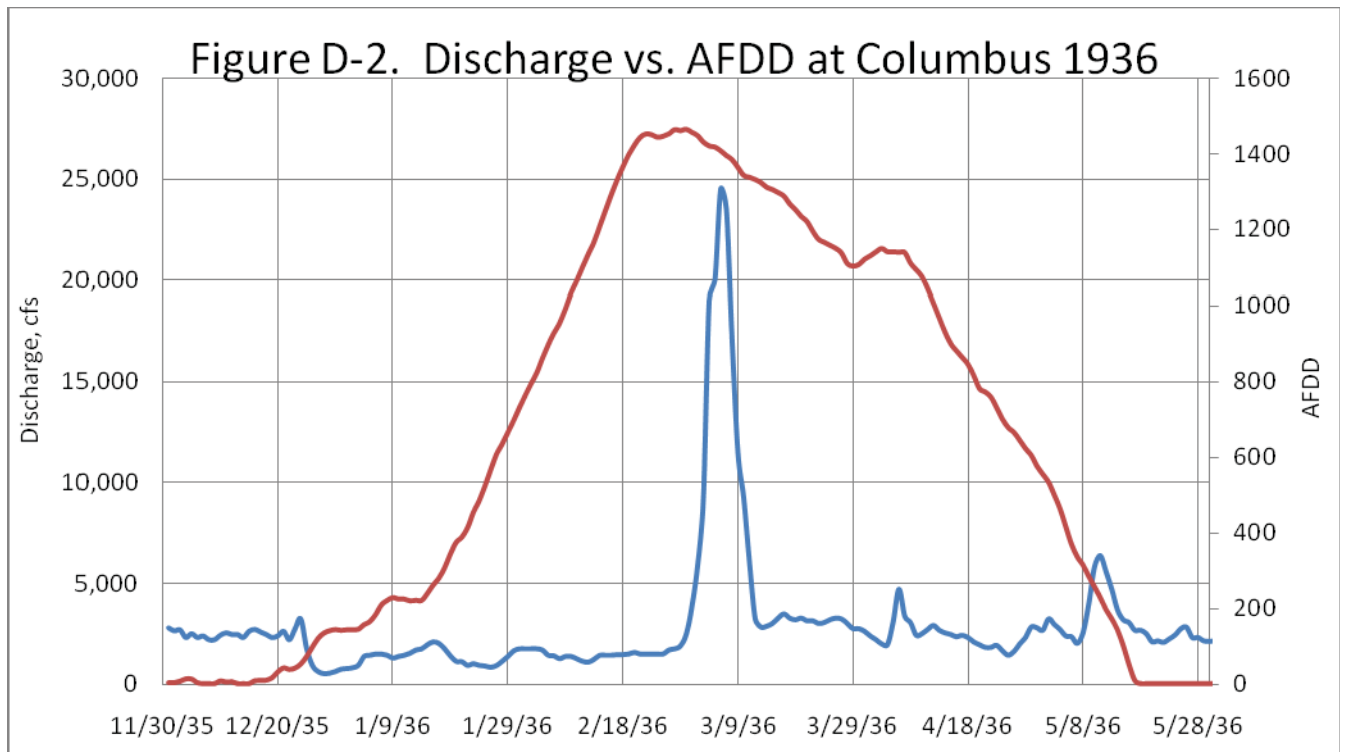
Year	Peak AFDD Date	Peak AFDD	Ice Thickness at Peak AFDD w/ C=0.4	Ice Thickness at Peak AFDD w/ C=0.6
1999 - 2000	2/1/2000	134	4.6	6.9
2000 - 01	3/6/2001	1091	13.2	19.8
2001 - 02	3/10/2002	242	6.2	9.3
2002 - 03	3/10/2003	429	8.3	12.4
2003 - 04	2/17/2004	599	9.8	14.7
2004 - 05	1/18/2005	395	7.9	11.9
2005 - 06	1/1/2006	238	6.2	9.3
2006 - 07	2/17/2007	614	9.9	14.9
2007 - 08	2/22/2008	682	10.4	15.7
2008 - 09	3/2/2009	561	9.5	14.2

The table above shows the peak AFDD value and corresponding estimated ice thickness at St. Paul.

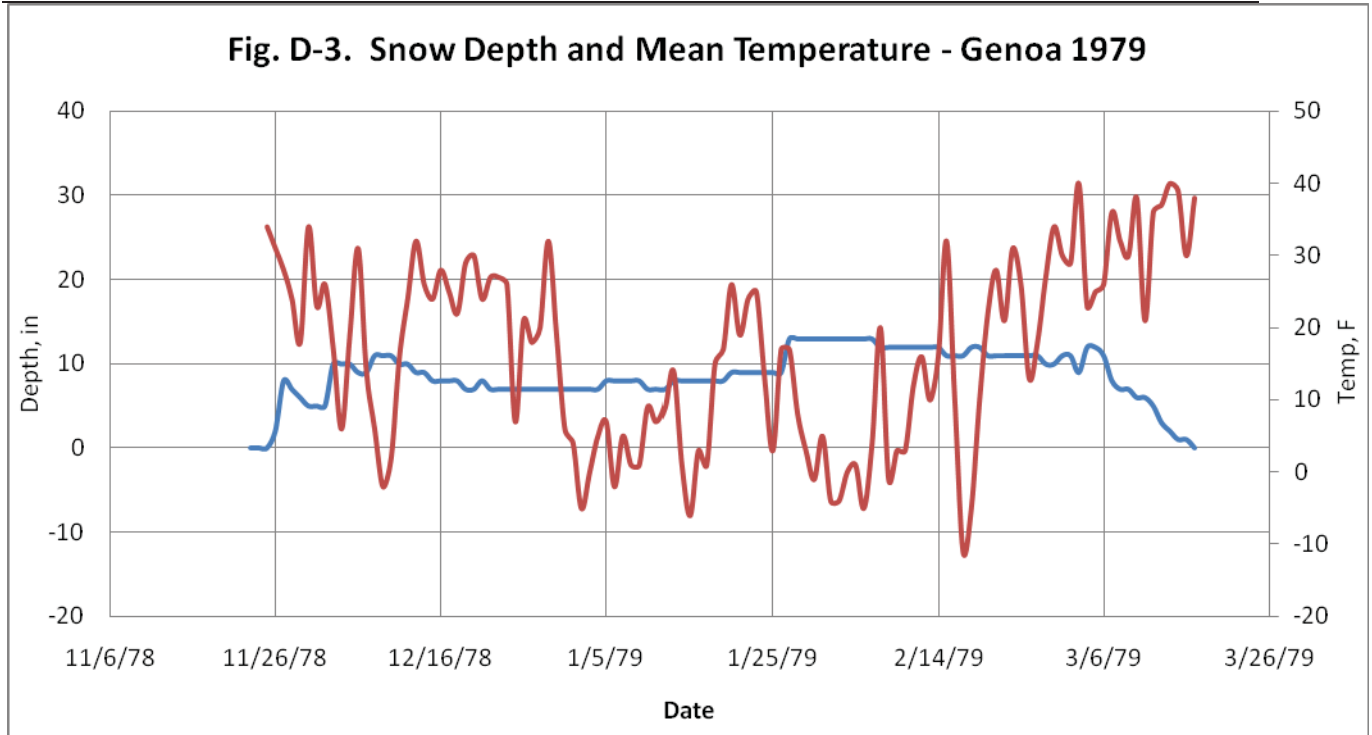
RELATIONSHIP BETWEEN SNOW COVER AND/OR RAIN AND ICE JAMS



The graph above shows the daily average temperatures and snow depth through the winter of 1979 at Columbus.



The table above shows the Loup River daily discharge at Columbus and the AFDD at Columbus.



The graph above shows the daily average temperatures and snow depth through the winter of 1979 at Genoa.

DYNARICE MODELING OF ICE TRANSPORT ON THE LOUP RIVER

DynaRICE Modeling of Ice Transport on the Loup River

Introduction

The transport of ice floes is beyond the capability of a one-dimensional model such as HEC-RAS. However, the two-dimensional DynaRICE ice-hydraulic numerical model has been successfully used to simulate ice transport through various channels and hydraulic structures as well as ice jam initiation. DynaRICE has simulated ice jam initiation at the Missouri-Mississippi River Confluence (Shen et al. 1998). The model was also used to analyze ice passage at Montgomery Lock and Dam on the Ohio River (Liu et al. 2001) and the Soo Locks (Tuthill et al. 2004). DynaRICE ice dynamics are linked to hydrodynamics that are two-dimensional-depth averaged and unsteady.

The main objective of the dynamic ice modeling is to detect differences in ice formation and ice jamming processes with- and without-diversions into the Power Canal. The DynaRICE modeling focuses on selected reaches of interest where ice formation and ice jamming processes may differ as a result of project operations (with and without the diversion into the canal).

Methodology.

DynaRICE (DR) hydraulic models were constructed for two areas of interest, the first upstream and downstream of the Power Canal Headworks on the Loup River and the second on the section of the Loup River that passes through Columbus. Figure 1 shows the two DynaRICE domains and other points of interest in the project area.

The Columbus reach was selected due to a history of damaging ice jam occurrences (both freezeup and breakup). The Loup River reach just upstream and downstream of the Headworks was modeled as it experiences the greatest incremental flow change due to Project operations and thus exhibits the greatest differences in flow regime and channel geometry.

Differences in ice cover formation and jam formation demonstrated by DynaRICE will be utilized in the Ice-Affected Hydraulics analysis as appropriate. DynaRICE simulations have been limited to existing conditions channel geometry. It was found in the Ice-Affected Hydraulics Analysis that the differences in channel geometry did not cause sufficient differences in ice conditions to warrant conducting a two-dimensional model simulation with modified channel geometry.

Data Sources.

USGS gage data and balanced hydrographs developed from the Hydrology studies were utilized in the DynaRICE modeling. The dynamic ice modeling used geometry data developed in the Ice Production and Freeze-up Jams and the Ice Breakup and Breakup Jam Formation studies. Most of the geometry data came from the geo-referenced HEC-RAS model which extended from the Headworks about 37 river miles (RM) downstream to a point near Loup-Platte River Confluence. Omaha District provided CRREL with detailed cross-section data from three additional locations: Sites 1 and 2, located about 5

and 4 miles upstream and downstream of the Headworks respectively, and Site 3 which lies just upstream of the Tailrace Return.

Two DynaRICE domains were constructed on the Loup River. The first 15-mile-long “Headworks Domain” extends from Site 1 to about 5 miles below the Genoa USGS Gage. Because no surveyed data exist between Site 1 and the Headworks, the bathymetry for this section of river was estimated from Google Earth composite imagery and USGS quadrangle data. For the section of the domain below the Headworks, the channel bathymetry came from 21 HEC-RAS cross sections at an average spacing of 1550 ft. plus 9 closely spaced cross sections at Site 2. Because so little data were available, only the active channel was modeled, assuming that flow would remain within bank during freeze-up flows. The Headworks domain has an upstream inflow boundary using discharge calculated as the sum of the flows reported at the USGS Loup River and Power Canal Gages near Genoa, NE. The downstream stage boundary is based on a rating curve calculated by HEC-RAS approximately 24,500 feet downstream of the Genoa gage. Freeze-up events were reviewed and typical values for formation flows were evaluated.

The “Columbus” domain with a length of about 6 RM extends from about 1 mile upstream of the Union Pacific Railroad Bridge to 3.5 miles downstream of the Highway 81/30 Bridge in Columbus. The domain is based on HEC-RAS geometry where the cross sections have an average spacing of about 860 ft and includes the overbank areas that were assumed to be inundated for a large event (based on the 1993 jam). The upstream flow boundary uses discharge data from the USGS gage at Columbus and synthesized flows for events after that gage was discontinued. The downstream stage boundary is based on a HEC-RAS calculated rating curve just downstream of the Platte-Loup confluence. Figures 2 and 3 show the Headworks and Columbus bed elevations for the domains used in the DynaRICE model.

Simulations

Because of the relatively close cross section spacing, the bathymetry in the Columbus domain is sufficiently well-defined to allow model stability in the breakup flow range. Low ice formation flows were not simulated because the spacing of data points is too coarse to represent such shallow flows in a 2D model. In the Headworks domain, the surveyed cross sections are absent for 3.5 miles above this structure and still widely spaced in the reach below the diversion. This led to modeling difficulties at low ice formation flows, particularly in the sharp bend below Genoa, a relatively flat section of the domain. This is likely an area where freezeup ice jamming occurs when the diversion is in operation.

Table 1 lists the four simulations attempted which gave reasonable results. Cases 1 and 2 are without-diversion (run of river) simulations of ice transport and jamming in the vicinity of the Headworks for high and medium formation flows respectively. Both these 24-hour simulations used an ice inflow with a surface concentration C_i of 40% and an ice floe thickness t_i of 0.1 ft. followed by a heavier inflow of $C_i = 60\%$ and floe thickness of 0.2 ft. Figure 4 shows the ice covers at 24 and 33 hours for Case 1. Figure 5 shows the ice covers at 24 and 39 hours for Case 2.

Cases 3 and 4 are breakup ice jam simulations in the Columbus domain. The Case 3 jam is assumed to form in the vicinity of the island located about 1 mile downstream of the Highway 81 Bridge. The breakup model was calibrated against USGS Gage data as well as detailed stage data from a report by Alan Abbott of the Nebraska Department of Roads dated 5/7/1993. Figure 6 shows the ice thickness for the 1993 event, using historical flows for with-diversion and synthetic flows for without-diversion cases. Figure 7 shows profiles for both Case 3 events. For the Case 4 jam, the jam was assumed to occur about ½-mile below the Highway 81 Bridge as per historical descriptions. The model was calibrated using the 1993 data and then run using the 21 March 1969 break-up jam flow. Figure 8 shows the ice thickness for the 1969 event for the historical 15,400 cfs flow. The breakup simulations used an ice inflow surface concentration C_i of 50% and an ice floe thickness of 1.1'. Manning's n for ice varied linearly with ice jam thickness between limits of 0.04 and 0.06.

Table 1. Simulations

Case	Domain	Condition	Upstream Inflow (cfs)	Diversion Outflow (cfs)	Loup R. Bypass (cfs)
1	Headworks	high formation flow	3,400	0	3,400
2	Headworks	medium formation flow	2,000	0	2,000
3	Columbus	7 Mar. 1993 breakup	34,000	3,300	30,700
4	Columbus	21 Mar. 1969 breakup	16,000	600	15,400

Discussion and Conclusions

Headworks Case 1 and Case 2 model without-diversion conditions, or operating conditions wherein the diversion is discontinued during ice formation flows. Both runs show a freeze-up jam occurring in the bend just downstream of the Genoa gage. A thin ice cover proceeds quickly upstream to the Headworks. The two different flows show the jam occurring in the same vicinity, but slightly further upstream for the medium formation flow. These results show that jams will occur under without-diversion conditions, and the diversion likely only reduces the amount of ice available in the bypass channel for jam formation.

The Columbus Cases 3 and 4 demonstrate that significant ice can build-up during break-up conditions, causing ice thicknesses greater than 2 ft at the Highway 81 Bridge. These ice thicknesses and resulting water surface correspond well to the high water marks measured following the 1993 event. Synthesized no-diversion discharge was used for

Case 3 and showed that similar, but larger, ice jams would form if flow is not diverted to the Power Canal. In these break-up cases, it appears that the influence of the diversion is to reduce the size of the jam and thus the water surface elevation and potential flooding.

For the originally-proposed downstream domain from above the Canal Outlet Tailrace to the Burlington Northern Railroad Bridge, much additional geometry data is needed. The downstream end of the HEC-RAS model appears to be close to the Loup-Platte Confluence. The Site 3 data provide some local bathymetry just upstream of the Canal Tailrace but no geometry exists for the one mile reach from there to the railroad bridge.

The limitation of the DynaRICE model proved to be the difficulty of modeling low formation flows with coarse bathymetric data. Additional DR model runs could possibly better define the impact of Power Canal diversions on ice formation in the Headworks reach under low flow conditions. However, much additional bathymetry data would be required to achieve an acceptable level of confidence. Were the additional geometry made available, it is not clear that DR would predict significant differences in ice cover formation for with and without-diversion conditions. This opinion is based on the observation that, under low flow conditions, the HEC-RAS predicted water velocities downstream of the Headworks with- and without-diversion were similar.

References

Liu, L., Tuthill, A. M. and H. T. Shen (2001) "Dynamic Simulation of Ice Conditions in the Vicinity of Locks and Dams" Proceedings, CRIPE 11th River Ice Workshop , May 2001, Ottawa

Shen, H.T., H. Shen and S. Tsai (1990) "Dynamic transport of river ice", Journal of Hydraulic Research, 28(6), p 659-671.

Shen, H. T., Liu, L, and A. M. Tuthill (1998) "A numerical model for ice jam evolution" Proceedings, IAHR 14th International Symposium on Ice, Potsdam, NY, 27-31 July 1998.

Tuthill, A. M., Liu, L. and H. T. Shen (2004) Modeling Ice Passage at Navigation Locks, ASCE J. Cold Regions Engineering, Vol. 18, No. 3, Sept, 2004.

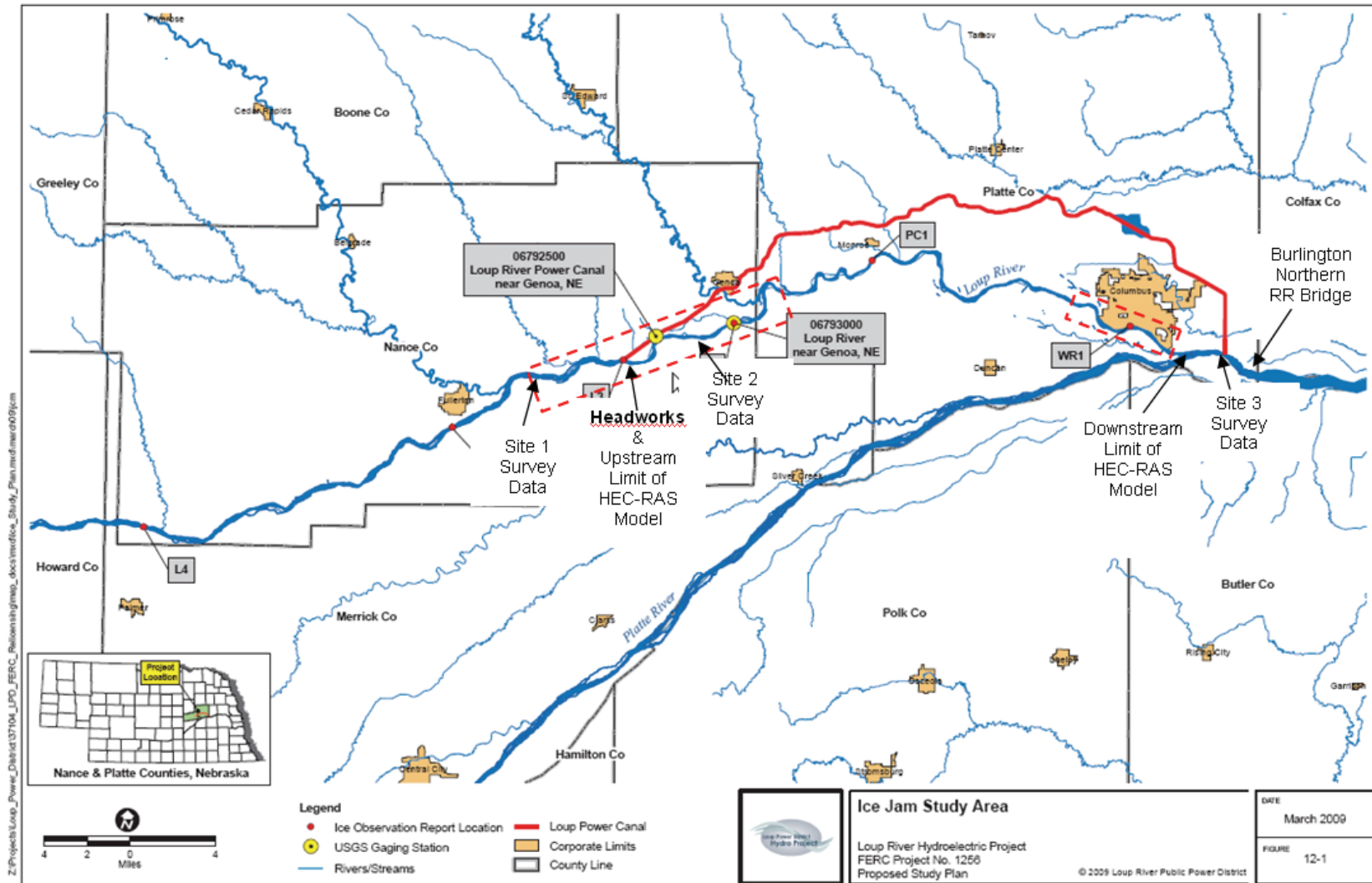


Figure 1. Map of project area showing DynaRICE domains (dashed red boxes) and sites of surveyed cross section data.

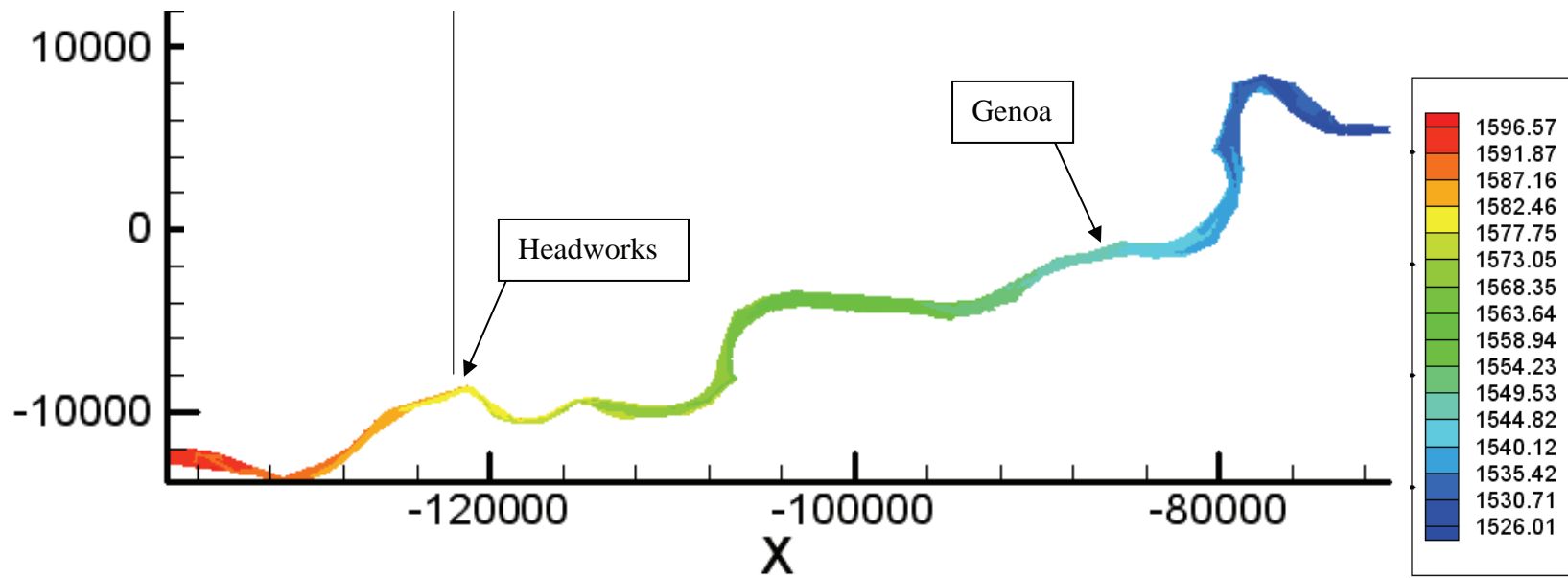


Figure 2: Bed elevations (ft) in Headworks domain.

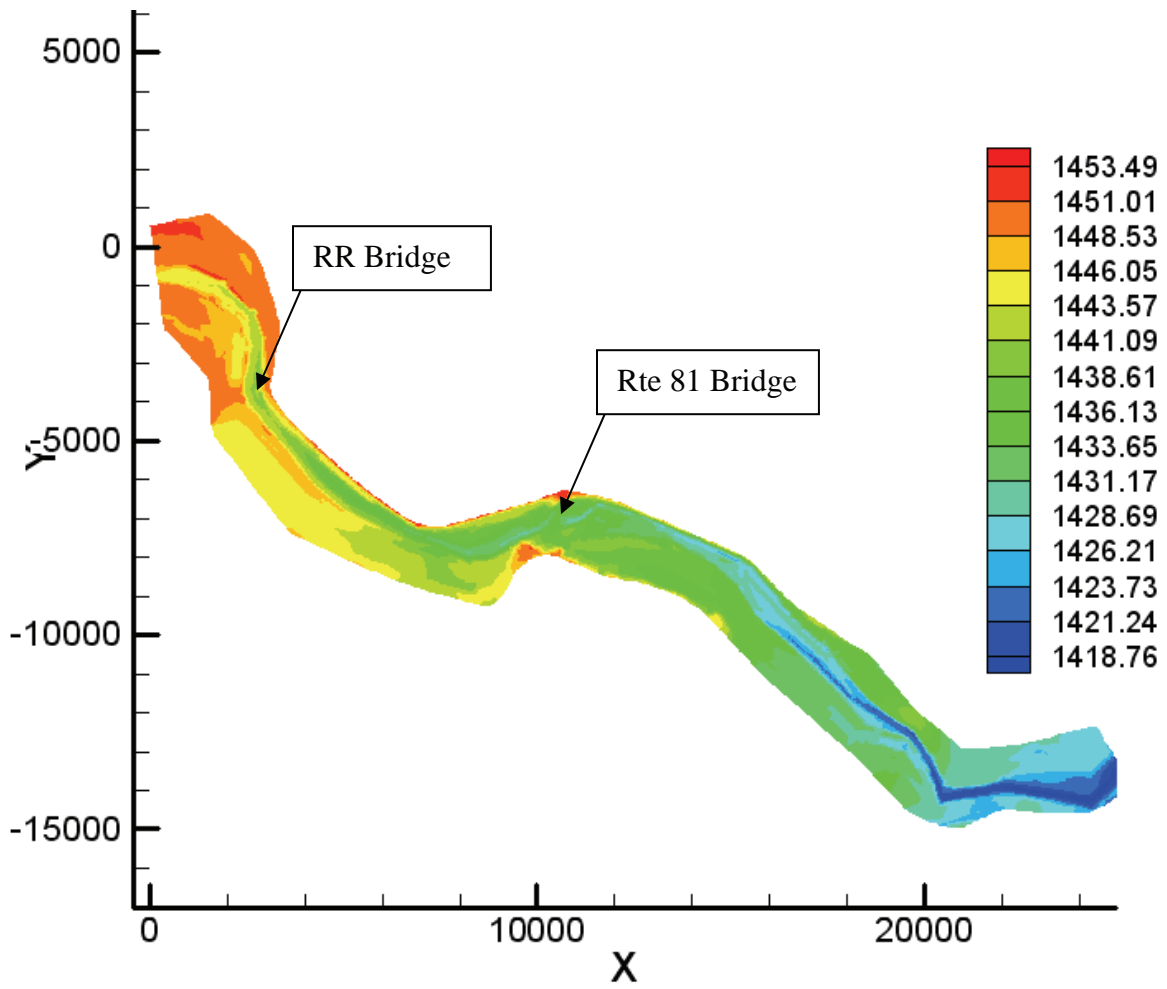


Figure 3: Bed elevations (ft) in Columbus domain.

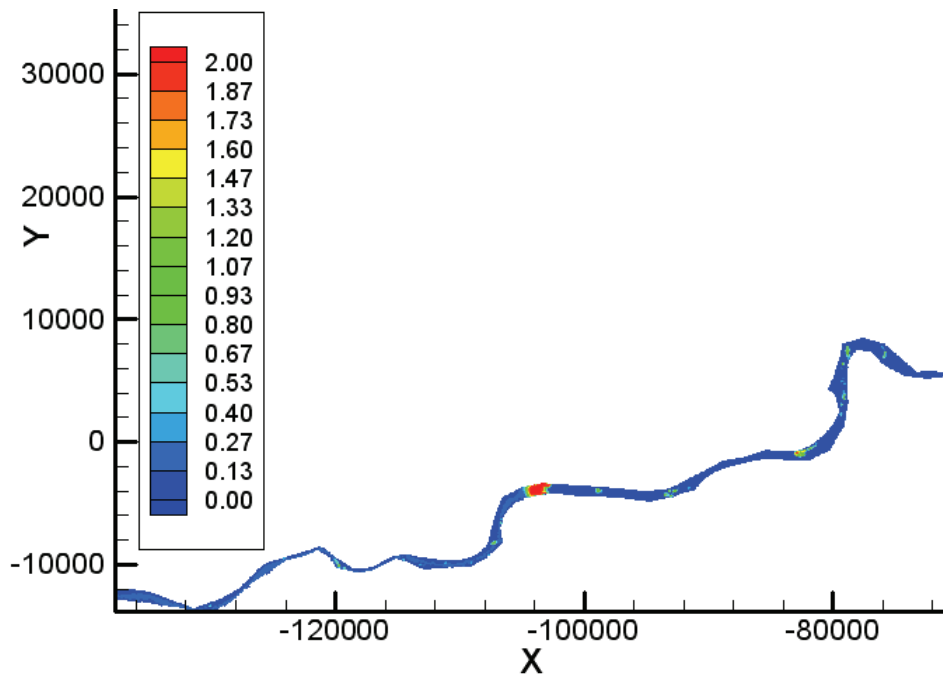
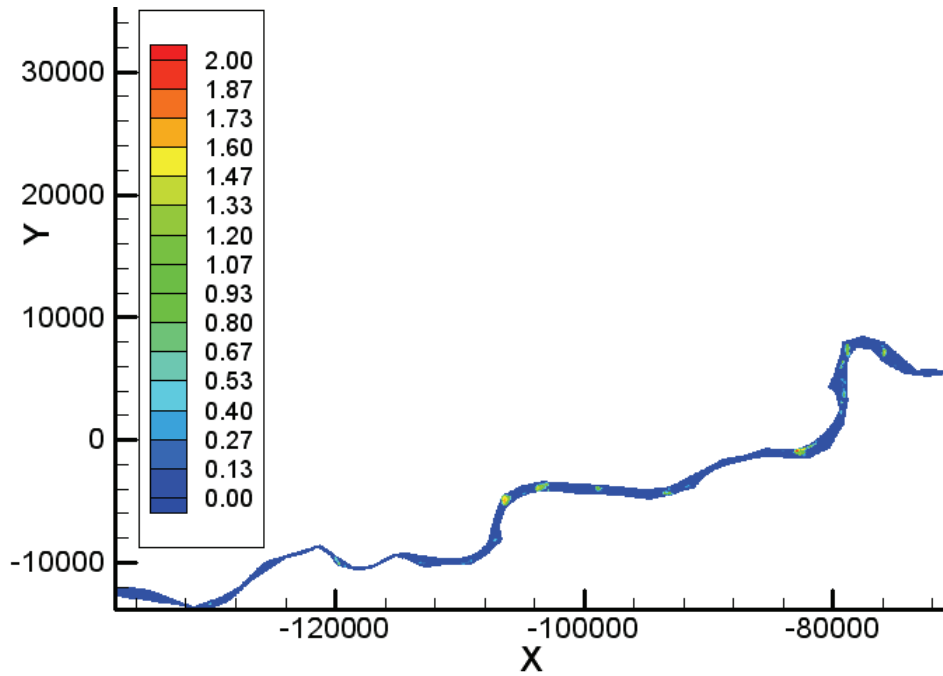


Figure 4: Case 1: Ice Formation for high 3400 cfs inflow. Top panel shows ice thicknesses after 24 hours of 40% concentration 0.1' ice floes. Bottom Panel shows ice formation at hour 33 (9 additional hours of inflows at 60% concentration and 0.2' floes)

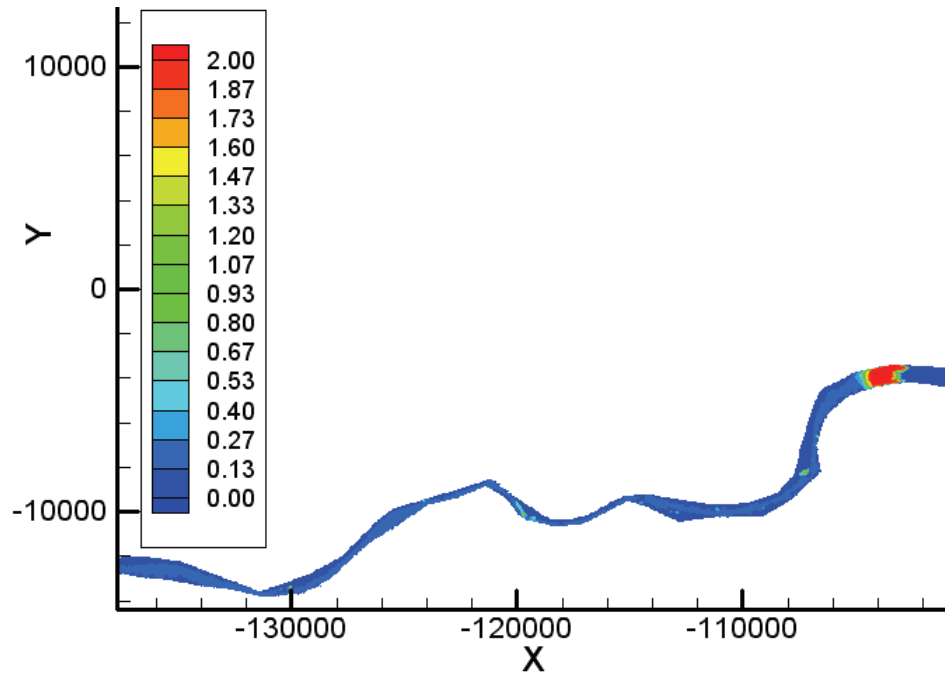


Figure 4a: Close-up of upstream half of domain, Case 1: Ice formation for high 3400 cfs inflow at 33 hours

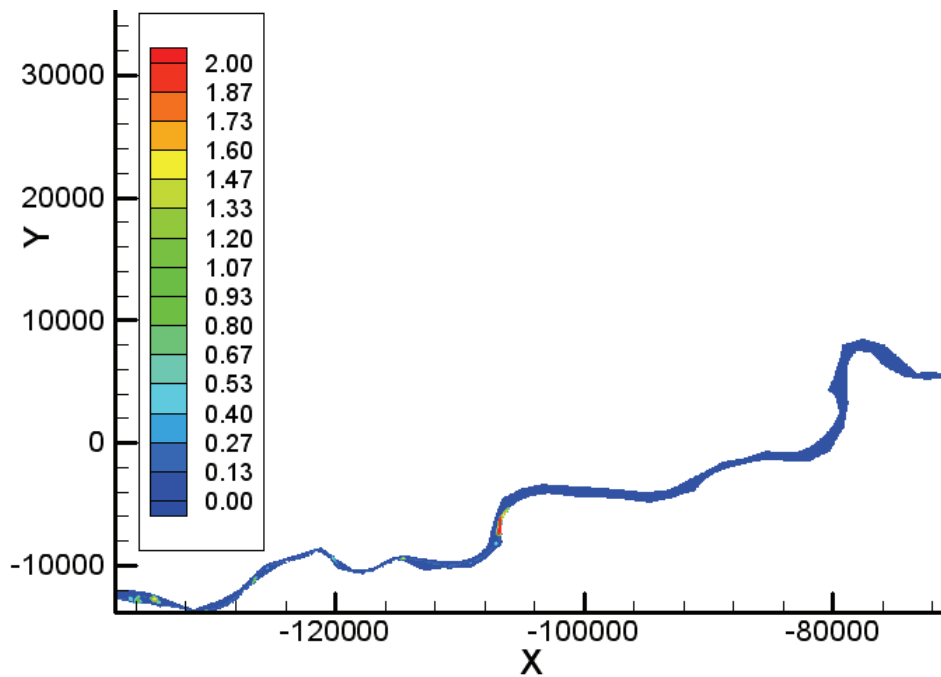
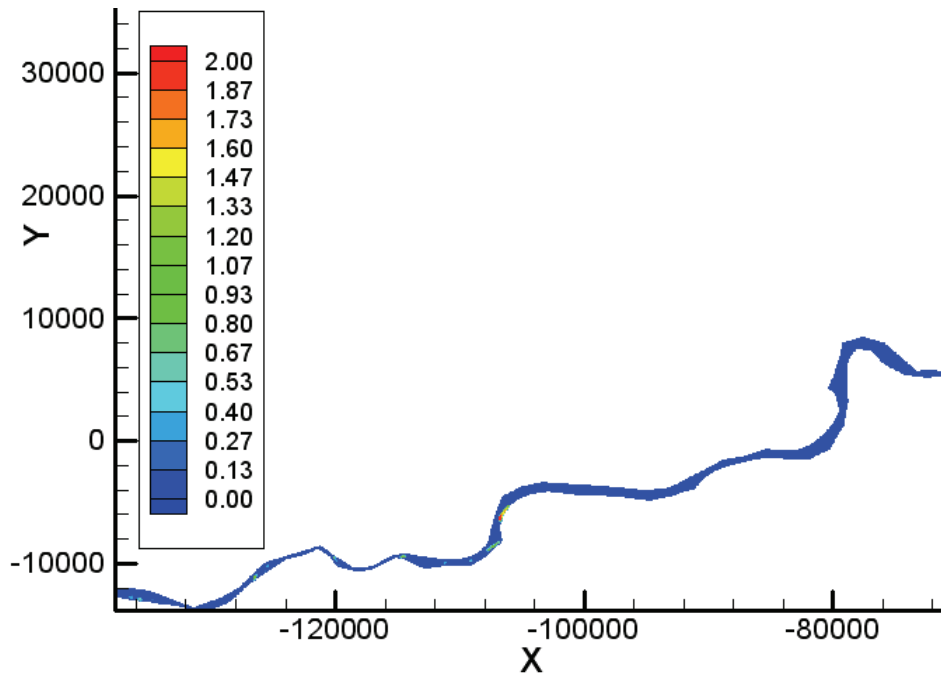


Figure 5: Case 2: Ice Formation for medium 2000 cfs inflow. Top panel shows ice thicknesses after 24 hours of 40% concentration 0.1' ice floes. Bottom Panel shows ice formation at hour 39 (18 additional hours of inflows at 60% concentration and 0.2' floes)

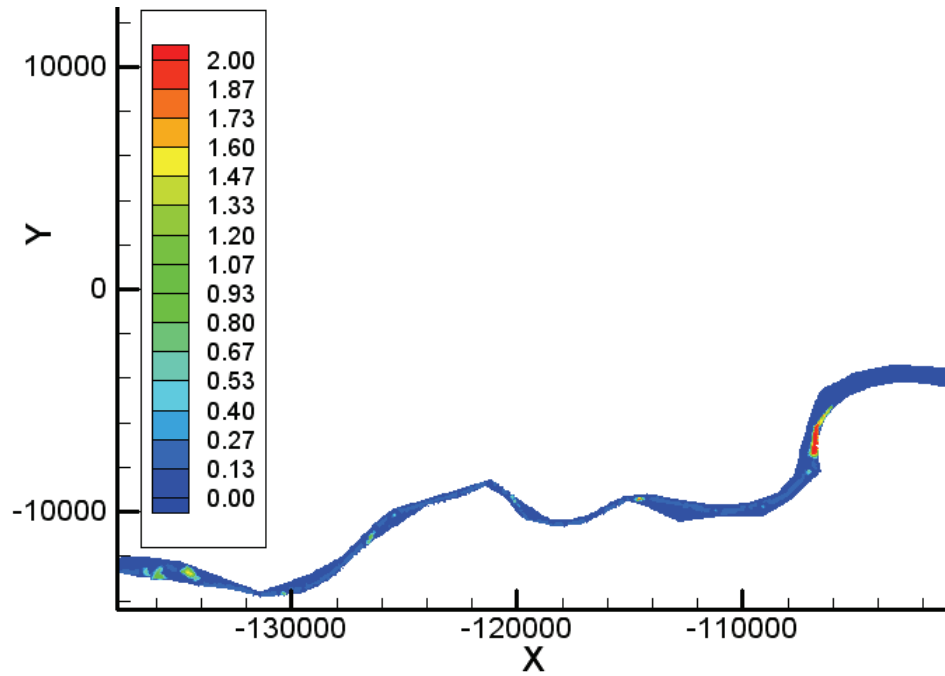


Figure 5a: Close-up of upstream half of domain, Case 2: Ice formation for medium 2000 cfs inflow at 39 hours

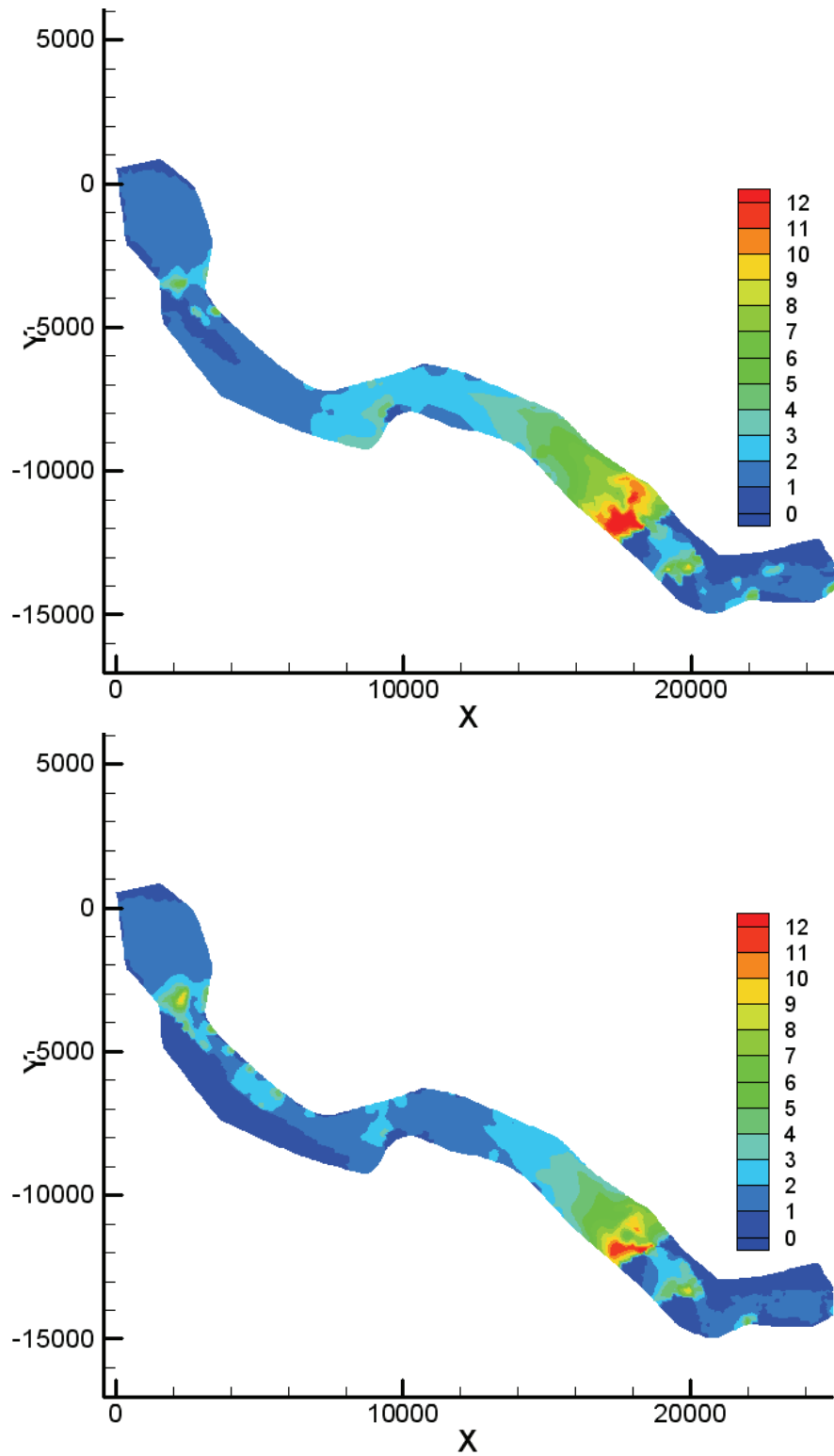


Figure 6: Case 3: Ice Thickness for the 1993 event. Top panel, 34,000 cfs assuming no diversion, bottom panel 30700 cfs with diversion

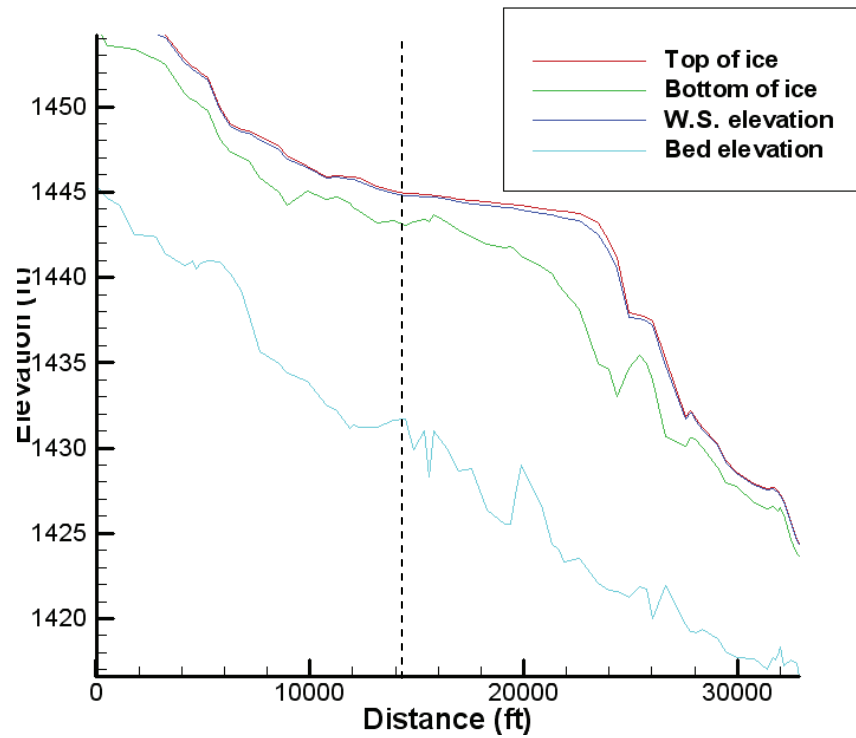
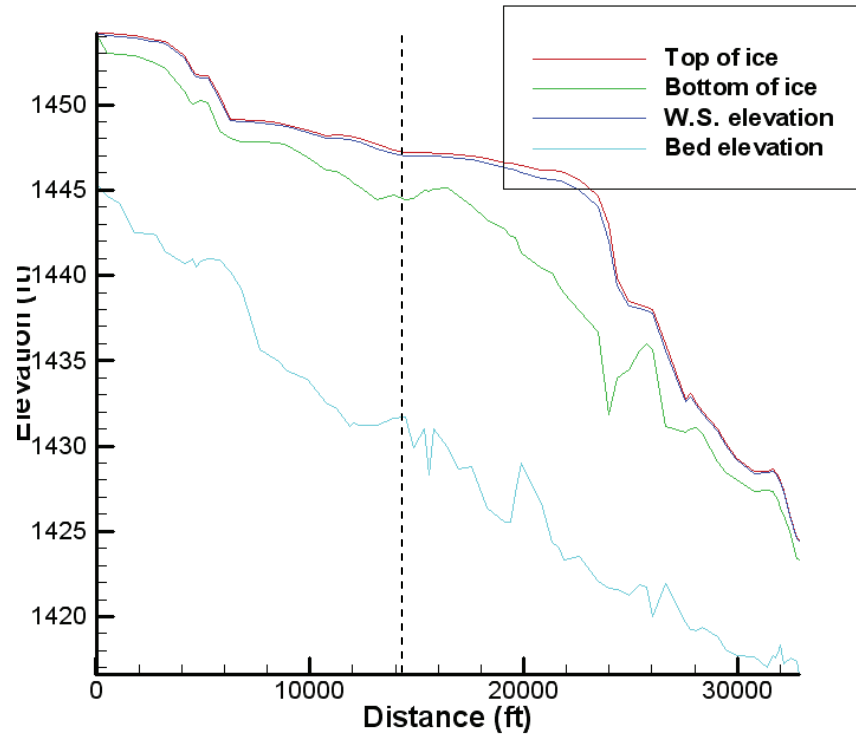


Figure 7: Case 3: Profiles for the 1993 event. Top panel, 34,000 cfs assuming no diversion, bottom panel 30,700 cfs with diversion. The Rte 81 Bridge is indicated by the dashed vertical line.

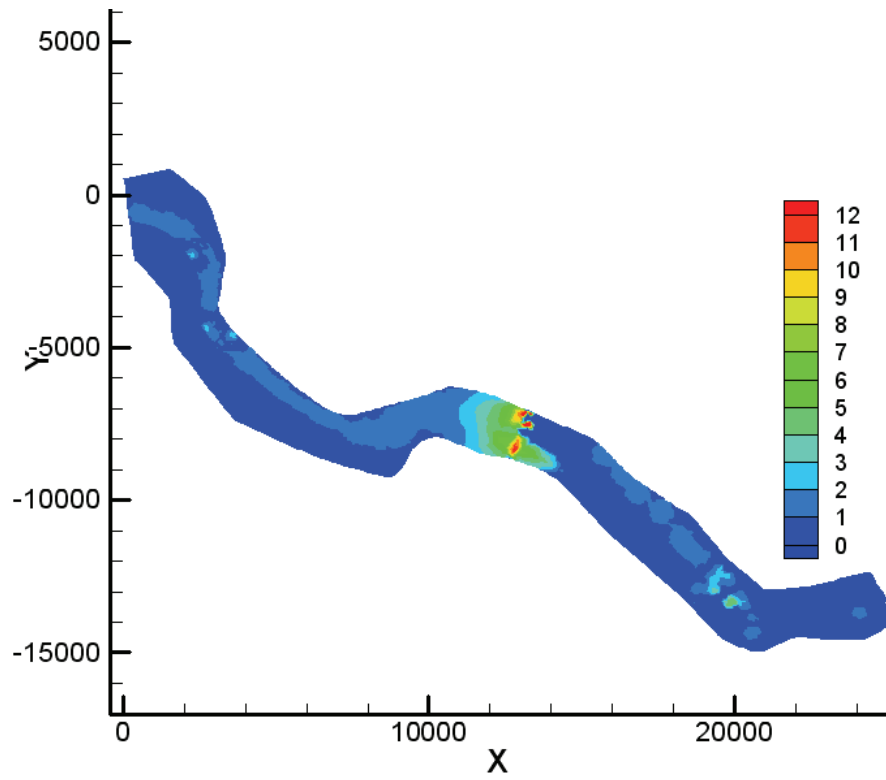


Figure 8: Case 4: Ice Thickness for the 1969 event. Only with diversion, 15,400 cfs is shown

Contract Report to:
Omaha District, US Army Corps of Engineers
1616 Capitol Ave., Omaha, NE 68102

by:
Meredith L. Carr, PhD
Andrew M. Tuthill, PE
Ice Engineering Group
US Army Cold Regions Research and Engineering Laboratory
72 Lyme Rd., Hanover, NH 03755